Characterization of Active and Inactive Hydrothermal Alterations in the Ethiopian Rift Valley System

BARDHIPAN SEEVARATNAM
February, 2013

SUPERVISORS:
Dr. C.A. Hecker
Prof. Dr. F. D. van der Meer

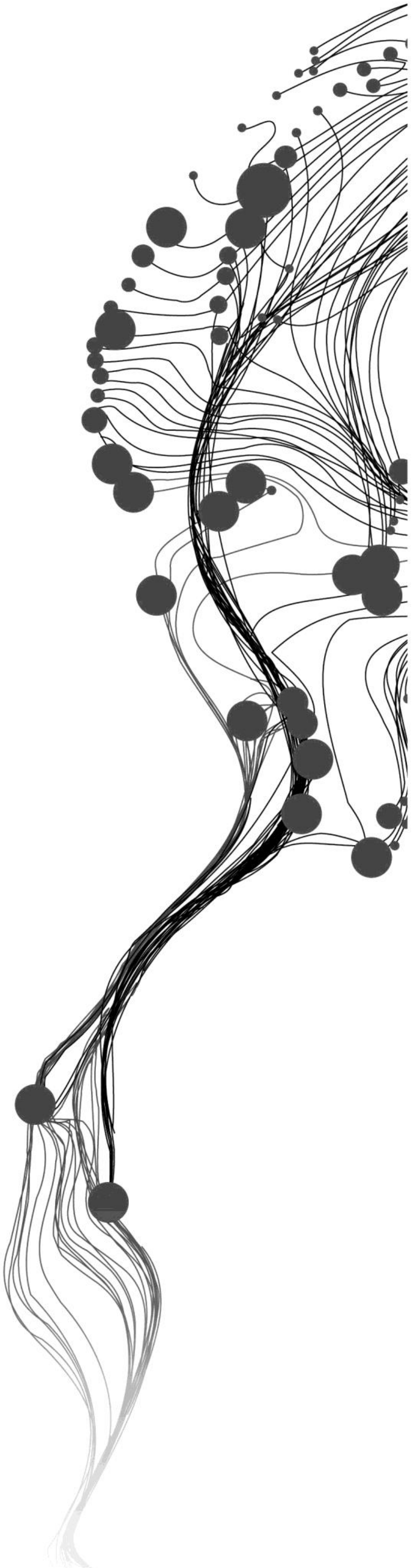

Characterization of Active and Inactive Hydrothermal Alterations in the Ethiopian Rift Valley System

BARDHIPAN SEEVARATNAM
Enschede, the Netherlands, February, 2013

Thesis submitted to the Faculty of Geo-Information Science and Earth Observation of the University of Twente in partial fulfilment of the requirements for the degree of Master of Science in Geo-information Science and Earth Observation.
Specialization: Applied Earth Sciences

SUPERVISORS:
Dr. C. A. Hecker
Prof. Dr. F. D. Van der Meer

THESIS ASSESSMENT BOARD:
Prof. Dr. F. D. Van der Meer (Chair)
Prof. Dr. S. M. (Steven) de Jong (External Examiner, Department of Physical Geography, University of Utrecht]

ABSTRACT

The characterization of active and inactive hydrothermal alteration provides information for geologists and stakeholders the recency of the system, thereby providing further knowledge about the geological phase a given hydrothermal alteration is in. Having this information is also crucial in making informed decisions for mining exploration, since it will illustrate the erosional processes of these two systems based on their exposed alteration zones.

The characterization of active and inactive hydrothermal alteration systems was studied using band ratios and corrected night-time TIR images from ASTER. Selected band ratios from literature were used to characterize the active and inactive alteration. The night-time thermal images were also used along with STcorr application to remove the artifacts, for better discriminate between active and inactive hydrothermal zones.

Band ratios on both inactive and active zones were inconclusive from both the dry and wet seasons. Band ratio values were high from using the Level 2 AST_07XT data product. The sensitivity issue was also studied in the results of the statistical tests and the results had shown statistical differences were found for areas that were visually similar in the box plots. This was due to the outliers in the data. Working with night-time imagery had also illustrated sensitivity to polynomial fits. The polynomial fit, which is user defined, results in different interpretation of active zones, while inactive zones, the polynomial fitting did not affect the discrimination. The study illustrate insight into the scale of temperature gradients, which are not localized to hydrothermal zones only, but actually have larger imprints that also influence other areas (active and inactive) in the Ethiopian Rift Valley system.

Keywords: Active Hydrothermal Alteration, Inactive Hydrothermal Alteration, ASTER, Ethiopian Rift Valley, Geothermal, Berecha, Tendaho

ACKNOWLEDGEMENTS

First and foremost, I would like to dedicate this thesis to my Father, who has always given me the love, support and knowledge for getting me through my tough times so that I could strive for my ambitions. It isn't often when two men find time to talk about research every weekend, especially if there is a quarter of a century of gap in our age and wisdom. But the time spent together as father and son will always be remembered. I would also like to take the opportunity to thank my mother and sister, for their unconditional love and support for keeping me grounded during these tough times.

I would like to express my gratefulness to both my supervisors, Dr. Freek van der Meer and Dr. Chris Hecker, for their support and **"patience"** in getting me through my graduate studies. It is an experience to remember, sitting in those weekly meetings with their dynamic personalities. In all honesty, I wouldn't have asked for better supervisors to really teach me what "science" really is and this token of enlightenment will always be with me. As the saying goes:

"Bardhi, your logic is like... eating chicken in the moon.."

Many thanks go out to the AES faculty for their academic support and advice. Without your time and hardwork, this would have not been possible. I wish you all the best for the years to come.

Lastly but not least, I would like to thank Angelo Meola, and the family of Angelo Gym for the relentless training and discipline for keeping me in order. The physical and mental training has been a gift and it will surely be continued when I return back home.

For those who are reading this, don't forget to reflect about yourself as a scientist. What I have learned is:

"Bad times have a scientific value. These are occasions a good learner would not miss."
-Ralph Waldo Emerson

TABLE OF CONTENTS

LIST OF FIGURES

LIST OF TABLES

1. INTRODUCTION

The presence and types of hydrothermal alterations under a geothermal setting have been recognized as key factors in modelling favourable areas for many mineral deposits types (Elder, 1981) and have long served as areas of interest for mining and mineral mapping purposes. Rift systems like the Ethiopian Rift Valley System (Oluwadebi, 2011) are a good prospective for hydrothermally altered rocks. Mineral commodities like gold, copper, and lead that occur in alterations have been prospected using conventional methods such as field-based surveying and drill-holes (Hemley et al., 1992; Stratex International, 2012; White, 1974). Advances in remote sensing have offered improved methods in detecting mineral deposits in hydrothermal alteration zones such as multispectral and hyperspectral remote sensing (Abrams et al., 1977; Omenda, 2005; Rowan et al., 2003; Yang et al., 1999). However, such studies have overlooked the importance of detecting between active and inactive hydrothermal systems. Such information for geologists and stakeholders is important in understanding the recency of the system, thereby providing further knowledge about the geological phase a given hydrothermal alteration is in. Having this information is crucial in making informed decisions for mining exploration. Despite the abundance of field knowledge, a systematic and *unbiased* method of detecting hydrothermal zones and characterizing active and inactive hydrothermal systems is a present necessity. In doing so, an enhancement of the methods in exploring as well as understanding the complexities of geological systems can be achieved in a methodological manner.

Remote sensing has played an important role in the identification of surface mineralogical composition(Van der Meer et al., 2012). In particular, the 0.45- to 2.5 μm region of the electromagnetic spectrum provides mineralogical information for differentiating iron, carbonate, hydrate and hydroxide minerals (Abrams et al., 1977; Rowan et al., 2003). Remote sensing datasets such as the Landsat Thematic Mapper (LTM) satellite images are widely used to interpret mineral composition (Abrams et al., 1977; Carranza & Hale, 2002). However, its broad spectral resolution limits the proper identification of hydrothermal rocks that have distinctive absorption features at the 2.2 μm region (Van der Meer et al., 2012). For this reason, the Advanced Spaceborne Thermal Emissions and reflectance Radiometer (ASTER) with its higher spectral resolution in the shortwave infrared (SWIR) as well as in the thermal infrared (TIR) regions offers more spectral leverage and has, in fact, become a very common multispectral optical sensor used for mapping hydrothermal alterations (Mars & Rowan, 2010; Van der Meer et al., 2012). By utilizing spectral enhancement techniques such as band ratios, ASTER imagery has proven useful in retrieving mineralogical information (Van der Meer et al., 2012). ASTER's night-time TIR is also capable of providing vital information on surface temperatures for studies related to volcanism, differences in surface energies, and geothermal mapping (Ulusoy et al., 2012).

Before delving deeper into remote sensing applications for hydrothermal alteration mapping, one must have a clear definition of the topic at hand. Hydrothermal alteration is a "change in the mineralogy as a result of interaction of the rock with hot water fluids, called 'hydrothermal fluids'" (Lagat, 2009, p. 2). An understanding of hydrothermal alterations is of great interest scientifically because it provides insight to how minerals are altered based on temperature, permeability, pressure, and other factors related to the hydrothermal activity of a given area (Lagat, 2009), thus also providing evidence whether a hydrothermal system is active or inactive (fossil). For this study, Mount Berecha and Tendaho, two hydrothermal alteration areas in the Ethiopian Rift Valley (ERV), are given particular attention. Both regions have shown similar alteration mineral assemblages but the former is characteristically described to be active while the latter inactive (Gianelli et al., 1998; Oluwadebi, 2011).

This thesis will focus on the unbiased characterization of active and inactive hydrothermal alterations in the Ethiopian Rift Valley, based on two known areas (Mount Berecha and Tendaho). The study will employ spectral indices in the form of ASTER-specific band ratios to investigate the spectral differences between active and inactive hydrothermal alterations and between altered and un-altered zones (Figure 1). This is important for understanding the erosional processes of these two systems based on their exposed alteration zones. Moreover, in doing so, the usefulness of band ratios can also be further examined in relation to their sensitivity to reflectance anomalies (Mars & Rowan, 2010). This study will also explore the differences in surface temperature between active and inactive systems using ASTER night-time thermal data. Since the Ethiopian Rift Valley has a thermal gradient that may influence hydrothermal alterations, characterization is vital to understanding not only the paleotemperature but also the localized differences in mineral assemblages between active and inactive systems. Overall, the study aims to not only reveal the complexities of characterizing alterations in the Ethiopian Rift Valley, but also to critically assess the use of multispectral sensors such as ASTER in producing relevant geological information.

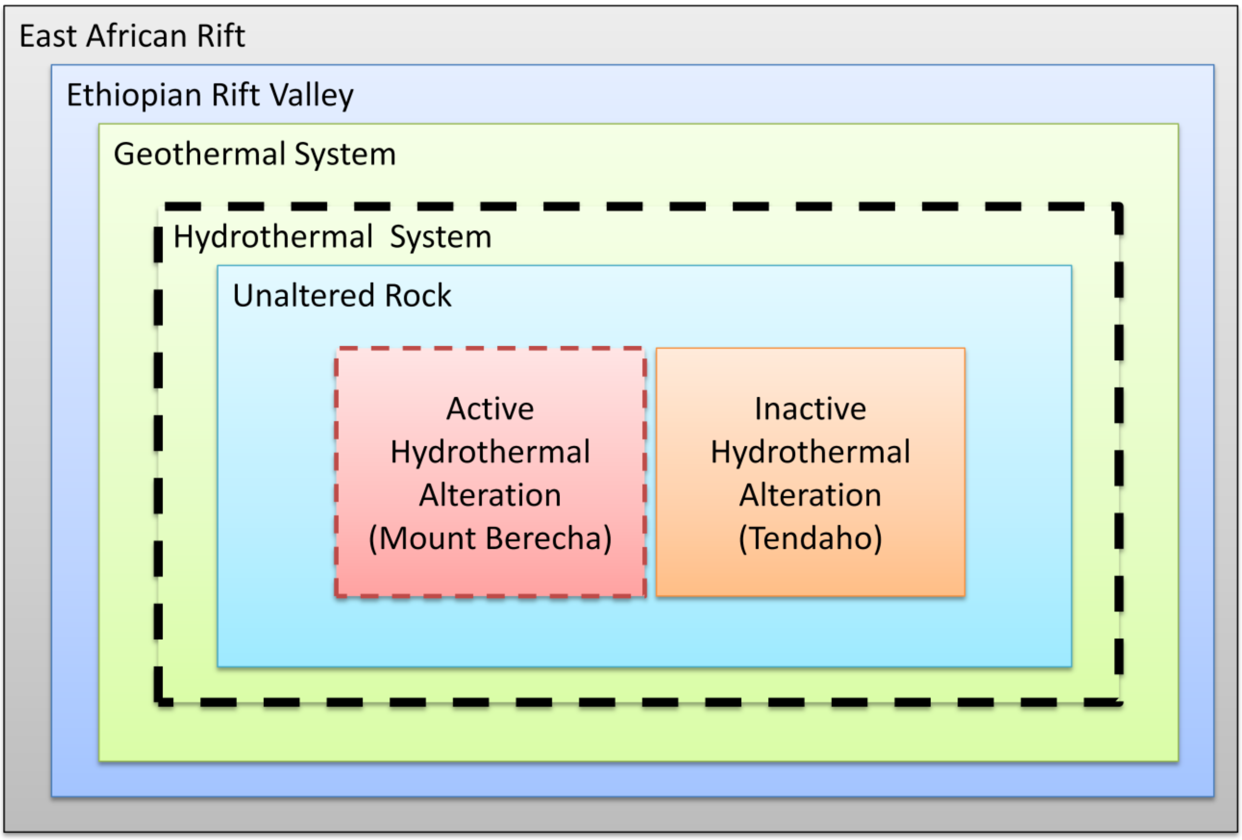

Figure 1. System Diagram of the geothermal setting in the Ethiopian Rift Valley. The focus of the study will be on the active hydrothermal alteration and Inactive hydrothermal alteration. The dashed lines represent the system co-exist of each other.

1.1 Research Problem

Up to the present, characterizing between active and inactive hydrothermal systems, especially those in the Ethiopian Rift Valley, has not been done, as the underlying factors in the development of these two systems is still quite unclear. For instance, the difference in the problem behaviour of surface temperatures between active and inactive systems is not known. Such dilemmas are difficult to solve, given that there has been no methodological framework in place to address such inquiries. Previous remote sensing applications have explored the use of a single multispectral dataset to detect hydrothermal systems, but are restricted due to the limitations of using a single dataset (Carranza & Hale, 2002; Rajesh, 2004). This leads to the question: Is there a methodological framework that integrates multiple remote sensing datasets and gives the ability to detect and differentiate between active and inactive systems in an unbiased manner? It is on these grounds that this study is undertaken and is by which the reliability of analyzing both ASTER day and night imagery through a systematic protocol, is tested.

1.2 Scientific Significance and Innovation Aspect

The scientific significance of this study can be partitioned into three aspects: (1) the task of characterizing between active and inactive hydrothermal systems within a geothermal setting (Ethiopian Rift Valley system); (2) undergoing this task using multiple remote sensing datasets; and (3) operating in an unbiased manner to produce a methodological framework. These three aspects constitute novelty; critical assessment and improvement of existing methods; and objectivity and repeatability—all these are hoped to achieved or demonstrated throughout the course of the study.

1.3 Research Objectives and Questions

The overall objective of this research is to investigate the applicability of using several multispectral datasets (ASTER both day and night) to characterize active and inactive hydrothermal alteration areas in the Ethiopian Rift Valley, and undertaking this through a systematic and unbiased approach. The following specific objectives and corresponding research questions are as follows:

Objective 1

To *spectrally* differentiate between known (a) active and inactive hydrothermal alteration areas and (b) altered and their surrounding unaltered zones using selected Day ASTER scenes.

1. Can active and inactive hydrothermal zones be differentiated using *existing mineral indices*? If so, which of these indices are useful for discriminating between active and inactive hydrothermal alterations?
2. Can mineral indices also be used to discriminate between altered and unaltered zones?

Objective 2

To *thermally* differentiate between (a) active and inactive hydrothermal alteration areas and (b) altered zones and their surrounding unaltered zones using selected night-time ASTER-TIR scenes.

1. Can surface temperatures of active and inactive hydrothermal zones be differentiated using night-time-TIR?
2. What is the optimal method for correcting temperature anomalies of night-time TIR imagery? How sensitive are thermal images in response to different regression techniques and how do these techniques affect the discrimination between active and inactive zones?
3. Can the correction between a small subset image and whole image show influence in the ability of thermal data to discriminate between active and inactive hydrothermal systems?

1.4 Research Setup

In order to answer the research questions, the following steps were made:

1. Literature Review – A review of the geology of the area was done to gain background knowledge on the relationship between geology and hydrothermally altered mineral assemblages in the area. An assessment of state-of-the-art in remote sensing applications in mineral and geothermal mapping was also done.
2. Selection and ordering of pre-processed ASTER scenes of the Mount Berecha and Tendaho (For both the Day and Night images)
3. Image processing, analysis and interpretation of the results of the mineral indices and surface temperature discrimination.
4. Discussion and outlook of the expected problems

1.5 Organization of Thesis

The thesis consists of seven chapters:

- Chapter one describes the research problem, the general and specific objectives (and questions) of the research.
- Chapter two gives a literature review of the characteristics between geothermal vs. hydrothermal systems as well as relevant literature on remote sensing applications in mineral and geothermal mapping.
- Chapter three offers an overview of the two study areas, their geologic setting and a brief review of exploration studies conducted in both areas.
- Chapter four discusses the methods and results for achieving Objective 1.
- Chapter five discusses the methods and results for achieving Objective 2.
- Chapter six is a chapter dedicated for the discussion of the outputs resulting from Objectives 1 and 2 and the problems encountered therewith.
- Chapter seven provides the conclusion and recommendations of the study.

1.6 Research Methodology Framework

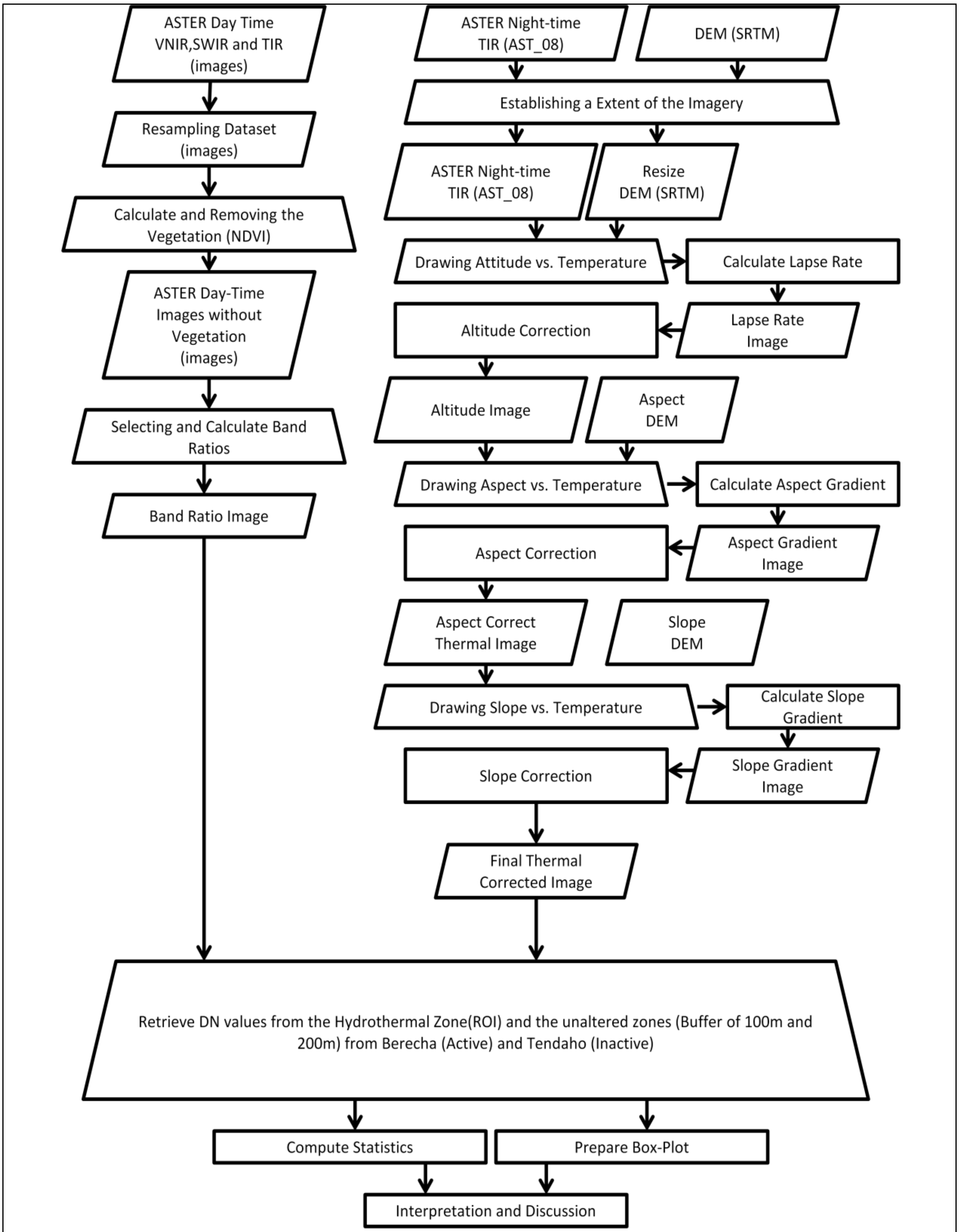

Figure2. Framework of the Research: The selected band ratios were computed using the ordered day imageries. The thermal correction followed similar patterns to Ulusoy et al. (2012) study using night-time imagery. The results were computed statistically and prepared by plotting them into box-plots for interpretation.

2. LITERATURE REVIEW

This chapter gives a review of literature pertaining to the Ethiopian Rift Valley—characteristics of geothermal and hydrothermal systems, geothermal explorations conducted in the area, and remote sensing applications in hydrothermal and geothermal mapping.

2.1. General Characteristics of Geothermal and Hydrothermal Systems

The term ***Geothermal*** and ***Hydrothermal*** have a specific definition for this study. Geothermal refers to a system that transfers heat from within the Earth to the surface, such examples Hot rocks, without water (Heasler et al., 2009). Hydrothermal is a subset of geothermal and means that the transfer of heat involve water (liquid or vapour)(Heasler et al., 2009).

The characteristics of geothermal systems are known to be non-uniform, varying from place to place due to thermal conductivity of rocks, igneous processes and structural setting (Elder, 1981). However, they can be described to possess three essential components (Elder, 1981):

- Subsurface heat source
- Fluid to transport the heat
- Faults, fractures or permeability within sub-surface (Allow heat source to reach to the surface).

The heat generated by the earth (heat flow) is one of the key factors that determine the temperature gradient of a given place (Elder, 1981). Another factor is the thermal conductivity of a certain rock type, or how well a rock insolates the generated heat (Elder, 1981). High heat flow will create higher temperature gradients, while an insulating blanket of sedimentary rocks over the heat source will trap that heat (Elder, 1981). Some rocks make better insulators than others, but in general, sedimentary rocks are generally good insulators (Denton, 1972; Elder, 1981). The East African Rift is an area well known for its high thermal gradients, where there is high heat flow with low thermal conductivity, making it a key area for hydrothermal alterations in a geothermal setting (Simmons & Browne, 2000).

There are several approaches for classifying geothermal system and this is based on the physical properties, convection versus non-convection, and permeable verse non-permeable formations (Denton, 1972; Elder, 1981).

Vapour-dominated geothermal systems (Hydrothermal system) produce superheated steam with little gases and with little or no water, with the steam acting as the controlling factor of temperature and phase (Denton, 1972). The heat from the rocks dries the fluid first to saturate the steam to a level of super-saturation (Denton, 1972). These steams can reach to 55^{O}C superheat with pressure ranging from 4 to 5 km/cm^2 (Denton, 1972). Most steam reservoirs may "cap" for the up flowing part of a major liquid dominated convection of a hydrothermal system (Denton, 1972).

Liquid-dominated convection geothermal systems (Hydrothermal system) are thermally driven convection systems from meteoric water, where the transfer of heat is from deep igneous sources (Denton, 1972). The thermal energy is stored both in the solid rock and in the water and steam which fill the pores and fractures (Denton, 1972). Hot liquid geothermal systems contain water at temperatures that is far past boiling because of the effects of high pressure. For example, the major zones in the main Ethiopian Rift Valley experience up-flow with coexisting steam and water that extends to the surface and as a result, geysers and boiling hot springs are formed (Denton, 1972; Oluwadebi, 2011). Such zones may be easy to detect, the capacity of these liquid-dominated systems in producing hydrothermal alterations is not known (Denton, 1972). The water in most hot liquid geothermal systems is a dilute aqueous solution that contains sodium, potassium, lithium, chloride, bicarbonate, sulphate, borate and silica (Denton, 1972). The silica and potassium/sodium ratio is dependent on temperature reservoir, which as a result can calculate the subsurface temperatures of the hot fluid (Denton, 1972).

Geopressured systems are deep sediment basins filled with sand, clay or shale (Denton, 1972). Geopressured geothermal systems occur in regions of heat flow trapped by insulating impermeable clay beds(Denton, 1972). Water in the geopressured zones are produced by compaction and dehydration of marine sediments and the aquifer systems are stored in regional horizontal faults (Denton, 1972). Water temperatures can range from 150^{O}C to 180^{O}C, with pressures ranging from 27.579 kPa to 41.368 kPa (Denton, 1972). Compared to other geothermal systems, the geopressured system is controlled by water, which is a poor conductor of heat when compared to minerals and caps that are excellent thermal insulators (Denton, 1972).

In the case of the Ethiopian Rift Valley, characterization of active and inactive hydrothermal systems is not straightforward, as there are many kinds of geothermal systems present in the entire system. Moreover, these systems are governed by several elements. Elder (1981) identifies these as:

1. *Scale*: The scale, whether localized or broad, has an important effect on the behaviour of the system, which could ultimately define the type of system(Denton, 1972).
2. *Closed, Open System or Sub-system*: The net discharge of a matter depends through a system(Denton, 1972). For example, geothermal areas with mass discharge in steaming grounds, hot springs, fumaroles and volcanic systems along a rift, imply that the system is active.
3. *Steady, Quasi-steady, Unsteady or Pulsatory system*: This element describes the temporal behaviour of a system(Denton, 1972). For instance, the characteristic feature of a surface zone of a volcanic system is being pulsatory is not a system that is steady state(Denton, 1972).
4. *Change of State*: Fluid elements within a system may experience one or more changes, or be in a continuous state of change(Denton, 1972). A dynamic system like this would have quite a different behaviour from a homogenous system(Denton, 1972).
5. *Changes of System Geometry*: A convection system may be capable of rearranging itself to such a degree that the system, from being active, becomes inactive(Denton, 1972). An example is a system undergoing lithosphere thinning due to interaction with the underlying mantle.

Tectonic geothermal systems in the East African Rift system is commonly occupied by lakes, where the hot mantle material is the primary driving energy source because of its high geothermal gradient (Prianjo, 2009). The deep-circulating meteoric waters have formed reservoirs in permeable stratigraph horizons (Prianjo, 2009). Fluids rise along graben faults and vents and resurface as hot springs or lakes. Such lakes as Lake Natron, Bogoria and Magadi have hot, saline springs discharging at 40-80^{O}C (Prianjo, 2009). Prianjo (2009) also stated that geopressured systems are typically found in sedimentary basins, where deep burial of aquifers result in overpressure reservoirs.

In a region of high heat flow such as the Ethiopian Rift Valley, thermal convection dominates the behaviour of water in permeable areas and fractured crust, creating hydrothermal zones in a geothermal system (Prianjo, 2009). But even with this process, one cannot deduce simply that a system is active or not by just looking at the surfacial hydrothermal expressions.

2.2. Geothermal Exploration in the East African Rift

Geothermal exploration started in Ethiopia in 1969 through the collaboration between the Ethiopian Government and the United Nations Development Program (UNDP) (Kebede, 2011). The main purpose of the exploration was to study the geology, geochemistry and hydrology of hot springs of the East African Rift System within Ethiopia. The study covered 150,000 km^2 area of the Ethiopian Rift including the Afar Rift and the Main Ethiopian Rift (MER) (Kebede, 2011). All fields for geothermal exploration in Ethiopia were located within the Rift, but particular interest was given to two areas: Aluto-Langano and Tendaho.

Aluto-Langano was studied in detail and promoted for deep exploration (Electroconsult, 1986). The drilling program revealed an active fault system (Wonji Fault Belt) with reservoirs containing fluids of high enthalpy and temperatures of 335^{O}C (Electroconsult, 1986). The Tendaho geothermal field, on the other hand, also showed the high temperatures at 270^{O}C, but with very low permeability, indicating that the area was located far from known active faults (Gebregziabher, 1998).

Moreover, the poor fluid circulation of the system proved that the system was inactive (Gebregziabher, 1998). The geothermal explorations demonstrated the importance of field investigations, as these reveal that geothermal elements such as high temperature, discharge/recharge of matter and permeability can differ within a geothermal system, and may even be localized to certain areas (Electroconsult, 1986; Gebregziabher, 1998; Kebede, 2011).

2.3. Hydrothermal Alteration in the Geothermal Field of East African Rift

Many geothermal fields in the East African Rift have revealed the presence of hydrothermal alterations through drill-hole samples. One of which is the Olkaria Domes geothermal field in Kenya (Lagat, 2009). The distribution and abundance of the hydrothermal minerals were obtained from the petrographic and XRD studies of drill cutting samples from exploration wells (Lagat, 2009). Hydrothermal minerals that were found include albite, amphibole, biotitie, calcite, chlorite, chalcedony, epidote, fluorite, garnet, illite, k-feldspar, sulphides, quartz, argillic and advanced argillic minerals (Lagat, 2009). Furthermore, the hydrothermal alteration was found to have undergone temporal changes from several drill sites, with some parts of the drill core indicating cooling whereas other parts indicated heating (Lagat, 2009). In other words, the system itself had been active and inactive over some geological time.

2.4. Remote Sensing for Hydrothermal and Geothermal Mapping

Past studies have used optical remote sensing for hydrothermal and geothermal mapping (Ulusoy et al., 2012; White, 1974). Today's state-of-the-art in mapping geothermal hotspots and hydrothermal alterations is slowly transitioning towards the use of hyperspectral remote sensing (Jones et al., 2010; Martini et al., 2004; Oluwadebi, 2011). Hyperspectral sensors have the ability to record surface reflectance in a large number of continuous spectral bands and "discriminate among earth surface features that have diagnostic absorption and reflection characteristics over narrow wavelength intervals" (Lillesand et al., 2004, pp. 384-385). Oluwadebi (2011) has demonstrated the potential of using hyperspectral datasets in identifying hydrothermal minerals. Furthermore, the detection of *active* hot spots, fumaroles, geothermal vents, mud pots, and thermal anomalies using the thermal infrared range of hyperspectral data was also illustrated byMartini et al. (2004).

Based on these studies, hyperspectral imagery has proved to be useful in mineral exploration, but there remains a need to further evaluate its potential, especially in detecting "certain target minerals, mineral assemblages and temperature data to deliver meaningful hyperspectral data products"(Jones et al., 2010, pp. 7).

2.5. Hyperspectral Remote Sensing Applications in the Ethiopian Rift Valley

Oluwadebi (2011) used Airborne Imaging Spectroradiometer for Application (AISA) Hawk Data to identify and map hydrothermal alteration minerals in Mount Berecha of the Main Ethiopian Rift Valley. Methods such as Wavelength of Minimum, Wavelength Mapping, Minimum Noise Fraction (MNF) and Spectral Angle Mapper (SAM) were applied to map alterations in the region (Oluwadebi, 2011). The study was able to successfully detect mineral assemblages in the study area, including Kaolinite, Halloysite, Opal, Montmorillonite, Nontronite, Calcite, K-alunite, and Illite (Oluwadebi, 2011). The methods applied showed a clear difference patterns between altered and unaltered areas as well as observable patterns within the altered areas (Oluwadebi, 2011). Moreover, the study was able to characterize Mount Berecha as an area of low sulfidation system that was active because of it high enthalpy (Oluwadebi, 2011). As a result, the widespread alteration essentially represented advanced argillic alteration assemblages which consisted of kaolinite, opal, smectite, and alunite minerals that could be traced back to steam-heated origins(Oluwadebi, 2011). Quartz veins and shallow silicifation was also reported in the area (Oluwadebi, 2011). The results showed to be very accurate when it was validated from field records. What the study did not detail is the neighbouring occurrences other alterations within Mount Berecha and failed to characterize if it was from the same or different alteration.

3. STUDY AREA REVIEW: BERECHA (ACTIVE) VS. TENDAHO (INACTIVE)

3.1. The East African Rift

The East African Rift System (EARS) is a series of complex rift systems that extends from Mozambique to the Afar depression in Ethiopia (Omenda, 2005). The EARS is split into two, forming the Eastern and the Western branches (Omenda, 2005) (Figure 3). For this study, the Eastern Branch is the area of interest. The Eastern branch includes the Afar, Ethiopian, Turkana and Kenya Rifts (Omenda, 2005).

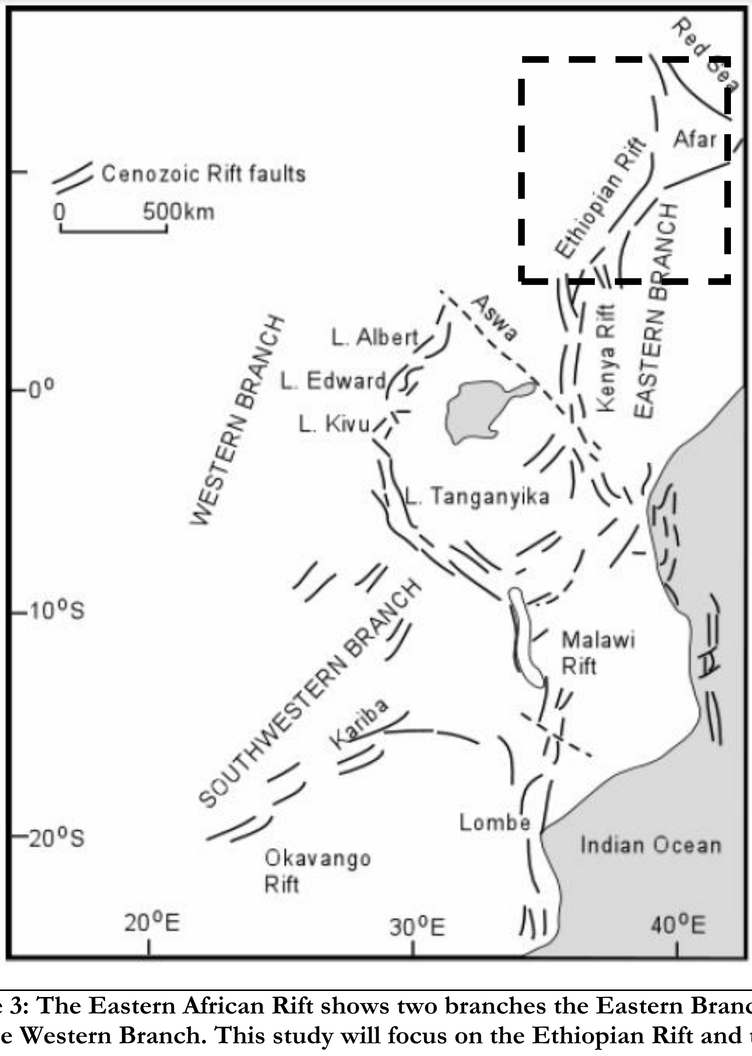

Figure 3: The Eastern African Rift shows two branches the Eastern Branch and the Western Branch. This study will focus on the Ethiopian Rift and the Afar Depression in the Eastern Branch as shown in the black dashed line.
Source: (Omenda, 2005)

The Western Branch includes the Albert, Kivu, Tanganyika, Rukwa and Malawi Rifts (Omenda, 2005). The model for the active rift formation in the Ethiopian Rift involves lithospheric extension, along with upwelling of the asthenospheric mantle (Omenda, 2005) (Figure 4). The decompression of the asthenosphere created large magmatic bodies within the crust. Brittle extension of the crust resulted in the down-faulting and the formation of graben (Omenda, 2005).

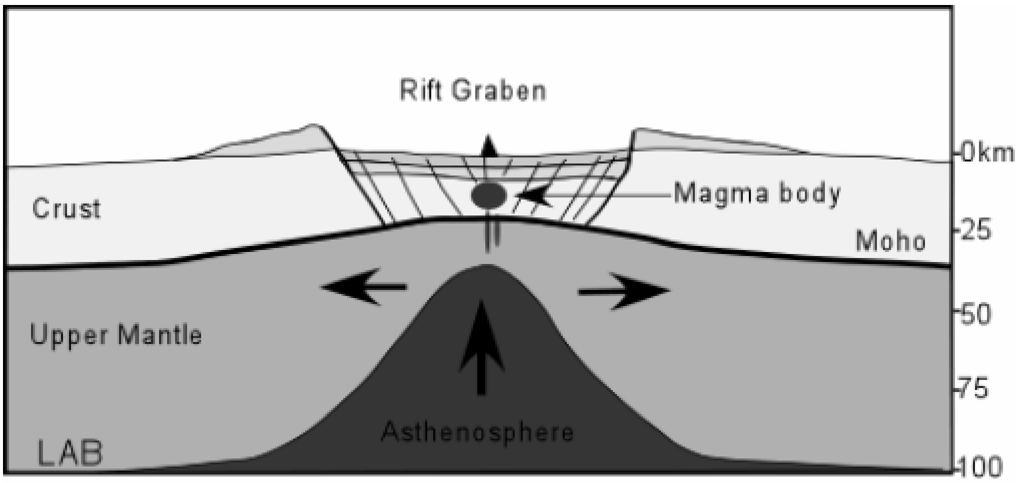

Figure 4: Model of the Last Stage of the Continental Rift
Source: (Omenda, 2005)

3.2. Ethiopia (General Information)

The study areas are located in the Ethiopian Rift Valley in Ethiopia. Its topography is generally flat, covering 1.14 million km² of broad plateau and low lands (Berhanu, 2008; Kebede, 2011). Some highlands exist as high as 4,600 m, while some low lands are 120 m below sea level (Berhanu, 2008; Kebede, 2011). The average annual rainfall in the highlands is 1,200 mm in the north, and ~1,800 mm in the south (Berhanu, 2008; Kebede, 2011). Lowlands annually receive 600 mm of rainfall (Berhanu, 2008; Kebede, 2011). About 70-80% of rain falls during mid-June to mid-September (Berhanu, 2008). (Teum, 2013) explains the seasons of Ethiopia can be divided into the following:

- **Summer** - June, July and August receive the heaviest rain falls throughout the year (Teum, 2013).
- **Spring** - September, October and November also known as the harvest season (Teum, 2013).
- **Winter** - December, January and February constitute the dry season, with morning frosts especially in January (Teum, 2013).
- **Autumn** - March, April and May receive occasional showers, with May as the hottest month in Ethiopia (Teum, 2013).

In the highlands the maximum monthly average temperature ranges between 23-27^{O}C and the minimum between 10-13^{O}C (Berhanu, 2008; Kebede, 2011). In the lowlands, the temperature range is much higher when compared to the highlands (Berhanu, 2008; Kebede, 2011).

3.3. The Ethiopian Rift

The Main Ethiopian Rift (MER) and the Afar Rift started to form 30 million years ago through a series of volcanic activities, such as uplift and eruptions of basalt (Omenda, 2005). This activity had progressed to the Miocene (23 – 5 millions year ago) , where "eruption of bimodal suite of basalts and alkaline silica lavas concentrated within the rift zones" (Omenda, 2005, pp 3). The axis of the rift which consists of rhyolite volcanoes, domes, ignimbrites and pyroclastics (Omenda, 2005). Along the Wonji Fault (axis of the rift) is a region of Quaternary crustal extension (Figure 5). The fault zone is offset along the Wonji Fault but the large volcanoes are located along the fault intersection (Omenda, 2005). The Afar Rift is an active segment of the Eastern African Rift, where large volcanoes of rhyolitic (in the south) and basaltic (in the north) nature are found (Omenda, 2005). The surface geology is ignimbrite (pyroclastic flow deposit) in the south and basalt sheet in the north (Omenda, 2005). The volcanic rocks overlie older sedimentary rocks (Omenda, 2005).

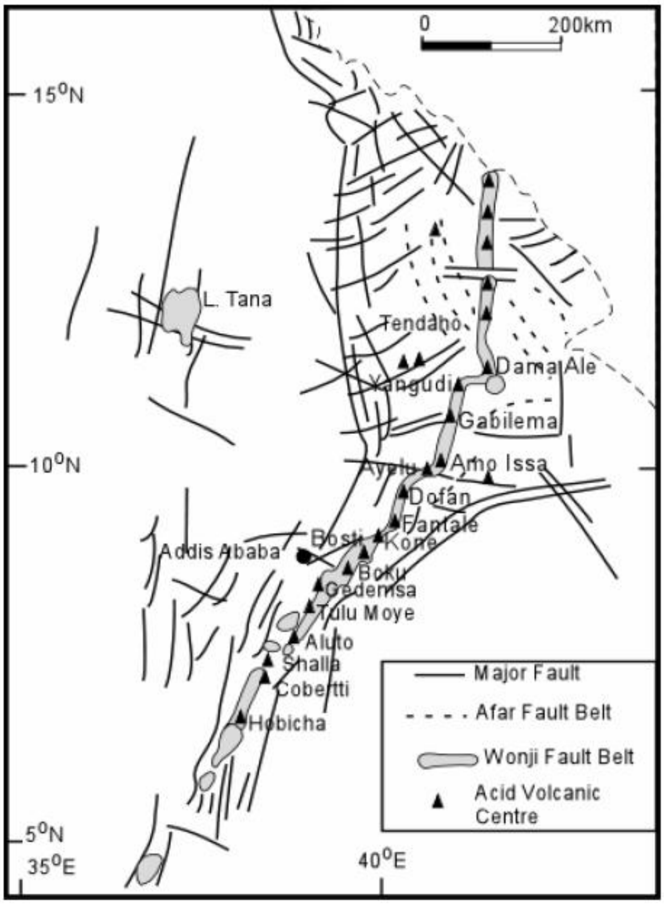

Figure 5: Wonji Fault (axis of the rift) is a region of Quaternary crustal extension (Omenda, 2005)

3.4. Study Area of Mount Berecha (Active)

The Mount Berecha area is located in the Main Ethiopian Rift (MER) near the Gademsa region (Figure 6).

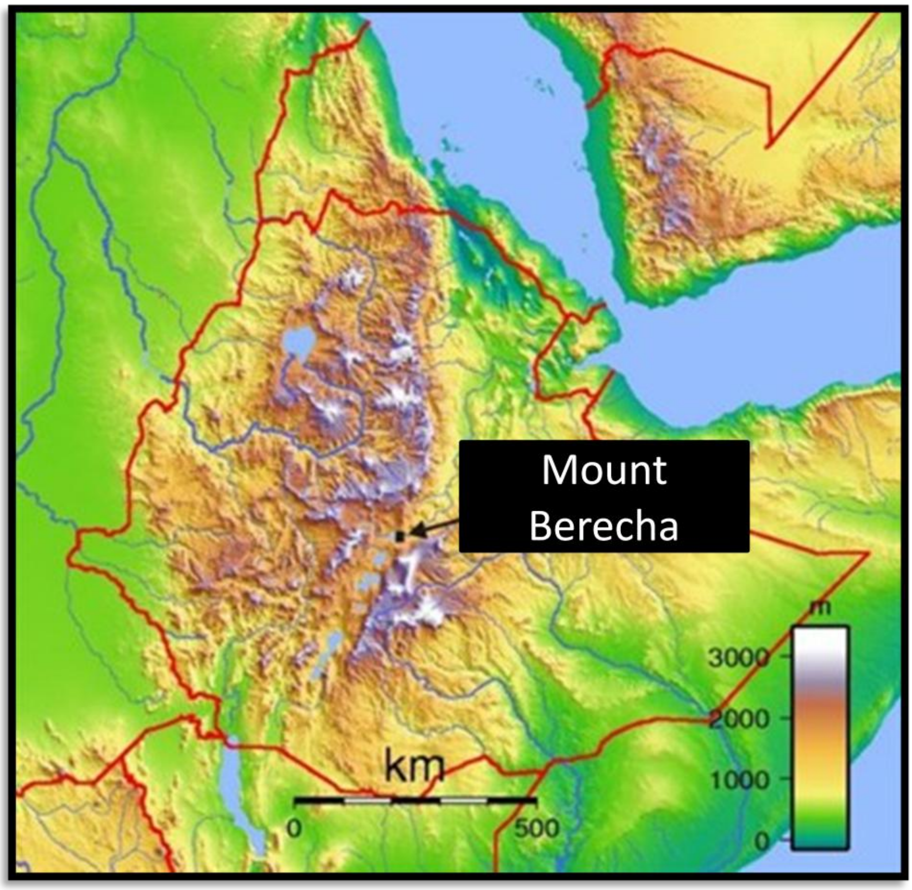

Figure 6. Location of Mount Berecha in Ethiopia
Source: (Modified Stratex International, 2012)

The Berecha area consists of Pleistocene-Holocene volcanic complex with volcano-sedimentary rocks which are recent (Ayele et al., 2002). Berecha is mostly covered by ignimbrite rock, which are units of volcanic complex that belong to a bimodal magmatic suite that erupted between 830 ka and 20 ka (Ayele et al., 2002).

The tectonic and structural setting of Mount Berecha is mainly characterized by NNW-SSE and NW- transverse normal faults (Ayele et al., 2002). The Wonji Faults Belt trends in NNE-SSW which affects Gademsa caldera faulting and also the Mount Berecha region (Ayele et al., 2002).

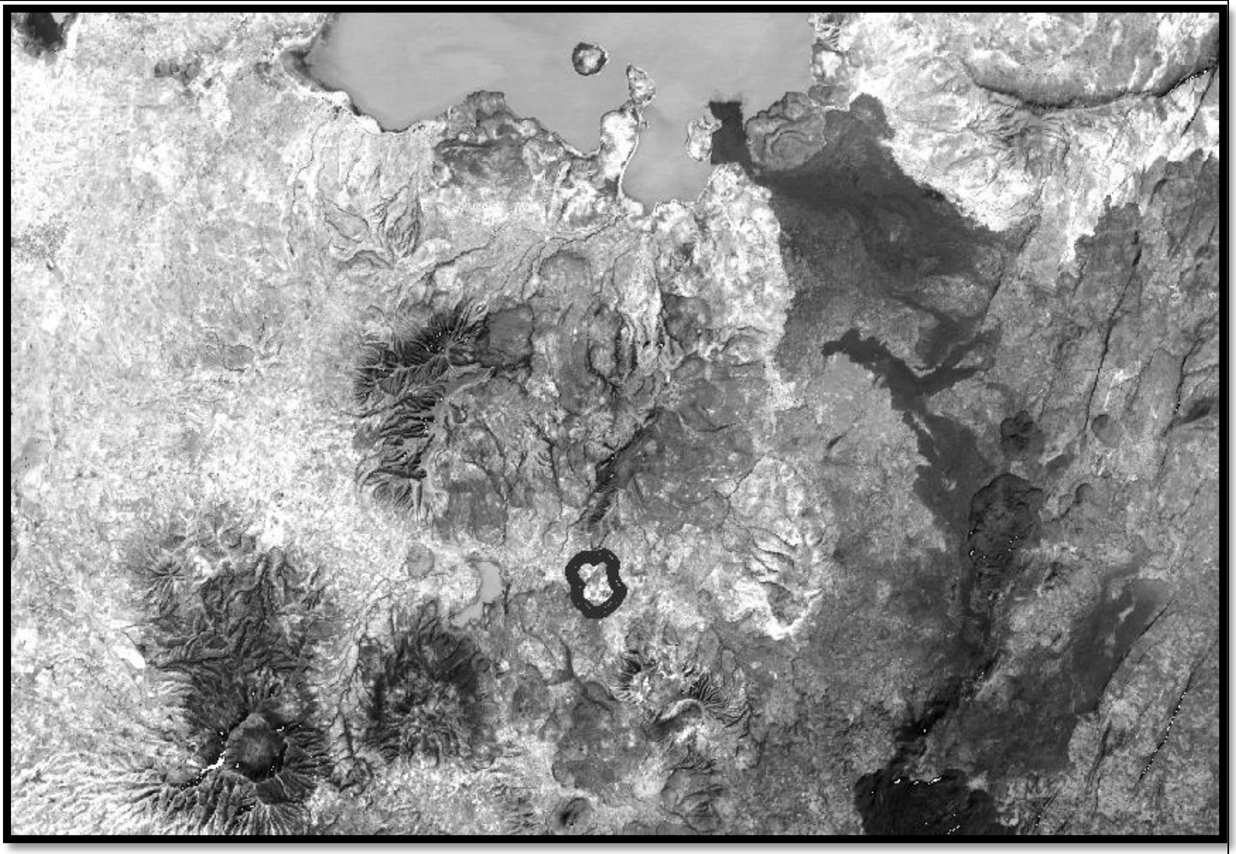

Scale of 1:125,000

Figure 7: Mount Berecha Study Area (Active Hydrothermal System)

The selected study area is in the active region of Mount Berecha, and has an area of approximately 71 hectares (0.714822 km^2) (Figure 7). This area was selected because of the conducted gravity surveys that showed high gravity anomalies due to relatively shallow magmatic intrusions, suggesting a major heat source (Ayele et al., 2002). The recent study of Oluwadebi (2011) revealed that Mount Berecha hosts many hydrothermal alteration minerals such as kaolinite and calcite. This makes it an ideal location for further investigating altered zones and surface temperatures.

3.5. Study Area of Tendaho (Inactive)

The Tendaho area is located in the Afar Depression (Figure 8). This depression refers to a rifting activity that began during the lower Miocene (Gebregziabher, 1998). The first stage of the rift formation was characterized by a change in the magmatic product—from transitional basalt, peralkaline granite and rhyolites to a more alkali and undersaturated composition (Gebregziabher, 1998). The age of the graben is about 25-15 million years(Gebregziabher, 1998).

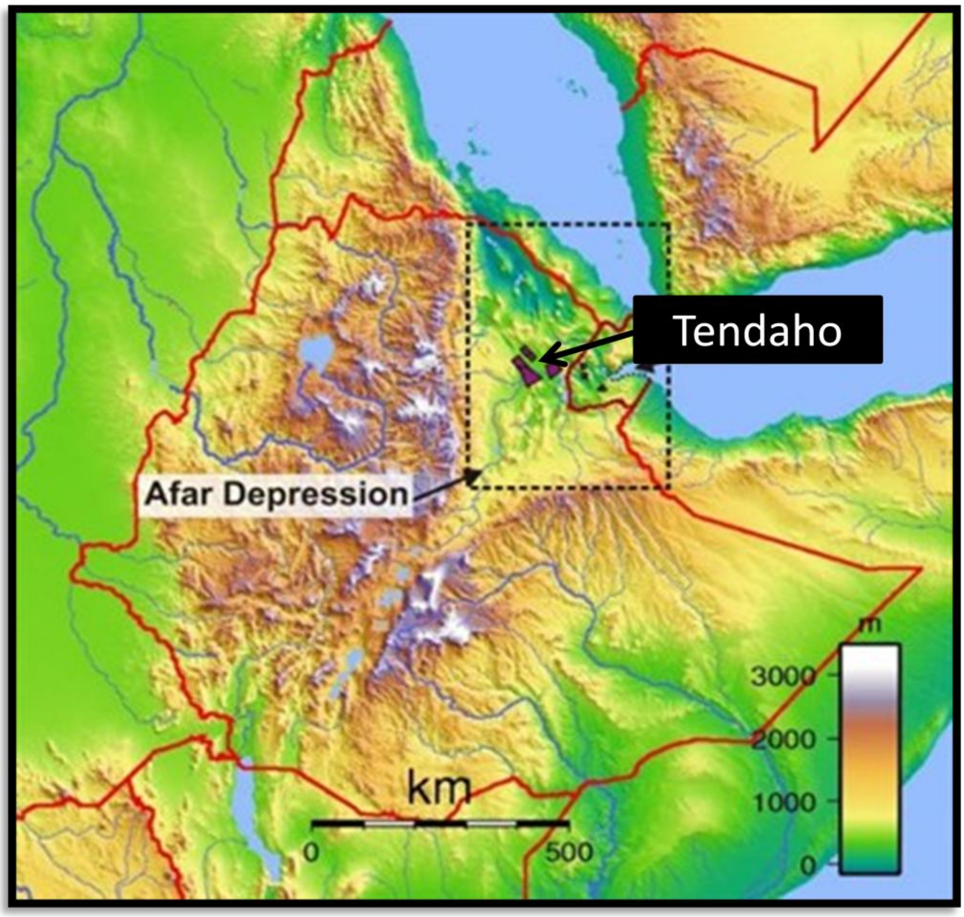

Figure 8: Location of Tendaho Graben in Ethiopia
Source: (Modified Stratex International, 2012)

The second stage is characterized by the deposition of a large volume of acid volcanic with basaltic and intermediate lava dated between 15.3 and 3.3 million(Gebregziabher, 1998). The third stage consists of placement of basaltic Dalha series from 8.0 to 4.9 million years (Gebregziabher, 1998). The inner part of the depression became affected by tensional tectonics, with intense volcanic activity, mostly fissure type Afar stratoid series (Gebregziabher, 1998). It is believed that the Afar depression reached its present geological setting during the Pleistocene period (Gebregziabher, 1998). The intense tensional tectonics affected the entire depression and as a result, formed complex mosaics of horst and graben which are still active only in localized sedimentary basins (Gebregziabher, 1998).

Hydrothermal manifestations occur in various parts of the Tendaho rift, mainly in the form of steaming grounds in the northern parts (i.e., Aerobera), hot springs in Allalobeda, as well as mud pots and fumaroles (Gebregziabher, 1998). Drilling projects have revealed hydrothermal mineralogical assemblages consisting predominantly of clay, calcite, quartz, stilbite, laumonite, wairakite, prehnite and epidote(Gebregziabher, 1998).

Based on the distribution of the alteration minerals, the wells showed zones from low to high temperature zeolites and clay minerals concomitant with increasing temperate down to the bottom of the wells (Gebregziabher, 1998).

The study area selected is within the inactive region of Tendaho, in the inner part of the Afar Depression. The Tendaho graben is technically considered as part of an active structure. However, the selected study area of 64 hectares (0.644190 km^2) has shown low enthalpy, making it a hydrothermal zone in an inactive site (Figure 9).

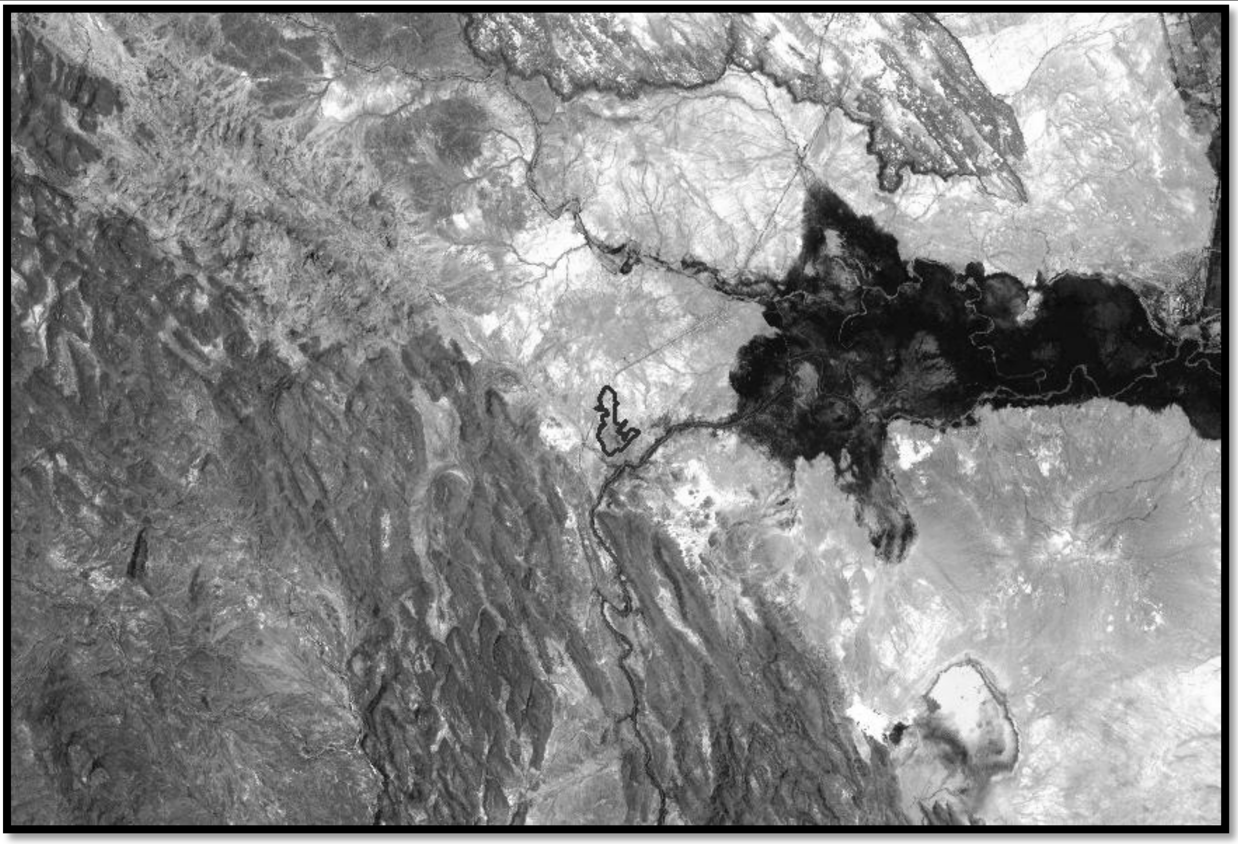

Scale of 1:125,000

Figure 9. Tendaho Study Area (Inactive Hydrothermal System)

The area of study was selected because it was known to be the first low-sulphidation epithermal within the Afar Depression, according to Stratex International (2012), an international mining exploration and development company. Stratex International (2012) describes the site as having identified regional alterations with a number of feeder structures comprised of fine chalcedonic silica vein outcrops at the surface and the preservation of steam heated sinster at the top of the system, suggesting that the system was once active.

4. SPECTRAL MINERAL INDICES FOR ACTIVE & INACTIVE HYDROTHERMAL ZONES

The use of spectral mineral indices (also referred to as band ratios) is an effective means of detecting minerals based on their spectral reflectance/absorption (Van der Meer et al., 2012). In principle, applying a series of band ratios over known active and inactive hydrothermal systems is simple and easy. However, assessing how these band ratios can be used to differentiate between altered and unaltered rock *and* between active and inactive systems is a different and more challenging endeavor. Van der Meer et al. (2012) had suggested the use of several bands ratios for mapping various mineral assemblages in relation to different styles of alteration. As a response, this chapter will investigate the use of said band ratios and assess their usefulness in discrimination by using several different ASTER day images.

4.1. Data Preparation and Rationalization of Data Selection

Several multispectral datasets in the form of ASTER imagery were chosen for this study. As previously discussed, ASTER, compared to other available multispectral sensors, has higher spectral leverage (although certainly not as high as hyperspectral scanners), with 14 bands covering the Visible-Near Infrared, Shortwave Infrared and Thermal Infrared regions (3 bands in the VNIR, 6 bands in the SWIR, and 5 bands in the TIR) and in various spatial resolutions. Furthermore, ASTER imagery were ordered by the data provider (NASA), thus adding to its justification for use.

ASTER data products of processing level 2 were selected for the study (Table 1). Level 2 data products have been converted into absolute reflectance and went through the following processing steps:

Processing Level	Short Name	ASTER Product	Res (m)
2	AST_07XT	Surface Reflectance – VNIR and Crosstrack Corrected SWIR: Surface reflectance containing atmospherically corrected data for both the Visible Near-Infrared (VNIR- 3 bands) and Shortwave Infrared (SWIR- 6 bands). The particular interest of using such a product is to differentiated minerals which can differentiate using SWIR. These minerals could include Carbonates, Silicates, and Kaolinite.	15, 30
2	AST_05	Surface Emissivity: Generated using the five thermal infrared (TIR) bands acquired during the day. It contains surface emissivity. The main goal of using this particular data is to accurately and precisely estimate mineral like silica in hydrothermal zones.	90

Table 1. ASTER Level 2 Image Processing

A total of six ASTER day scenes were selected for the task of investigating the potential of spectral mineral indices in differentiating between active/inactive systems and altered/unaltered rocks. These datasets have the following metadata:

Tendaho	Berecha
Oct 11, 2003 (Wet Season)	Jan 12, 2003 (Dry Season)
Jan 25, 2002 (Dry Season)	Feb 05, 2006 (Dry Season)
Jan 01, 2005 (Dry Season)	Oct 16, 2005 (Wet Season)

Table 2. Selection of ASTER Imagery

The differences in the seasonality are expected to show variance that would, in turn, be useful for discrimination between the two systems. The different seasons may also help identify and eliminate the noise and variations that influence the result of the band ratios.

4.2. Data Processing: Removal of Vegetation and Selected Band Ratio (s)

Prior to image processing, the vegetation was masked from all the images. This was done by applying an NDVI and masking values that showed high NDVI index values. The cut-off values were determined from field images from Stratex and Google Map of where vegetation was occurring (The threshold cut-off were different for each season). This was done to enhance the spectral contrast of the mineral indices without the spectral influence of vegetation.

Several band ratios have been proposed to map mineral indices in a hydrothermal setting (see review by Van der Meer et al., 2012). Mineral band ratios were created by dividing the pixel values of the appropriate band by the same pixel values of another selected band. For this study, eight mineral indices as listed by Van der Meer et al. (2012) were used:

Carbonate/Mafic Minerals Common Ratio	
Carbonates/Chlorite/Epidote	(7+9)/(8)
Silicates Common Ratio	
Sericite/Muscovite/Illite/Smectite (Phyllic Alteration)	(5+7)/(6)
Alunite/Kaolinite/ Pyrophyllite	(4+6)/(5)
Kaolinite	(7/5)
Alteration	(4/5)
Silica Common Ratio	
Silica	(11/10)
Silica	(11/12)
Silica	(13/10)

Table 3. Several band ratios have been proposed to map mineral indices in a hydrothermal setting

These ratios were what authors have found useful for mapping various mineral assemblages in relation to different styles of alteration (Van der Meer et al., 2012). Secondly, these indices correspond to minerals already found in Mount Berecha and Tendaho (see Review from Chapter 3).

4.3. Defining Regions of Interest (ROI) and Buffer Zones

ROI and buffer were used to extract pixel values from images for statistical analysis. To begin the unbiased discrimination of active and inactive alteration systems, a Region of Interest (ROI) was created and used as base for impending interpretation of results. Buffers of 100 m and 200 m were created around the ROI to assess possible differences between these buffer zones and the ROI. Both 100 m and 200 m buffers were selected to assess whether or not alterations occurred within those regions, but also investigate if differences can also be observed between the two buffer zones, as we move further away from the center of alteration.

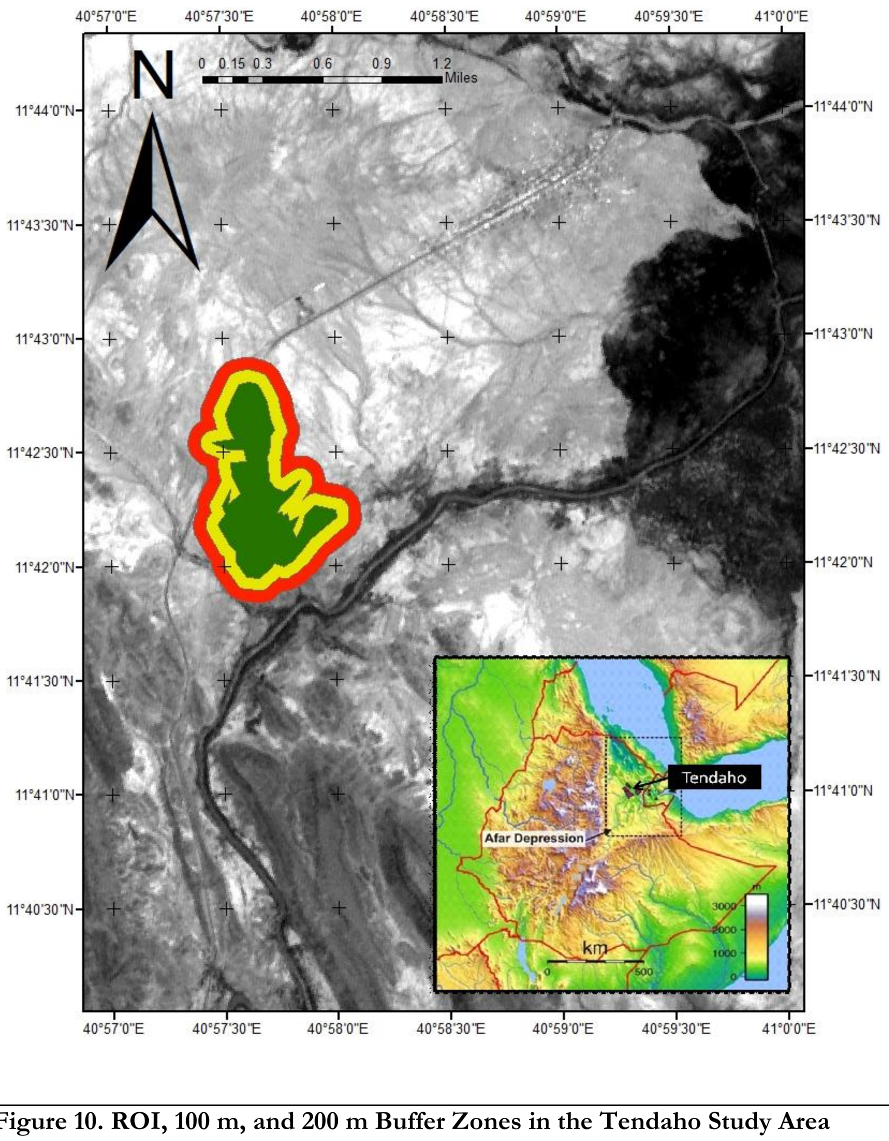

Figure 10. ROI, 100 m, and 200 m Buffer Zones in the Tendaho Study Area

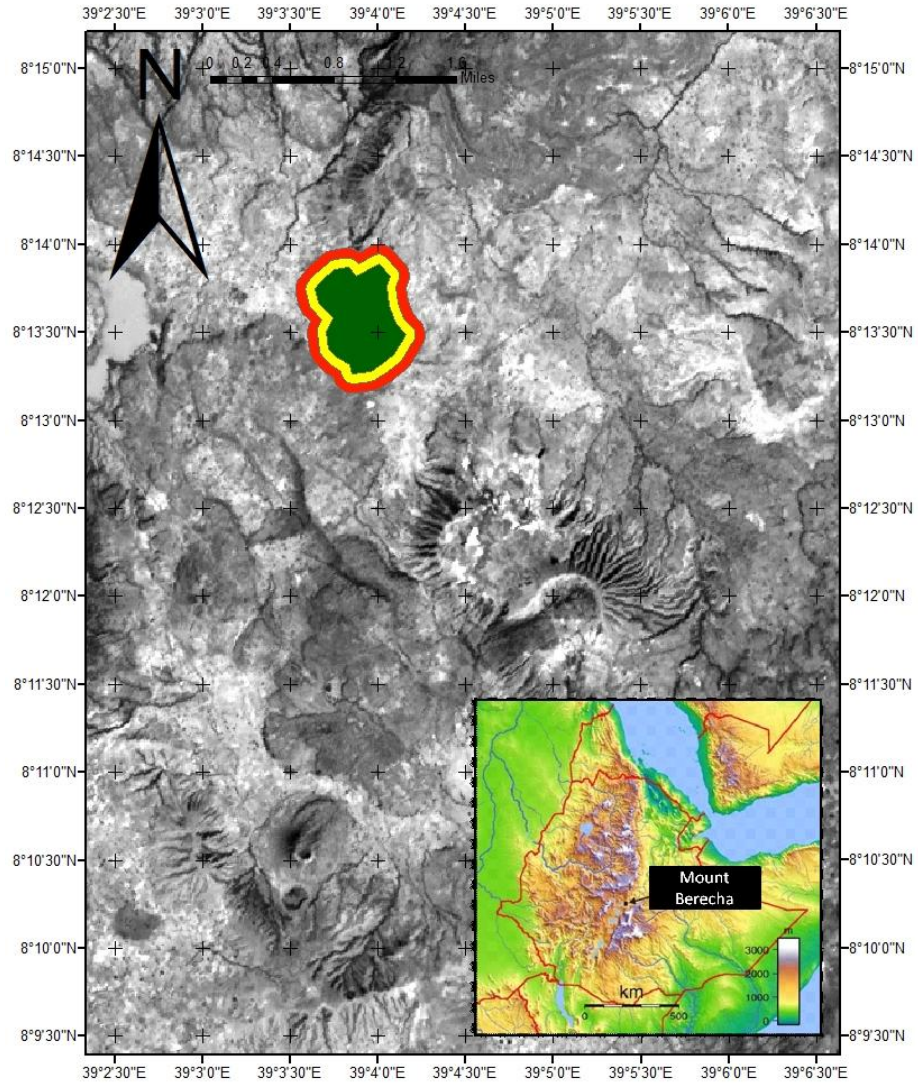

Figure 11. ROI, 100 m, and 200 m Buffer Zones in the Mount Berecha Study Area

Figures 10 and 11 illustrate the ROI set-up along with their corresponding buffer zones for both Mount Berecha and Tendaho. The green zone represents the known (active/inactive) hydrothermal alteration. The yellow and red zones represent the 100m and 200m buffers, respectively. The advantage of this arrangement is to understand the anomalies within these regions that can be plotted against hydrothermal zones and the buffer areas to see if patterns can be recognized. In this case, it would be the discrimination difference between the hydrothermal zones (ROI) and the unaltered zones (Buffer Zones).

4.4. Plotting Band Ratios DN Values using Box-and-Whisker and Statistical Tests

All pixel values from the various band ratios were plotted using the box-and-whisker for visual representation, which generally shows patterns and the spread of the values.

The groups that were evaluated on three requirements:

1. Hydrothermal Zone vs. 100m Buffer from the Hydrothermal Zone ROI
2. Hydrothermal Zone vs. 100m and 200m Buffer from the Hydrothermal Zone ROI
3. 100 m Buffer from Hydrothermal Zone ROI vs. 100m and 200m Buffer from Hydrothermal Zones ROI

This allows for easy assessment in the differences between the mean, median, extremes and quartiles of the hydrothermal zones and the buffer zones for each season/image. As a result, it was easy to establish the relationship between ratios that could be grouped to describe relationships between active and non-active hydrothermal alterations.

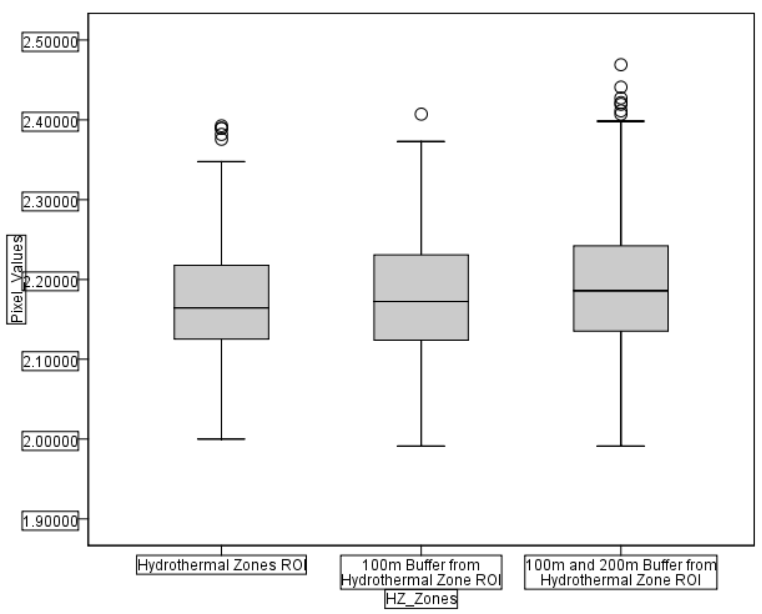

Figure 12. Example of a Box-and-Whisker Plot for for the hydrothermal zone (ROI) and the two buffer zones for the carbonates, chlorite and epidote mineral indices for Berecha October 16, 2005.

The grouping of results was based on the pixel values within the hydrothermal zones and the 100 m and 200 m buffer zones for each index for both Berecha and Tendaho. Figure 12 is an example of the box-and-whisker plots for the hydrothermal zone (ROI) and the two buffer zones for the carbonates, chlorite and epidote mineral indices for Berecha October 16, 2005. On the y-axis, the pixel values resulting from the said band ratios are plotted. The bottom and top of the box represent the lower and upper quartiles while the line inside the box represents the median. The ends of the whiskers are the minimum and maximum data values. The circles beyond the whiskers represent the outliers of the dataset.

Apart from visually displaying summary statistics of the data, statistical tests were conducted to quantify the level of discrimination between the hydrothermal zones and the buffered zones. The ANOVA Post Hoc test with unequal variance and sample size was computed. More specifically, the Tamhane's T2 and Dunnett's T3 test were used to calculate to allow for multiple comparisons among the hydrothermal and buffer zones wherein population variances are large and for different population sizes. The Tamhane's T2 test the conservative pair wise comparisons test based on the t test (SPSS, 2013). The test is appropriate when the variance is unequal (SPSS, 2013). The Dunnett's T3 test is a pair wise comparison test based on the Studentized maximum modulus(SPSS, 2013). This test is also appropriate when the variance is also unequal (SPSS, 2013).

4.5. Results

Two conditions were evaluated using the spectral mineral indices: (1) visual discrimination between the hydrothermal zones vs. buffer zones using box plots; and (2) statistical discrimination between the hydrothermal zones vs. the buffer zones using the ANOVA Post Hoc test.

Box plots were used to visualize the distribution of the pixel values of the hydrothermal zones and the buffer zones as obtained from each mineral index applied. Figure 13 is an example of a box plot showing the results of the Alunite/Kaolinite/Pyrophyllite mineral index (B4+B6/B5) applied to the images of Berecha for the following dates: Jan 12, 2003, Oct 16, 2005 and Feb 5, 2006:

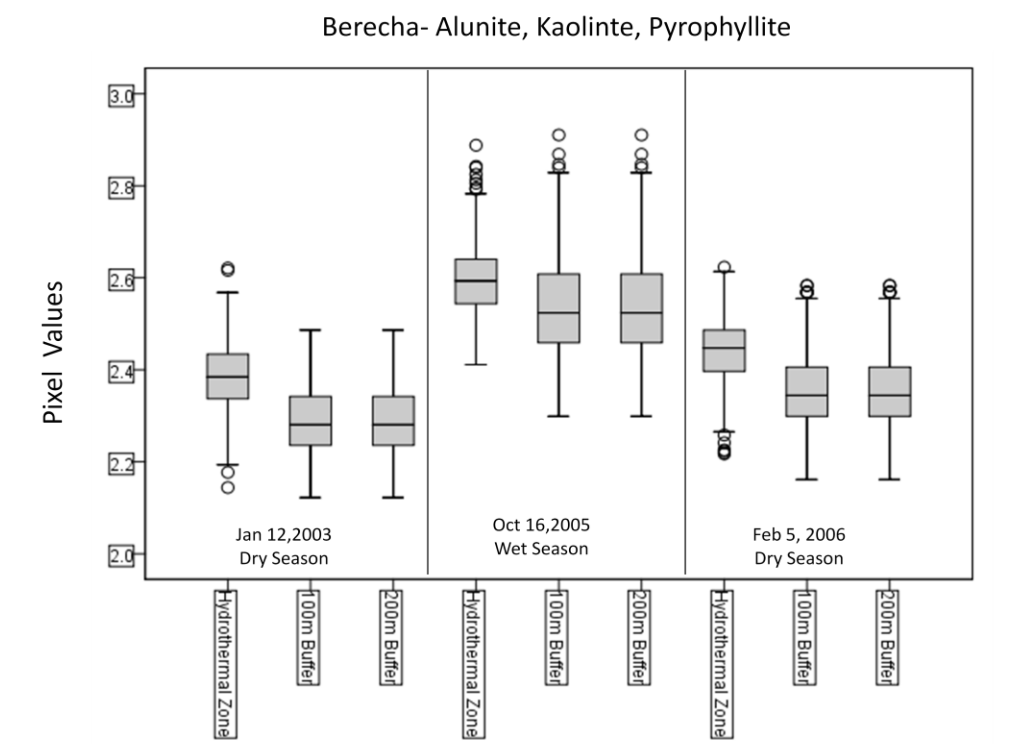

Figure 13. Results of the Alunite/Kaolinite/Pyrophyllite Mineral Index applied to Berecha.

In this figure, hydrothermal zones can be differentiated with the unaltered zones (100m and 200m buffer zones) during the dry season but not for the wet season. For example, for Jan 12, 2003 the hydrothermal zone shows a median value close to 2.4, while the buffer zones show a median value of 2.3. This suggests that the alunite, kaolinite, and/or pyrophyllite are better detected in the hydrothermal zones than in its corresponding buffer zones. In the case of the wet season (Oct 16, 2005), the median values between the hydrothermal zone and the buffer zones are different, but the overall spread of values for all three cases is similar. For example, the upper quartile of the 100m and 200 m buffer zones coincide with the median value of the hydrothermal zone. Moreover, the large values (outliers) are evident in all three zones. This indicates that their values are comparable, making it difficult to separate Alunite, Kaolinite, and/or Pyrophyllite during in the wet seasons.

Another example is the application of the Silica mineral index (B11/B10) on the Tendaho images for the following dates: Jan 25, 2002, Oct 11, 2003 and Jan 1, 2005 (Figure 14).

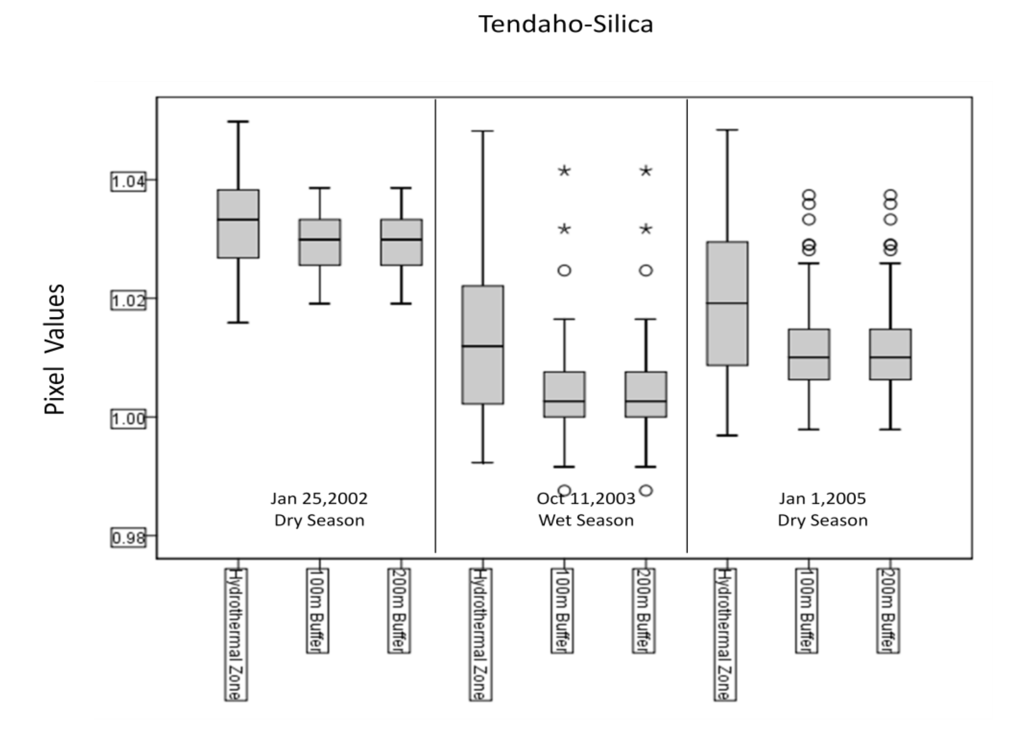

Figure 14. Silica mineral index (B11/B10) on the Tendaho images for the following dates: Jan 25, 2002, Oct 11, 2003 and Jan 1, 2005

Unlike the results of the Alunite/Kaolinite/Pyrophyllite mineral index on the Berecha zones, the results of the Silica band ratio showed no visible difference in the box plot values of the hydrothermal zone and the buffer zones. For both dry and wet seasons, the hydrothermal zone exhibited silica values ranging from 0.95 to 1.05. The values for the buffer zones were also in the same range, although having smaller variance. The similarity in the range of the three zones renders the silica band ratio useless for discriminating between altered and altered zones in Tendaho. More importantly, this similarity implies the presence of silica in the buffer zones.

As a further step in the analysis, the use of the ANOVA Post Hoc test was employed to find significant differences (if any) in the pixel values of the images, as derived from the application of band ratios. For instance, the Alunite/Kaolinite/Pyrophyllite mineral index was found to be useful in differentiating hydrothermal zones from unaltered zones in Berecha during the dry seasons, but not during the wet season. In the results of the ANOVA, however, the wet season values of the buffer zones were found to be statistically different from the values of the hydrothermal zone at a 0.05 level of significance (see table 4). No significant difference was found between the values of 100m and 200m buffer zones, as also visualized through the box plot, and as expected, since both characterize unaltered rock.

An explanation was sought for the disagreement between the box plot and ANOVA results for the wet season image of Berecha. It appears that the outliers in the box plots of the buffer zones may have influenced the statistical outcome. The values of these outliers were traced back in the image and it was found that these were actually representations of large manifestation of kaolinite in low lying fields within the buffer zones, as shown in Figure 15. This suggests that the buffer zones also have hydrothermal alterations.

Figure 15. Low lying areas with surface manifestations of kaolinite(White). Source: (Oluwadebi, 2011)

Multiple Comparisons

Dependent Variable:Pixel Values

	(I) HZ_Zones	(J) HZ_Zones	Mean Difference (I-J)	Std. Error	Sig.	95% Confidence Interval Lower Bound	Upper Bound
Tamhane	Hydrothermal Zones ROI	100m Buffer from Hydrothermal Zone ROI	.00602286*	.00224767	.022	.0006493	.0113964
		100m and 200m Buffer from Hydrothermal Zone ROI	.00894166*	.00196521	.000	.0042439	.0136395
	100m Buffer from Hydrothermal Zone ROI	Hydrothermal Zones ROI	-.00602286*	.00224767	[illegible]	-.0113964	-.0006493
		100m and 200m Buffer from Hydrothermal Zone ROI	.00291880	.00194198	.348	-.0017244	.0075620
	100m and 200m Buffer from Hydrothermal Zone ROI	Hydrothermal Zones ROI	-.00894166*	.00196521	.000	-.0136395	-.0042439
		100m Buffer from Hydrothermal Zone ROI	-.00291880	.00194198	.348	-.0075620	.0017244
Dunnett T3	Hydrothermal Zones ROI	100m Buffer from Hydrothermal Zone ROI	.00602286*	.00224767	.022	.0006495	.0113962
		100m and 200m Buffer from Hydrothermal Zone ROI	.00894166*	.00196521	.000	.0042440	.0136393
	100m Buffer from Hydrothermal Zone ROI	Hydrothermal Zones ROI	-.00602286*	.00224767	.022	-.0113962	-.0006495
		100m and 200m Buffer from Hydrothermal Zone ROI	.00291880	.00194198	.348	-.0017242	.0075618
	100m and 200m Buffer from Hydrothermal Zone ROI	Hydrothermal Zones ROI	-.00894166*	.00196521	.000	-.0136393	-.0042440
		100m Buffer from Hydrothermal Zone ROI	-.00291880	.00194198	.348	-.0075618	.0017242

*. The mean difference is significant at the 0.05 level.

Jan 12,2003

Multiple Comparisons

Dependent Variable:Pixel Values

	(I) HZ_Zones	(J) HZ_Zones	Mean Difference (I-J)	Std. Error	Sig.	95% Confidence Interval Lower Bound	Upper Bound
Tamhane	Hydrothermal Zones ROI	100m Buffer from Hydrothermal Zone ROI	.05475465*	.00619122	.000	.0399340	.0695753
		100m and 200m Buffer from Hydrothermal Zone ROI	.05917970*	.00485343	.000	.0475789	.0707805
	100m Buffer from Hydrothermal Zone ROI	Hydrothermal Zones ROI	-.05475465*	.00619122	[illegible]	-.0695753	-.0399340
		100m and 200m Buffer from Hydrothermal Zone ROI	.00442504	.00678471	.886	-.0118061	.0206562
	100m and 200m Buffer from Hydrothermal Zone ROI	Hydrothermal Zones ROI	-.05917970*	.00485343	.000	-.0707805	-.0475789
		100m Buffer from Hydrothermal Zone ROI	-.00442504	.00678471	.886	-.0206562	.0118061
Dunnett T3	Hydrothermal Zones ROI	100m Buffer from Hydrothermal Zone ROI	.05475465*	.00619122	.000	.0399353	.0695740
		100m and 200m Buffer from Hydrothermal Zone ROI	.05917970*	.00485343	.000	.0475793	.0707801
	100m Buffer from Hydrothermal Zone ROI	Hydrothermal Zones ROI	-.05475465*	.00619122	.000	-.0695740	-.0399353
		100m and 200m Buffer from Hydrothermal Zone ROI	.00442504	.00678471	.885	-.0118050	.0206551
	100m and 200m Buffer from Hydrothermal Zone ROI	Hydrothermal Zones ROI	-.05917970*	.00485343	.000	-.0707801	-.0475793
		100m Buffer from Hydrothermal Zone ROI	-.00442504	.00678471	.885	-.0206551	.0118050

*. The mean difference is significant at the 0.05 level.

Oct 16, 2005

Multiple Comparisons

Dependent Variable:Pixel Values

	(I) HZ_Zones	(J) HZ_Zones	Mean Difference (I-J)	Std. Error	Sig.	95% Confidence Interval Lower Bound	Upper Bound
Tamhane	Hydrothermal Zones ROI	100m Buffer from Hydrothermal Zone ROI	.08009132*	.00491777	.000	.0683240	.0918587
		100m and 200m Buffer from Hydrothermal Zone ROI	.08669644*	.00384234	.000	.0775129	.0958800
	100m Buffer from Hydrothermal Zone ROI	Hydrothermal Zones ROI	-.08009132*	.00491777	[illegible]	-.0918587	-.0683240
		100m and 200m Buffer from Hydrothermal Zone ROI	.00660513	.00487438	.440	-.0050588	.0182691
	100m and 200m Buffer from Hydrothermal Zone ROI	Hydrothermal Zones ROI	-.08669644*	.00384234	.000	-.0958800	-.0775129
		100m Buffer from Hydrothermal Zone ROI	-.00660513	.00487438	.440	-.0182691	.0050588
Dunnett T3	Hydrothermal Zones ROI	100m Buffer from Hydrothermal Zone ROI	.08009132*	.00491777	.000	.0683248	.0918578
		100m and 200m Buffer from Hydrothermal Zone ROI	.08669644*	.00384234	.000	.0775132	.0958797
	100m Buffer from Hydrothermal Zone ROI	Hydrothermal Zones ROI	-.08009132*	.00491777	.000	-.0918578	-.0683248
		100m and 200m Buffer from Hydrothermal Zone ROI	.00660513	.00487438	.440	-.0050580	.0182682
	100m and 200m Buffer from Hydrothermal Zone ROI	Hydrothermal Zones ROI	-.08669644*	.00384234	.000	-.0958797	-.0775132
		100m Buffer from Hydrothermal Zone ROI	-.00660513	.00487438	.440	-.0182682	.0050580

*. The mean difference is significant at the 0.05 level.

Feb 5, 2006

Table 4. Results of the ANOVA Post Hoc test on the Alunite/Kaolinite/Pyrophyllite pixel values for the Berecha images. The red boxes explain the statistical significance, while the green represent not sig. Values that are not significant.

As previously discussed, the application of the Silica mineral index (B11/B10) for the Tendaho images showed no visual difference in the box plots. The statistical results of the same ratio, however, reveal the opposite. The ANOVA Post Hoc test results show a significant difference (at 0.05) between the band ratio values of hydrothermal zones and the buffer zones in both wet and dry seasons. When reflecting back on Figure 13, the box plot of the hydrothermal zone showed high variability in pixel values, compared to the pixel values of both the 100m and 200m buffer zones. Recall that the ANOVA Post Hoc test looks at the difference not only in sample means but also in sample variances. The pixel values for the hydrothermal zone for Jan 1, 2005, for instance, had values ranging from 0.985 to 1.05 but the buffer zones showed a different range, from 1.00 to 1.023. This subtle difference in the range of values between the altered and unaltered zones may have caused the statistical difference. The results of the visual test and the statistical test cannot be reconciled with each other, and as a consequence, the differentiation between altered and unaltered zones using this specific band ratio cannot be determined.

Next, the results from each index were summarized into a table, to distinguish when indices can be used to discriminate between active and inactive systems. The results showed that not all band ratios work and that the outcome of whether the site was active or inactive. For discriminating carbonate, chlorite and epidote, table 5 shows this that ratio would be difficult to use for discriminating between active and inactive sites, neither between altered vs. Unaltered.

On the contrary, band ratio's for discriminating sericite, muscovite, illite, smectite and general alteration can be use to discriminated for an active site like Berecha. Unfortunately, these band ratios do not apply for discriminating the inactive region of Tendaho. There are special cases where the discrimination is appealing. For instance, for discriminating kaolinite, alunite and pyrophyllite for an active region is possible only in the dry seasons and not for the wet season. Also for the silica, the results illustrate the discrimination is very difficult among both the active and inactive regions. Coincidently, the only scenario where Tendaho is possible to discriminate is the silica band ratio of (b13/b10) and (b11/b12) for Jan 25, 2002 (HZ vs. 100m and 200m), Oct 11, (HZ vs. 200m) and Jan 1, 2005 (HZ vs. 200m). The silica band ratio's (b11/b10) don't show convenient results for discrimination for Tendaho.

In general most band ratios showed some various sensitivity of discrimination in the active regions but not for the inactive regions. It is difficult to tabulate proper results for the inactive region, since the results did not correspond to the visual differences and the statistical results.

The table 5 is a summary of the tabulated indication, where the red box describes the differentiation is no possible, while the green box illustrates differentiation is possible. The (*) is an indication of the mean difference being significant at 0.05 level. The tabulated results show a comparison between Hydrothermal Zones vs. 100m (HZ vs. 100m), Hydrothermal Zones vs. 200m buffer (HZ vs. 200m) and 100m Buffer vs. 200m Buffer (200m vs. 100m).

Table 5. Summary of the Band Ratio and Statistical test discrimination between the HZ and buffered zones. The tabulated indication, where the red box describes the differentiation is not possible, while the green box illustrates differentiation is possible. The (*) is an indication of the mean difference being significant at 0.05 level.

Mineral Feature	**Berecha**								
	Jan 12,2003 (Dry Season)			Oct 16,2005 (Wet Season)			Feb 5,2006 (Dry Season)		
Carbonate/Chlorite/Epidote (b7 + b9 / b8)	HZ vs. 100m	HZ vs. 200m	100m vs. 200m	HZ vs. 100m	HZ vs. 200m	100m vs. 200m	HZ Vs. 100m	HZ Vs. 200m	100m vs. 200m
Box Plot Visual Differences									
ANOVA Tamhane's Test					*	*			
ANOVA Dennett's Test					*	*			
	Tendaho								
	Jan 25,2002 (Dry Season)			Oct 11,2003 (Wet Season)			Jan 1, 2005 (Dry Season)		
Box Plot Visual Differences									
ANOVA- Tamhane's Test	*	*		*	*		*	*	
ANOVA- Dennett's Test	*	*		*	*		*	*	

Mineral Feature	**Berecha**								
	Jan 12,2003 (Dry Season)			Oct 16,2005 (Wet Season)			Feb 5,2006 (Dry Season)		
Sericite/ Muscovite/ Illite/ Smectite (b5 + b7 / b6)	HZ vs. 100m	HZ vs. 200m	100m vs. 200m	HZ vs. 100m	HZ vs. 200m	100m vs. 200m	HZ Vs. 100m	HZ Vs. 200m	100m vs. 200m
Box Plot Visual Differences									
ANOVA Tamhane's Test	*	*	*	*	*	*	*	*	*
ANOVA Dennett's Test	*	*	*	*	*	*	*	*	*
	Tendaho								
	Jan 25,2002 (Dry Season)			Oct 11,2003 (Wet Season)			Jan 1, 2005 (Dry Season)		
Box Plot Visual Differences									
ANOVA- Tamhane's Test	*	*		*	*		*	*	
ANOVA- Dennett's Test	*	*		*	*		*	*	

Mineral Feature	**Berecha**								
	Jan 12,2003 (Dry Season)			Oct 16,2005 (Wet Season)			Feb 5,2006 (Dry Season)		
Alunite/ Kaolinite/ Pyrophyllite (b4 + b6 / b5)	HZ vs. 100m	HZ vs. 200m	100m vs. 200m	HZ vs. 100m	HZ vs. 200m	100m vs. 200m	HZ Vs. 100m	HZ Vs. 200m	100m vs. 200m
Box Plot Visual Differences									
ANOVA Tamhane's Test	*	*		*	*		*	*	
ANOVA Dennett's Test	*	*		*	*		*	*	
	Tendaho								
	Jan 25,2002 (Dry Season)			Oct 11,2003 (Wet Season)			Jan 1, 2005 (Dry Season)		
Box Plot Visual Differences									
ANOVA- Tamhane's Test	*	*		*	*	*	*	*	
ANOVA- Dennett's Test	*	*		*	*	*	*	*	

Mineral Feature	**Berecha**								
	Jan 12,2003 (Dry Season)			Oct 16,2005 (Wet Season)			Feb 5,2006 (Dry Season)		
Kaolinite (b7 / b5)	HZvs. 100m	HZ vs. 200m	100m vs. 200m	HZ vs. 100m	HZ vs. 200m	100m vs. 200m	HZ Vs. 100m	HZ Vs. 200m	100m vs. 200m
Box Plot Visual Differences									
ANOVA Tamhane's Test	*	*		*	*	*	*	*	
ANOVA Dennett's Test	*	*		*	*	*	*	*	
	Tendaho								
	Jan 25,2002 (Dry Season)			Oct 11,2003 (Wet Season)			Jan 1, 2005 (Dry Season)		
Box Plot Visual Differences									
ANOVA- Tamhane's Test	*	*		*	*		*	*	

ANOVA- Dennett's Test	*	*		*	*		*	*	

Mineral Feature	Berecha								
	Jan 12,2003 (Dry Season)			Oct 16,2005 (Wet Season)			Feb 5,2006 (Dry Season)		
Alteration (b4 / b5)	HZ vs. 100m	HZ vs. 200m	100m vs. 200m	HZ vs. 100m	HZ vs. 200m	100m vs. 200m	HZ Vs. 100m	HZ Vs. 200m	100m vs. 200m
Box Plot Visual Differences									
ANOVA Tamhane's Test	*	*	*	*	*		*	*	*
ANOVA Dennett's Test	*	*	*	*	*		*	*	*
	Tendaho								
	Jan 25,2002 (Dry Season)			Oct 11,2003 (Wet Season)			Jan 1, 2005 (Dry Season)		
Box Plot Visual Differences									
ANOVA- Tamhane's Test	*	*			*		*	*	
ANOVA- Dennett's Test	*	*			*		*	*	

Mineral Feature	Berecha								
	Jan 12,2003 (Dry Season)			Oct 16,2005 (Wet Season)			Feb 5,2006 (Dry Season)		
Silica (b11 / b10)	HZ vs. 100m	HZ vs. 200m	100m vs. 200m	HZ vs. 100m	HZ vs. 200m	100m vs. 200m	HZ Vs. 100m	HZ Vs. 200m	100m vs. 200m
Box Plot Visual Differences									
ANOVA Tamhane's Test		*		*	*				
ANOVA Dennett's Test		*		*	*				
	Tendaho								
	Jan 25,2002 (Dry Season)			Oct 11,2003 (Wet Season)			Jan 1, 2005 (Dry Season)		
Box Plot Visual Differences									
ANOVA- Tamhane's Test	*	*		*	*		*	*	
ANOVA- Dennett's Test	*	*		*	*		*	*	

Mineral Feature	Berecha								
	Jan 12,2003 (Dry Season)			Oct 16,2005 (Wet Season)			Feb 5,2006 (Dry Season)		
Silica (b11 / b12)	HZ vs. 100m	HZ vs. 200m	100m vs. 200m	HZ vs. 100m	HZ vs. 200m	100m vs. 200m	HZ Vs. 100m	HZ Vs. 200m	100m vs. 200m
Box Plot Visual Differences									
ANOVA Tamhane's Test							*	*	
ANOVA Dennett's Test							*	*	
	Tendaho								
	Jan 25,2002 (Dry Season)			Oct 11,2003 (Wet Season)			Jan 1, 2005 (Dry Season)		
Box Plot Visual Differences									
ANOVA- Tamhane's Test	*	*		*	*		*	*	
ANOVA- Dennett's Test	*	*		*	*		*	*	

Mineral Feature	Berecha								
	Jan 12,2003 (Dry Season)			Oct 16,2005 (Wet Season)			Feb 5,2006 (Dry Season)		
Silica (b13 / b10)	HZ vs. 100m	HZ vs. 200m	100m vs. 200m	HZ vs. 100m	HZ vs. 200m	100m vs. 200m	HZ Vs. 100m	HZ Vs. 200m	100m vs. 200m
Box Plot Visual Differences									
ANOVA Tamhane's Test	*	*					*	*	
ANOVA Dennett's Test	*	*					*	*	
	Tendaho								
	Jan 25,2002 (Dry Season)			Oct 11,2003 (Wet Season)			Jan 1, 2005 (Dry Season)		
Box Plot Visual Differences									
ANOVA- Tamhane's Test	*	*		*	*		*	*	
ANOVA- Dennett's Test	*	*		*	*		*	*	

5. NIGHT-TIME TIR IMAGERY FOR ACTIVE & INACTIVE HYDROTHERMAL ZONES

This chapter aims to investigate the surface temperature differences between active and inactive hydrothermal zones. Night-TIR is utilized because it is less affected by solar irradiation during the day, thereby making it easier to identify possible anomalies. However, thermal effects due to differential solar heating and shadowing that are greatly dependent on the acquisition time may be present in the Night-TIR images. Hence, corrections for removing false anomalies such as lapse rate, slope and aspect effect, must be considered (Ulusoy et al., 2012).

Before going into the methods of processing the Night-TIR imagery used in this specific part of the research, an understanding of the above mentioned thermal effects must be made. Such knowledge is crucial for assessing image quality before even attempting image processing. One such effect is the lapse rate, which is the negative change of actual temperature with altitude (-dT/dz) (Ulusoy et al., 2012). Lapse rate is region- and season-specific. The two study areas in this research are geographically different, and would therefore need different lapse rate corrections. In particular, the lapse rate would have a strong effect on the TIR imagery because of the considerable difference in altitude for both study areas. For Berecha the elevation ranges from 1500m to 2500m, while Tendaho is from 350m to 650m.

Another correction that would need to be taken into account is the absorbed solar radiation, which is the function of surface albedo and the illumination effect (Ulusoy et al., 2012). This can be examined by looking at the aspect and the slope values of a pixel (Ulusoy et al., 2012). Different geological surface properties respond differently to solar radiation, resulting in various surface temperatures (Ulusoy et al., 2012). A demonstration of this effect is in the strong anomalies in uncorrected images caused by warmer sun-facing slopes (Ulusoy et al., 2012). Also, night-time images carry residual temperature differences from the day that are still visible and need to be corrected from the aspect and slope. In the case of the Ethiopian Rift valley where the topographic slopes are gradual, this effect may be minimal, but should still be taken into account in order to detect thermal anomalies.

5.1. Code of IDL of Methodology of STcorr: Topographic Correction of ASTER Images

STcorr is an Interactive Data Language (IDL) code for the correction of altitude, aspect and slope effects in the night-time thermal imagery using an image based polynomial regression analysis (Ulusoy et al., 2012). The code uses surface kinetic temperature image, digital elevation model (DEM), aspect image and the slope image to help remove lapse rate and illumination effects and generate an output image with actual thermal anomalies (Ulusoy et al., 2012).

Some of the limitation to this application; There is no albedo and thermal inertia corrections(Ulusoy et al., 2012). The albedo is important since the night-time images, the albedo affects are noticeable in the ASTER night images(Ulusoy et al., 2012). For the thermal inertia, the correction does not take into account the difference of geological material being heated and cooled off(Ulusoy et al., 2012).

The STcorr IDL code is implemented through a standalone application in ENVI is specifically designed to correct ASTER night time surface temperature images (Ulusoy et al., 2012). The application has important capabilities in detecting geothermal anomalies as. For further information on the regression algorithm used in STcorr, the reader is guided to the paper of Ulusoy et al. (2012). The steps involved in TIR image correction are as follows:

Step (s)	Image Normalization	Purpose of the Correction/Formula
1	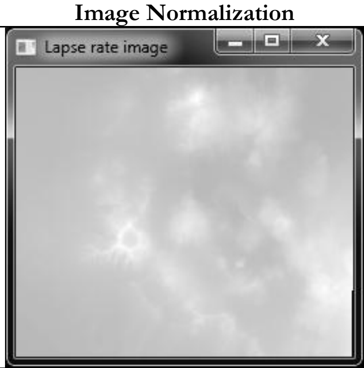	Lapse Rate produced using the surface kinetic temperature and the DEM. This image represents the lapse rate according to the relationship between altitude and surface temperature.
2	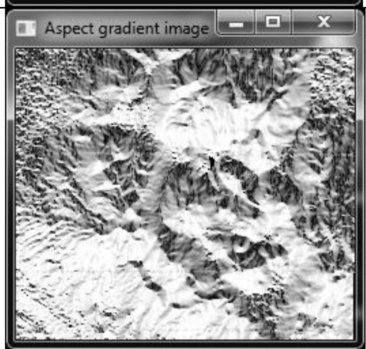	Aspect correction is achieved using the relation between altitude and the lapse rate corrected thermal image. This is a gradient image used to normalize the surface temperature anomaly to produce aspect-correct image.
3	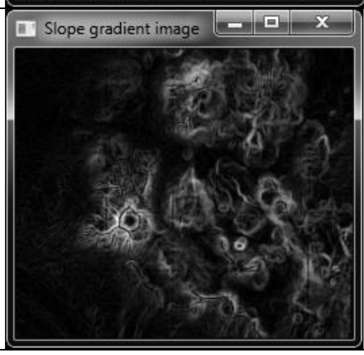	Slope correction, uses the aspect-corrected image and the slope image to generate a slope corrected image.

Figure 16. Steps Involved in STcorr Correction of ASTER Night TIR Imagery

5.2. Data Selection and Preparation

ASTER night TIR imagery of level 2 processing was selected for the study. A total of four images were selected for the task of investigating the surface temperature differences between active/inactive systems and altered/unaltered rocks. These datasets have the following image processing steps and metadata:

Level	Short Name	ASTER Product	Res (m)
2	AST_08	Surface Kinetic Temperature: This specific data contains 1 band with surface temperature at 90m spatial resolution. Surface kinetic Temperature was selected because of it requirements with STcorr application. Previous studies have used this specific data to study volcanism, thermal inertia, and surface temperature for geothermal studies.	90
Data Product	**Capture Resolution**	**Pixel Resolution**	
SRTM – Filled	3 arc second	90m	

Table 6. The data used for the thermal correction

The AST_08 and the SRTM were basic requirements to run the STcorr application. The DEM was resampled to the AST_08 images resolution before any processing was executed. The STcorr also required aspect image and slope image from the resampled DEM. Aspect and slope images need to be between 1 and 360^{o}. Figure 16 provides an overview of the data preparation of Berecha required for STcorr.

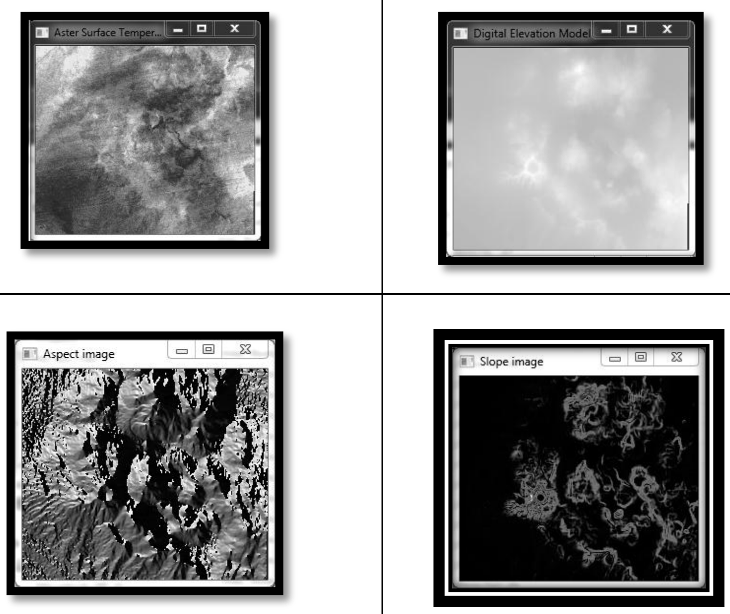

Figure 16. Data Preparation of Tendaho for STcorr Correction

5.3. Regression Computation for Corrections

The initial corrections are based on regression fits to create the images related to lapse rate, gradient and the slope correction. The regression is based on polynomial fits to the image and these polynomials fits can be fitted from the 1st to 6th degree. These generate images of the lapse rate, slope and aspect image to help normalize the thermal anomalies and improve the quality of the true anomaly. The basic concept of this polynomial fit is to correct for the relict illumination (remove artifacts), which occurs during cooling at nights(Ulusoy et al., 2012).

5.4. Methodology for Analysis of Thermal Anomalies

The regions of interest and buffer zones used for the thermal imagery analysis are identical to those used in the analysis of mineral indices (see Section 4.3). Similar ROIs and buffer zones were required for this analysis in order to integrate later on the results of both the spectral mineral indices and the surface temperature differences. Likewise, the visual and statistical analyses for the surface temperature anomalies also follow the same procedure as described in Section 4.4. In this case, however, the analysis is conducted on the corrected thermal images of the STcorr.

Similar to section 4.5, two conditions of were evaluated; (1) visual discrimination between the hydrothermal zones vs. buffer zones using the box plot, (2) statistically discrimination between the hydrothermal zones vs. the buffer zones using the ANOVA Post Hoc test (Tamhane's and Dennett's because of unequal variance and sample size).

5.5. Results

The results of the differentiation between surface temperature of active and inactive sites are illustrated using scatter plots of Temperature vs. Altitude, Aspect and Slope was investigated (Figure 18).

An inverse relationship exists between temperature and altitude, with decreasing temperature as elevation increases. The Berecha area has varying altitudes, resulting in temperature gradients (see Figure 17). In Figure 17, the green areas represent thermal anomalies in the caldera area, suggesting that these areas are active. Meanwhile, the red areas depict surface temperatures caused by night-time katabatic winds, which take air from high elevation down slopes (Tucker & Pedgley, 1977). The corresponding scatter plot shows the "real" active areas as well as the cold areas.

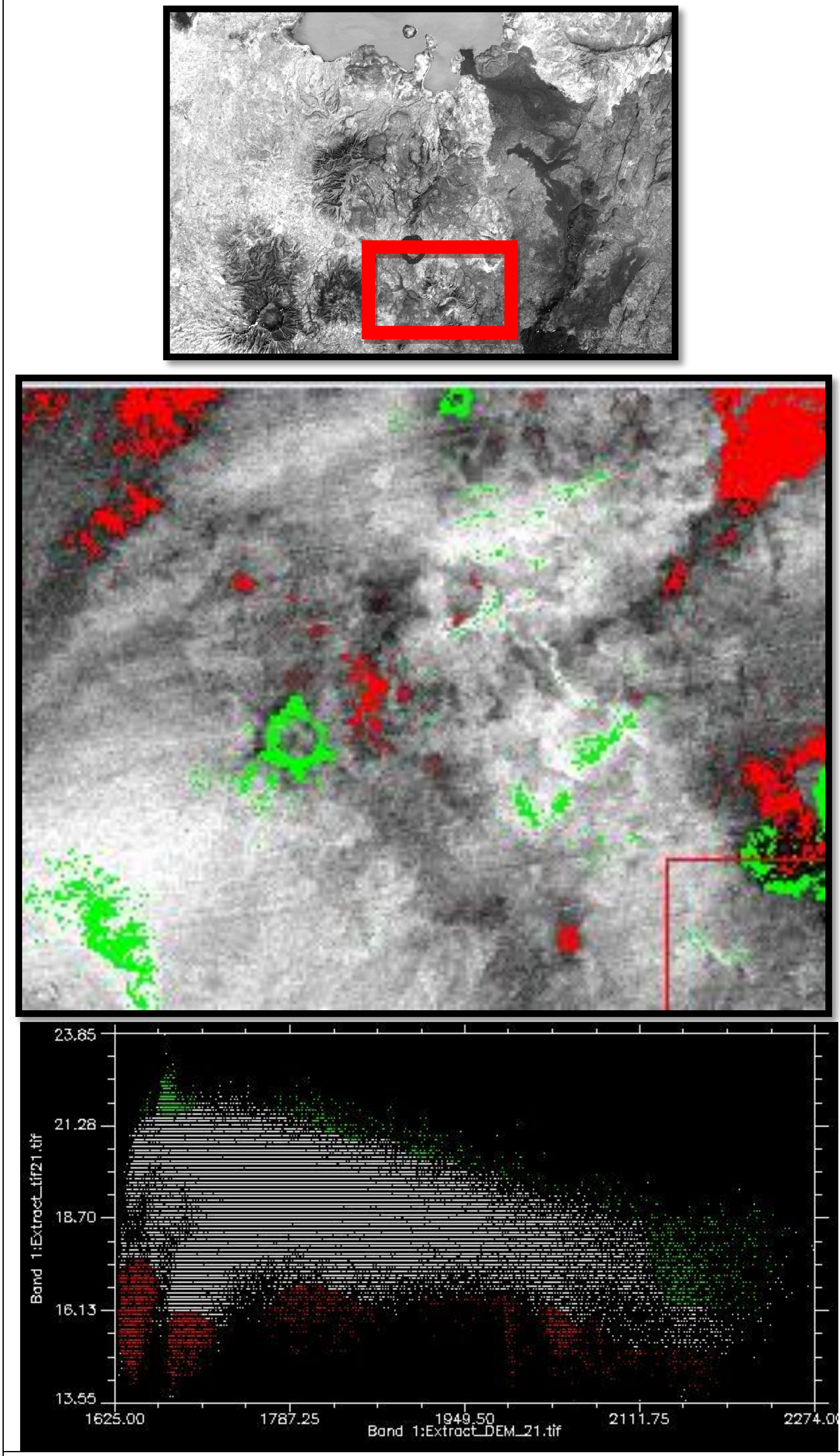

Figure 17. Mount Berecha the Image Extraction

When investigating the corrections for the "Temperature versus Aspect", the corrections show the aspect to have consistent temperature ranges from 5^{O}C to -5^{O}C (Figure 18). The altitude was corrected for extreme temperature anomalies for better contrast. The lapse rate is the main contributing factor for creating false anomalies due to the elevation. In the case of the "Temperature Anomaly verse Aspect", the plot reveals the aspect has less of a contributing factor for correction when compared to the elevation (Figure 18). For the "Temperature Anomaly verse Slope" graphs, the change of temperature anomaly with respect to slope shows a constant trend, indicating a constant temperature with varying slope conditions. The slope effect is relatively less when compared to the aspect and the altitude.

The end result is the anomalies corrected according to the user definitions and these can be used to discriminate between the hydrothermal zones and the buffer zones for both Berecha and Tendaho.

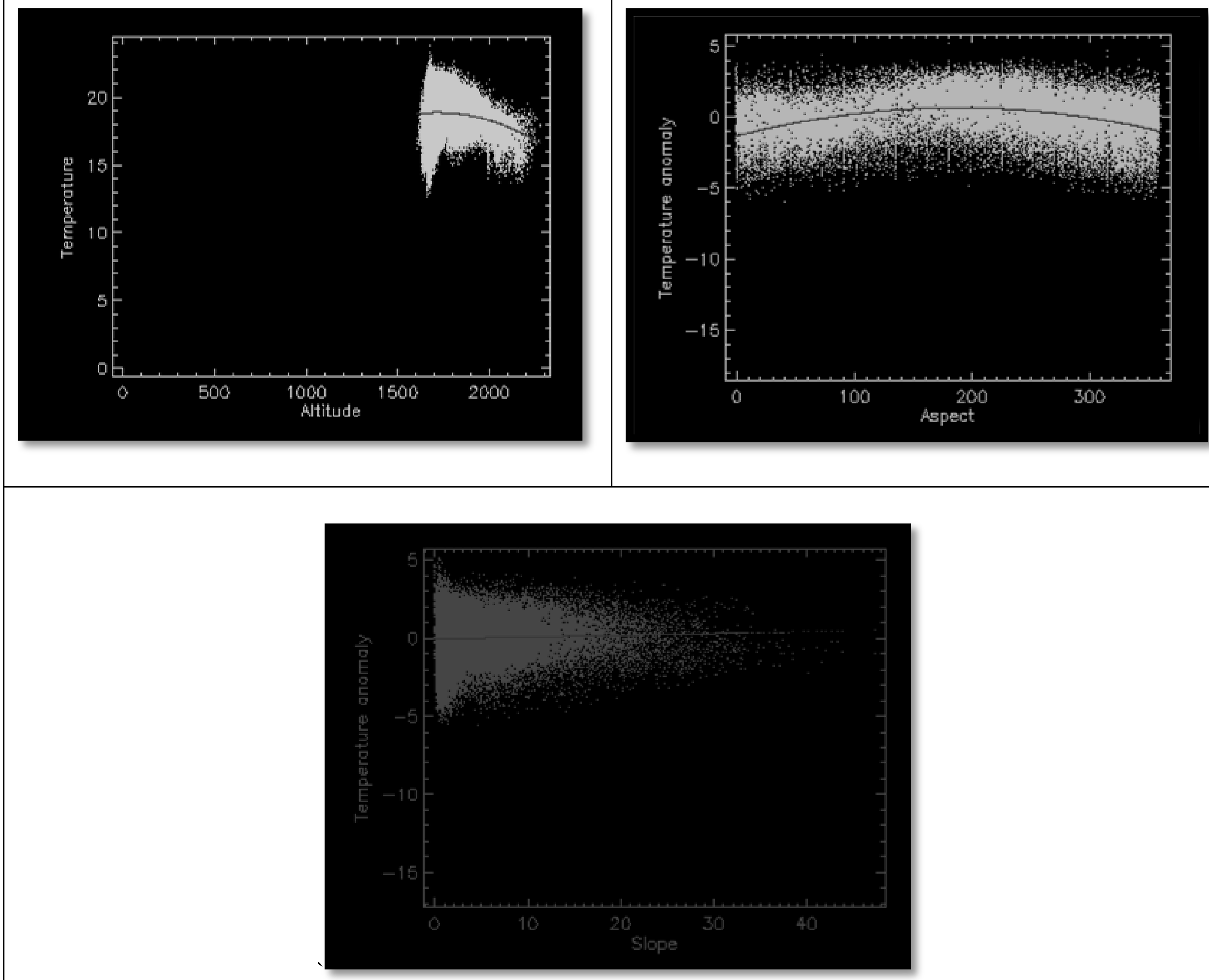

Figure 18. Illustrated using scatter plots of Temperature vs. Altitude, Aspect and Slope

To better understand the sensitivity of the results from different settings, images of different seasons were experimented with several polynomial fits. Sensitivity to scale was also tested between small image subsets and the entire image.

Table 7 summarizes the results from the box plot and the ANOVA analysis. For the case of Berecha, using the 1st polynomial fit, the box plot showed that the active hydrothermal zone could not be differentiated from the 100m buffer zone but was differentiable from the 200m buffer zone. Statistically, however, the difference between the 100m buffer zone and the hydrothermal zone were found to be significant, thus, adding to the list of mixed results of the visual and statistical tests. Moreover, for the wet season (Aug 8, 2010), it is completely impossible to tell apart visually and statically the altered and unaltered zones.

For the 2nd polynomial fit, the box plot showed hardly noticeable differences between the hydrothermal zone and the buffer zones. Statistically, however, the difference between the altered zone and the 200 m buffer zone was significant in both wet and dry season images. In general, the box plots for Berecha region could not differentiate between altered and unaltered zones, either in wet or dry seasons, except in the isolated case of the first polynomial fit of HZ_ROI vs. 200 m.

For Tendaho (Inactive region), the surface temperatures could not be discriminated between the hydrothermal zone and the buffer zones visually or statistically, suggesting little or no contrast between the surface temperatures. This is expected since the hydrothermal zone is an inactive region and should not exhibit observable contrast in surface temperatures.

When investigating the sensitivity of the thermal image from that of a small subset versus the whole image, the sensitivity is less reliable when it comes to discriminating active regions. The small subset area, demonstrate discrimination is more receptive as compared to the entire image. This is due to the fact that the entire images have a higher effect of relict diurnal heat, making it difficult to discriminate from a framework of a known hydrothermal alteration. What this reveals is an issue correction if the study was to investigate surface temperature from **unknown** alterations. In that case for Tendaho, the results confirm there is no contrast between the masked subset image and the whole image since this is an inactive area.

Table 7. The results is the summary of the thermal discrimination, where red boxes mean it can't be discriminated, while the green box indicates that discrimination is possible. The (*) indicate there is statistical significance at 0.05

Polynomial Fit Type (Small Extent)	**Berecha (Active)**					
	Feb 2, 2003 (Dry Season)			Aug 8,2010 (Wet Season)		
1st Polynomial Fit	HZ_ROI vs. 100m	HZ_ROI vs. 200m	100m vs. 200m	HZ_ROI vs. 100m	HZ_ROI vs. 200m	100m vs. 200m
Box Plot Visual Differences						
ANOVA Tamhane's Test	*	*				
ANOVA Dennett's Test	*	*				
	Berecha (Active)					
2nd Polynomial Fit	HZ_ROI vs. 100m	HZ_ROI vs. 200m	100m vs. 200m	HZ_ROI vs. 100m	HZ_ROI vs. 200m	100m vs. 200m
Box Plot Visual Differences						
ANOVA- Tamhane's Test		*		*		
ANOVA- Dennett's Test		*		*		

Polynomial Fit Type (Small Extent)	**Tendaho (Inactive)**					
	Sept 30, 2002 (Wet Season)			Mar 2,2010 (Dry Season)		
1nd Polynomial Fit	HZ_ROI vs. 100m	HZ_ROI vs. 200m	100m vs. 200m	HZ_ROI vs. 100m	HZ_ROI vs. 200m	100m vs. 200m
Box Plot Visual Differences						
ANOVA Tamhane's Test						
ANOVA Dennett's Test						
	Tendaho (Inactive)					
2rd Polynomial Fit	HZ_ROI vs. 100m	HZ_ROI vs. 200m	100m vs. 200m	HZ_ROI vs. 100m	HZ_ROI vs. 200m	100m vs. 200m
Box Plot Visual Differences						
ANOVA- Tamhane's Test						
ANOVA- Dennett's Test						

Imagery Difference	**Berecha (Active)**					
	Feb 2, 2003 (Dry Season)			Aug 8,2010 (Wet Season)		
Small Subset Image	HZ_ROI vs. 100m	HZ_ROI vs. 200m	100m vs. 200m	HZ_ROI vs. 100m	HZ_ROI vs. 200m	100m vs. 200m
Box Plot Visual Differences						
ANOVA Tamhane's Test	*	*				
ANOVA Dennett's Test	*	*				
	Berecha (Active)					
Whole Image	HZ_ROI vs. 100m	HZ_ROI vs. 200m	100m vs. 200m	HZ_ROI vs. 100m	HZ_ROI vs. 200m	100m vs. 200m
Box Plot Visual Differences						
ANOVA- Tamhane's Test		*				
ANOVA- Dennett's Test		*				

Imagery Difference	**Tendaho (Inactive)**					
	Sept 30, 2002 (Wet Season)			Mar 2,2010 (Dry Season)		
Small Subset Image	HZ_ROI vs. 100m	HZ_ROI vs. 200m	100m vs. 200m	HZ_ROI vs. 100m	HZ_ROI vs. 200m	100m vs. 200m
Box Plot Visual Differences						
ANOVA Tamhane's Test						
ANOVA Dennett's Test						
	Tendaho (Inactive)					
Whole Image	HZ_ROI vs. 100m	HZ_ROI vs. 200m	100m vs. 200m	HZ_ROI vs. 100m	HZ_ROI vs. 200m	100m vs. 200m
Box Plot Visual Differences						
ANOVA- Tamhane's Test						
ANOVA- Dennett's Test						

6. DISCUSSION

In this chapter, results from chapter 5 and 6 are discussed in the context of the original research objectives.

6.1. Characterization of Hydrothermal Zones using Mineral Indices.

The objective of Chapter 4 was to assess whether applying mineral indices on ASTER datasets would yield differences in the pixel values between hydrothermal zones and buffered zones for both the active and inactive systems. The results showed that the characterization of active and inactive hydrothermal alterations using band ratios is very difficult. The summary of the results of the 8 band ratios (Table 14) suggest that the use of the said band ratios in achieving its assigned purpose was inconclusive. Some band ratios were found to be efficient in distinguishing between a hydrothermal zone and an adjacent unaltered zone (e.g., 100 m buffer) in an active system (e.g., Kaolinite band ratio for Berecha), but not for an inactive system. Likewise, bands ratios such as silica were able to distinguish the hydrothermal zones from the unaltered buffer zone for Tendaho (inactive system) but not for Berecha. Regardless, there were also major inconsistencies for establishing which band ratios were useful, since the comparison between the visual box-plot and statistical analysis were not matching.

The statistical results also posed another complexity, especially in areas where discrimination was apparently difficult, as evidenced by the box plots where values of an ROI and a 100 m area were visually the same. The ANOVA test may, at certain instances, suggest that these two areas are statistically different at a 95% level of significance, despite hardly noticeable difference in the box plot. This was attributed to the fact that statistical tests such as the ANOVA post-hoc takes into account not only the means, but also the variance in the unequal sample size that it is analyzing. For example, for Tendaho the discrimination for several band ratios (e.g. Silica) illustrate no differences visually but the statistical test explains the hydrothermal zones and the buffer zones are statistically significant. Still, when looking back to the box plot it was clear that the number of outliers had numerically defined the test to be significant, while the visual observations showed no discrimination. In this circumstance, it would be best to accept the visual interpretation since methodological framework was designed by known occurrences of hydrothermal alterations and its surrounding. The results suggest that certain band ratios are ideal for discriminating between hydrothermal zones and unaltered zones in certain systems, but such results would need to be further investigated for clarification.

Many concerns have risen regarding the proper selection of mineral indices for discrimination between altered and unaltered rock. One factor is the selection of the buffer zones and if the buffers were optimally selected for discriminating between altered and unaltered rock.

From literature, it is known that these hydrothermal systems are much localized but are also scale dependent (Elder, 1981). Buffer zones of 100 meter and 200 m were selected in an unbiased manner. However, these sizes may not be sufficient for discriminating between altered and unaltered zones. For example, the results from the Alunite/Kaolonite/Porphyllite band ratio suggest that the buffer zones may still be actually be part of the designated hydrothermal zone. Determining the size of so-called localized alteration zones is unclear, much more the determination of the start of unaltered rock.

For the case of Berecha, the study area is situated in an active area beside a lake, where active hydrothermal alterations are occurring. But to truly discriminate in an "unbiased" manner, it would better to select several study sites in Berecha and test if the mineral indices show similar patterns. This also opens the idea of examining if possible classifications might be needed, if several study sites tend to show different mineral characteristic within an active system. This will also follow the same framework for differentiating inactive systems.

6.2. Issues of Sensitivity of Band Ratios and Methodological Framework

Using band ratios for the discrimination between altered and unaltered zones poses a lot of difficulties that further pose problems when reconciling the characterization of active and inactive systems. One issue is the "sensitivity" of band ratios to differences in seasonality, active and inactive systems, and to the selected regions (for altered and unaltered areas). This sensitivity issue was also evident in the statistical results, wherein differences were seemingly found for areas that visually, were clearly similar. This has to do with the outliers affecting the statistical significance for discrimination. In this case, the box plot illustrates a better representation of the true geological scenario, since the hydrothermal zones were selected from known sites.

Another concern was the standard AST_07XT data products used to compute the band ratios. Mars and Rowan (2010) have stated that the AST_07XT radiative transfer model was inaccurate, there is a wide spectral variation in the SWIR. The authors also addressed the concern for the low band 5 reflectance's in the AST_07XT, which affect the discrimination for minerals like alunite. Mars and Rowan (2010) then suggested the use of ASTER Refl1b data as this was more consistent and spectrally more correct than the AST_07XT. Since the latter was used for this study, the spectral discrimination between minerals such as alunite and kaolinite was not possible without proper spectral calibration. As a consequence, the results from band ratios could be inaccurate as the pixel values from the SWIR were higher than normal at values around 2.0 μm.

Another concern is the framework for which discrimination was implemented. Only one sample study area was essentially used for both the active and inactive areas. Since the statistical tests are being sampled for different ratios, the concern is on the accuracy, let alone, the appropriateness of using one sample to represent for both active and inactive sites. Ideally, it would not be significant to conduct statistical tests under one site over numerous band ratios to accurately characterize a region. In the statistical context, this is a case of over-parameterizing, wherein one dependent variable (1 ROI = 1 sample) is being tested with numerous independent variables (which in this case, are the pixel values resulting from the band ratios). It is difficult to be convinced that the results gained from Mount Berecha can be conclusive for all other active hydrothermal systems; and the same premise goes for Tendaho for other inactive systems.

6.3. Characterization of Hydrothermal Zones using Night-time TIR and its Sensitivity

The objective was to assess whether applying corrected night-time images available with ASTER datasets would yield differences in surface temperatures between hydrothermal zones and unaltered zones for both the active and inactive systems. The results had shown that characterization is very sensitive to seasonalities for an active region (Berecha). The active hydrothermal zones shows some contrast during the dry season but is hindered during the wet season. For areas with contrast the box plot visualizations did not seem to agree with their statistical equivalents. This is particularly exemplified between the hydrothermal zone and the buffer zones for both the 1st and 2nd polynomial fits. For the case of Tendaho, the results showed no observable temperature contrasts between altered and unaltered zones. This is expected, since this is an area where there is very little enthalpy from a system that has been inactive. In conclusion, active and inactive hydrothermal zones can be differentiated using night-time TIR. However, for the active regions, two aspects need to be taken into account for discrimination.

The first aspect is that discrimination is largely dependent on the regression fitted to the image. The sensitivity is highly dependent on the regression fitted by the *user*. In this case for the 1st polynomial fit of Berecha at Feb 2, 2003, the visual distinction between the hydrothermal zone and the 100m buffer zone is not clear, but can be characterized between the 200m. What this suggests is the imprint of the surface temperature for an active system is larger, when compared to the hydrothermal zone outlined in the framework. For the case of a 2nd polynomial fit of Feb 2, 2003, the results show no visual difference between the box plot but the statistical results showed otherwise, due to outliers in both the 100m and 200m buffer zones. Overall, the sensitivity to different regression fits can hinder the conclusion of differentiation for active systems from inactive hydrothermal zones. Furthermore is the user-dependent selection of the proper fit, which is subjective.

The second circumstance is the sensitivity of discrimination between a small subset versus the entire image. Small image subsets yield better discrimination for active hydrothermal alterations. Moreover, working with entire images may hamper proper discrimination of active systems, due to the effects of diurnal heating on a large scale. For the Ethiopian Rift, a large area may also be largely influenced by the differential cooling rate of various lithology (sediments).

6.4. Optimal Method for correcting night-time TIR

Producing an optimal framework for correcting images was a very difficult task. Preferably working with images as a whole would be better with the justification that the masking out of large thermal anomalies such as water bodies, hot springs and correcting for the differential cooling for the various lithology in the Ethiopian Rift can be done for a large area. This was clear when investigating the difference between working with a mask subset as compared to the entire image. The mask subset images showed better discrimination between the active and inactive zones. However, selecting various seasons for correction is an excellent means for comparing differences in the image to and to suggest if a region is active or inactive. Again, it is important to note that the different regression fits can also be heavily affected by seasons. It was clear from section 6.3 that different fits can influence the sensitivity for an active system but more importantly, these can hinder the interpretation of an unknown area between active and inactive regions. It is apparent from a known hydrothermal framework that sensitivity is erratic to different polynomial fits. Basically, the different regression techniques can affect the sensitivity of the thermal images, and as a result can affect the discrimination between active and inactive zones.

7. CONCLUSION AND RECOMMENDATIONS

In this research the characterization of active and inactive hydrothermal alteration systems was studied using band ratios and corrected night-time TIR images. The results from the application of band ratios on both inactive and active zones and in different seasonality were inconclusive. Band ratio values were unusually high for AST_07XT images. The sensitivity issue was also reflected in the results of the statistical tests: statistical differences were found for areas that were visually similar in the box plots, and this was due to the outliers in the data.

Working with night-time imagery had also illustrated sensitivity to polynomial fits. Any chosen polynomial fit, which is user defined, results in different interpretation of active zones. For inactive zones, however, the polynomial fitting did not affect the discrimination, but this is expected since this is a region that is inactive.

Nevertheless, the study gave insight into the scale of temperature gradients, which are not localized to hydrothermal zones only, but actually have larger imprints that also influence other areas (active and inactive) in the Ethiopian Rift Valley system.

7.1. Recommendations

Based on the results and issues discussed in this research, certain precautious should be kept in mind when attempting characterization of active and inactive hydrothermal systems. The following points are recommended:

- Use of mineral band ratios and ANOVA Post Hoc tests or other statistical tests
- Select more than one sample site for both active and inactive regions in order to properly characterize active and inactive hydrothermal zones.
- The use of AST_07XT data is not recommended, rather, the use of ReL1b data (see Mars & Rowan, 2010) for the corrected spectra
- Create several ROI and buffer zones for active and inactive zones; use the corrected thermal images to see if discrimination is possible.
- Look at the profiles of the corrected surface temperature images and establish possible markers for active and inactive zones
- Test the accuracy of the characterizations of active and inactive regions by applying it to an entire (larger) image.

LIST OF REFERENCES

Abrams, M. J., Ashley, R. P., Rowan, L. C., Goetz, A. F. H., & Kahle, A. B. (1977). Mapping of hydrothermal alteration in the Cuprite mining district, Nevada, using aircraft scanner images for the spectral region 0.46 to 2.36μm. *Geology, 5*(12), 713-718. doi: 10.1130/0091-7613(1977)5<713:mohait>2.0.co;2

Ayele, A., Teklemariam, M., & Kebede, S. (2002). Geothermal Resource Exploration in The Abaya and Tulu Moye-Gedemsa Geothermal Prospects, Main Ethiopian Rift (H.-E. G. a. G. Department, Trans.): Geological Survey of Ethiopia.

Berhanu, G. (2008). Geothermal Exploration and Development in Ethiopia *Geothermal Training Programme*. Reykjavik, Iceland: United Nations University.

Carranza, E. J. M., & Hale, M. (2002). Mineral imaging with Landsat Thematic Mapper data for hydrothermal alteration mapping in heavily vegetated terrane. *International Journal of Remote Sensing, 23*(22), 4827-4852. doi: 10.1080/01431160110115014

Denton, J. C. (1972). *Geothermal energy : a national proposal for geothermal resources research : final report of the geothermal resources research conference, 18 - 20 September, Seattle, Washington*. . University of Alaska.

Elder, J. (1981). *Geothermal systems*. London etc.: Academic Press.

Electroconsult, E. (1986). Exploration of Aluto-Langano Geothermal Resources, feasibility report *Geothermal Exploration Project*: Ethiopian Institue of Geological Survey.

Gebregziabher, Z. (1998). Geology and hydrothermal alteration in wells TD-5 and TD-6, Tendaho geotheraml field, Ethiopia. *Geothermal Training Programme*. Reykjavik, Iceland: The United Nations University.

Gianelli, G., Mekuria, N., Battaglia, S., Chersicla, A., Garofalo, P., Ruggieri, G., . . . Gebregziabher, Z. (1998). Water–rock interaction and hydrothermal mineral equilibria in the Tendaho geothermal system. *Journal of Volcanology and Geothermal Research, 86*(1–4), 253-276. doi: http://dx.doi.org/10.1016/S0377-0273(98)00073-0

Heasler, H. R., Jaworowski, C., & Foley, D. (2009). *Geothermal System and monitoring hydrothermal features*. Colorado: Geological Society of America.

Hemley, J. J., Cygan, G. L., Fein, J. B., Robinson, G. R., & d'Angelo, W. M. (1992). Hydrothermal ore-forming processes in the light of studies in rock-buffered systems; I, Iron-copper-zinc-lead sulfide solubility relations. *Economic Geology, 87*(1), 1-22. doi: 10.2113/gsecongeo.87.1.1

Jones, K. L., Schulenburg, N. W., & Wright, C. (2010). Hyperspectral remote sensing techniques for locating geothermal areas. 76870J-76870J. doi: 10.1117/12.855444

Kebede, S. (2011). Status of geothermal exploration and development in Ethiopia. In U. N. U. G. T. Programme (Ed.). Geological Survey of Ethiopia.

Lagat, J. (2009). Hydrothermal Alteration Mineralogy in Geothermal Fields with case examples from Olkaria Domes Geothermal Field, Kenya. In U. N. U. G. T. Programme (Ed.), (Vol. 1). Geological Survey of Ethiopia.

Lillesand, T. M., Kiefer, R. W., & Chipman, J. W. (Eds.). (2004). *Remote sensing and image interpretation* (5th ed.). New York, NY: Wiley & Sons.

Mars, J. C., & Rowan, L. C. (2010). Spectral assessment of new ASTER SWIR surface reflectance data products for spectroscopic mapping of rocks and minerals. *Remote Sensing of Environment, 114*(9), 2011-2025. doi: http://dx.doi.org/10.1016/j.rse.2010.04.008

Martini, B. A., Cocks, T. D., Cocks, P. A., & Pickles, W. L. (2004, 20-24 Sept. 2004). *Operational airborne hyperspectral remote sensing for global geothermal exploration*. Paper presented at the Geoscience and Remote Sensing Symposium, 2004. IGARSS '04. Proceedings. 2004 IEEE International.

Oluwadebi, A. G. (2011). *Characterization of hydrothermal alteration in mount Berecha area of main Ethiopian rift using hyperspectral data*. University of Twente Faculty of Geo-Information and Earth Observation (ITC), Enschede. Retrieved from http://www.itc.nl/library/papers_2011/msc/aes/oluwadebi.pdf

Omenda, P. A. (2005). The Geology and Geothermal Activity of the East African Rift System. In U.-G. a. KengGen (Ed.), *Workshop for Decision Makers on Geothermal Projects Management*. Kenya.

Prianjo, F. (2009). *Hydrothermal processes and mineral systems : e-book*. Dordrecht: Springer
Geological Survey of Western Australia.

Rajesh, H. M. (2004). Application of remote sensing and GIS in mineral resource mapping - An overview. *Journal of Mineralogical and Petrological Sciences, 99*(3), 83-103.

Rowan, L. C., Hook, S. J., Abrams, M. J., & Mars, J. C. (2003). Mapping hydrothermally altered rocks at Cuprite, Nevada, using the advanced spaceborne thermal emission and reflection radiometer (Aster), a new satellite-imaging system. *Economic Geology, 98*(5), 1019-1027.
Simmons, S. F., & Browne, P. R. L. (2000). Hydrothermal Minerals and Precious Metals in the Broadlands-Ohaaki Geothermal System: Implications for Understanding Low-Sulfidation Epithermal Environments. *Economic Geology, 95*(5), 971-999.
SPSS. (2013). Anova Post Hoc Test (Version 17): IBM. Retrieved from http://publib.boulder.ibm.com/infocenter/spssstat/v20r0m0/index.jsp?topic=%2Fcom.ibm.spss.statistics.help%2Fovervw_auto_0.htm
Stratex International. (2012). Megenta, Tendaho, 2012, from http://www.stratexinternational.com/operations/exploration/ethiopia-djibouti/afar-project/tendaho.aspx
Teum, T. (2013). Ethiopian Tresures- Climate Retrieved January 13,2013, 2013, from http://www.ethiopiantreasures.co.uk/pages/climate.htm
Tucker, M. R., & Pedgley, D. E. (1977). Summer winds around the southern Red Sea. *Archiv für Meteorologie, Geophysik und Bioklimatologie, Serie B, 25*(3), 221-231. doi: 10.1007/bf02243054
Ulusoy, İ., Labazuy, P., & Aydar, E. (2012). STcorr: An IDL code for image based normalization of lapse rate and illumination effects on nighttime TIR imagery. *Computers & Geosciences, 43*(0), 63-72. doi: http://dx.doi.org/10.1016/j.cageo.2012.02.012
Van der Meer, F. D., van der Werff, H. M. A., van Ruitenbeek, F. J. A., Hecker, C. A., Bakker, W. H., Noomen, M. F., . . . Woldai, T. (2012). Multi- and hyperspectral geologic remote sensing: A review. *International Journal of Applied Earth Observation and Geoinformation, 14*(1), 112-128. doi: http://dx.doi.org/10.1016/j.jag.2011.08.002
White, D. E. (1974). Diverse Origins of Hydrothermal Ore Fluids. *Economic Geology, 69*(6), 954-973.
Yang, K., Huntington, J. F., Boardman, J. W., & Mason, P. (1999). Mapping hydrothermal alteration in the Comstock mining district, Nevada, using simulated satellite-borne hyperspectral data. *Australian Journal of Earth Sciences, 46*(6), 915-922. doi: 10.1046/j.1440-0952.1999.00754.x

8. APPENDICES A

Berecha- Carbonate Mafic Minerals

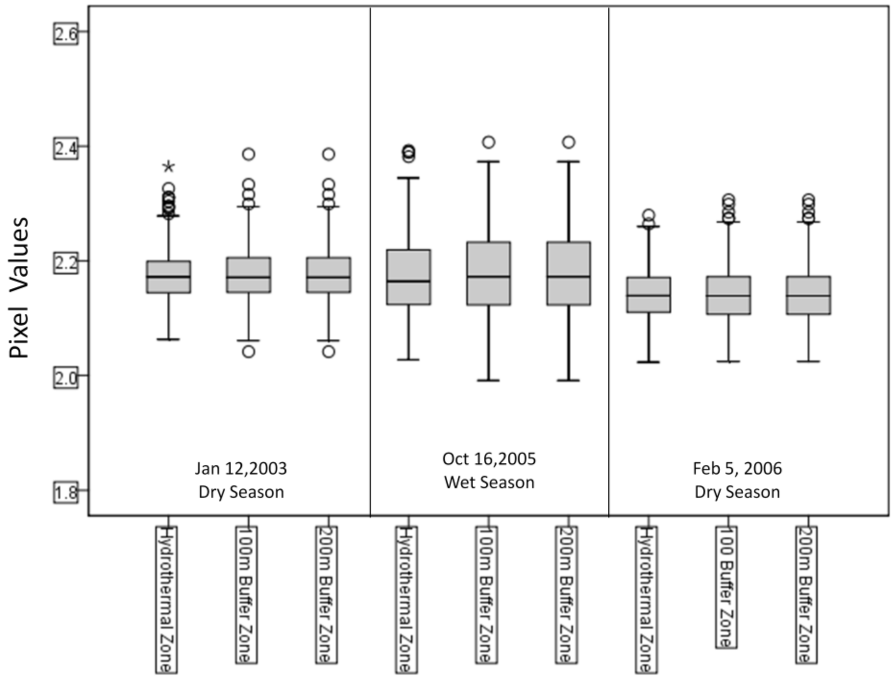

Tendaho- Carbonate Mafic Minerals

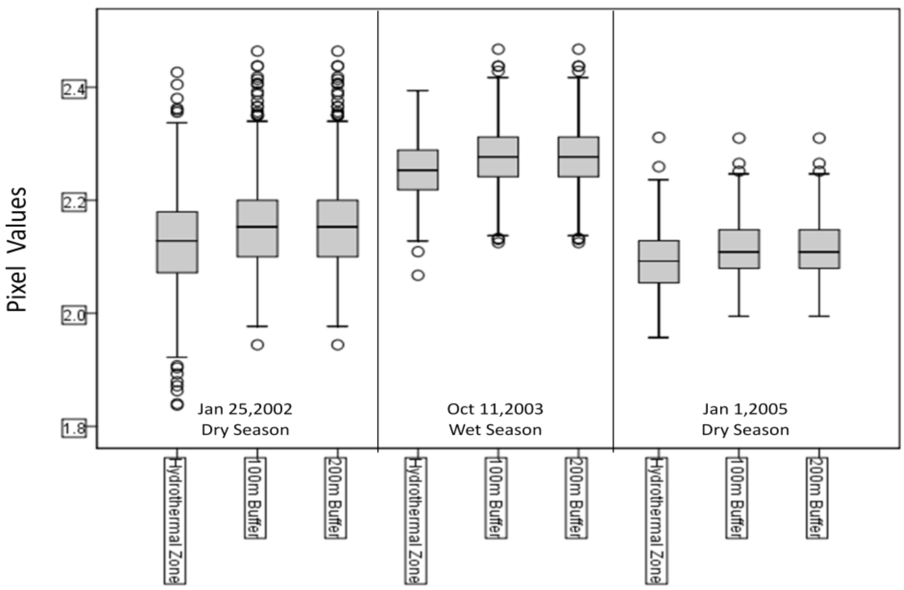

Berecha- Sericite, Muscovite, Illite, Smectite

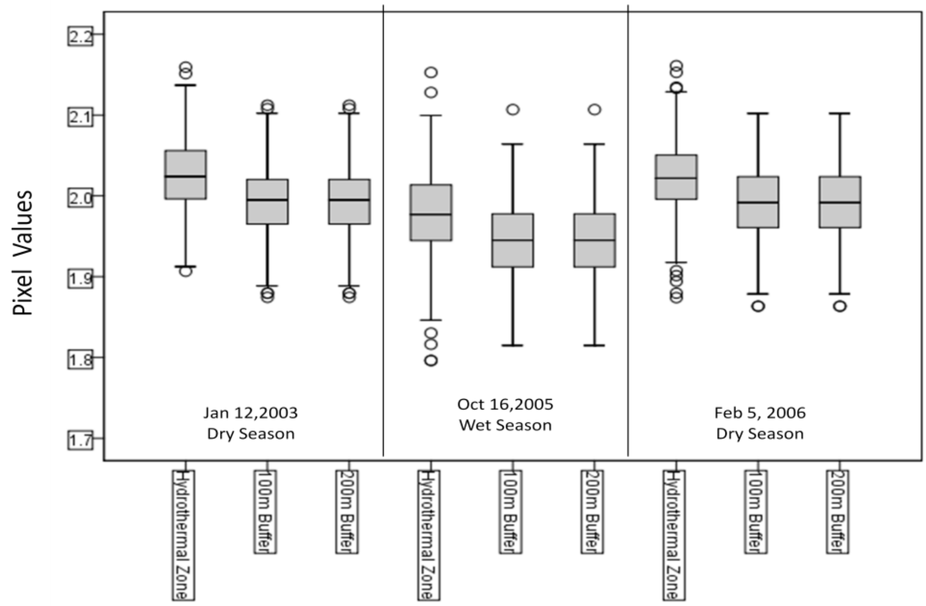

Tendaho- Sericite, Muscovite, Illite, Smectite

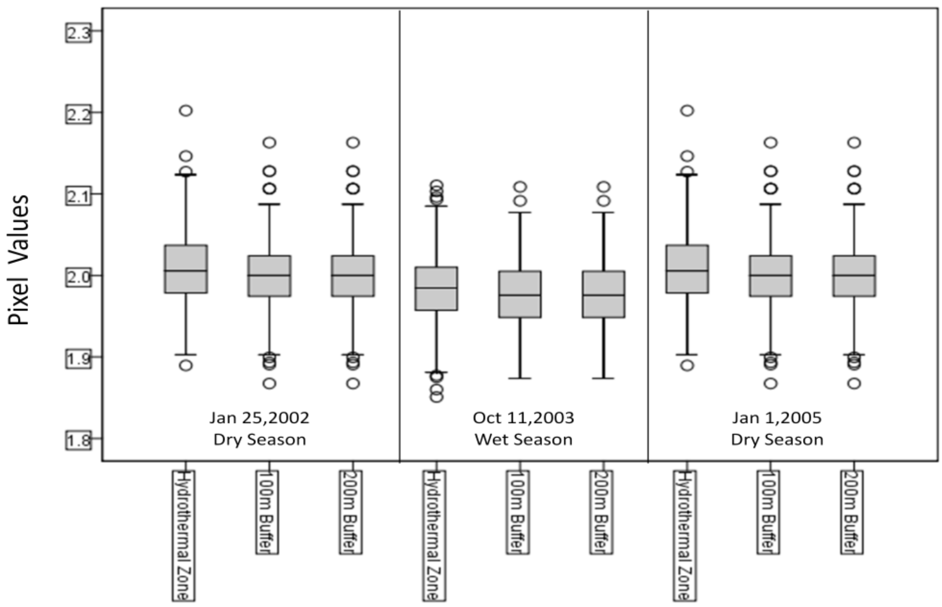

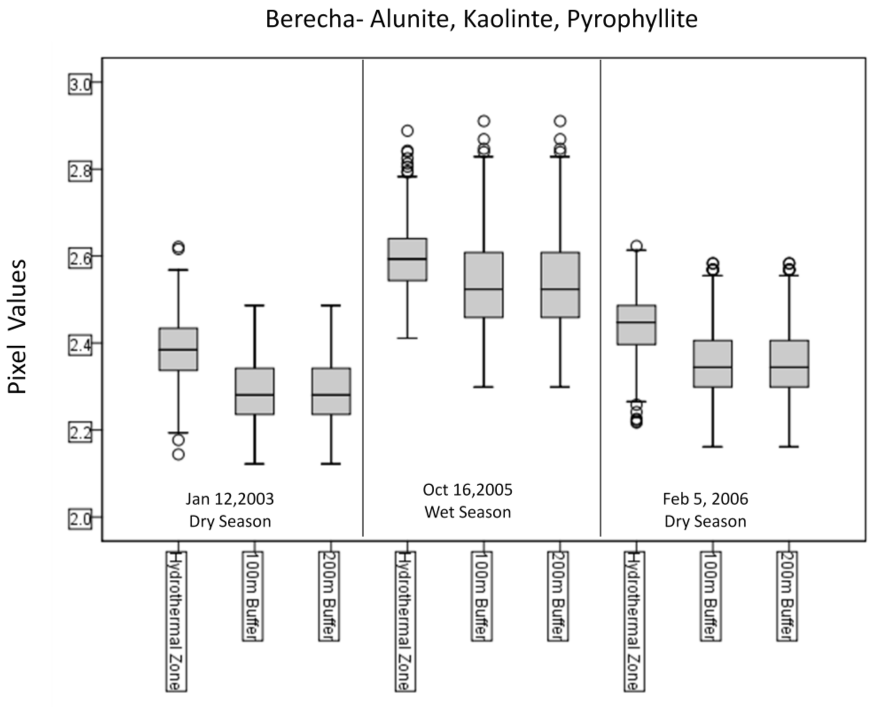
Berecha- Alunite, Kaolinte, Pyrophyllite
Pixel Values
3.0
2.8
2.6
2.4
2.2
2.0
Jan 12,2003
Dry Season
Oct 16,2005
Wet Season
Feb 5, 2006
Dry Season
Hydrothermal Zone
100m Buffer
200m Buffer
Hydrothermal Zone
100m Buffer
200m Buffer
Hydrothermal Zone
100m Buffer
200m Buffer

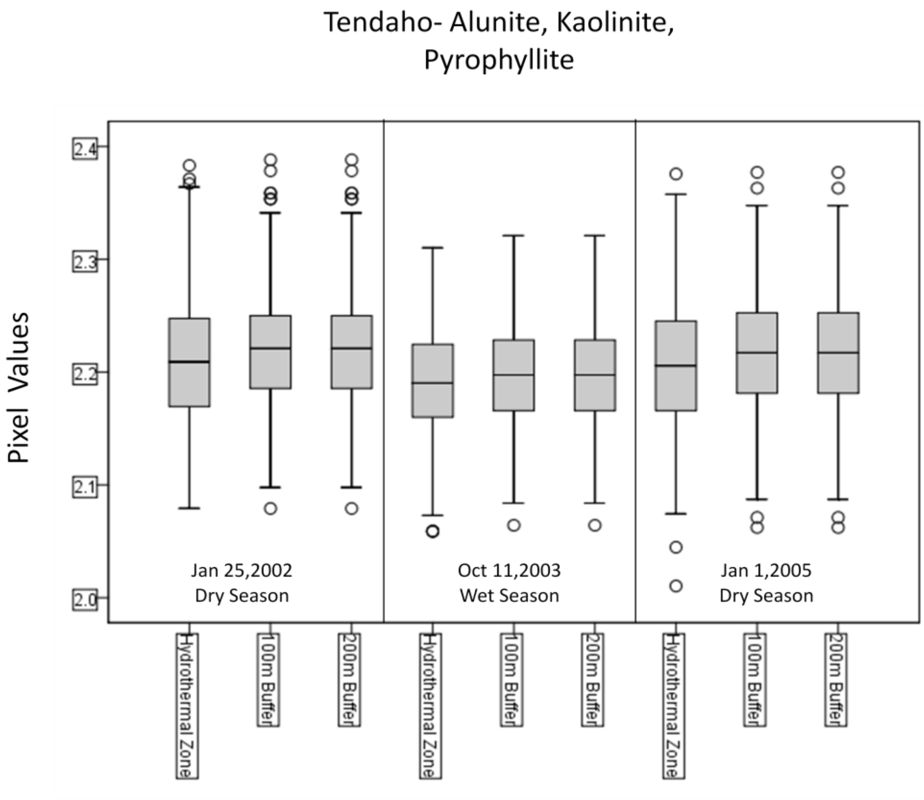
Tendaho- Alunite, Kaolinite,
Pyrophyllite
Pixel Values
2.4
2.3
2.2
2.1
2.0
Jan 25,2002
Dry Season
Oct 11,2003
Wet Season
Jan 1,2005
Dry Season
Hydrothermal Zone
100m Buffer
200m Buffer
Hydrothermal Zone
100m Buffer
200m Buffer
Hydrothermal Zone
100m Buffer
200m Buffer

Berecha- Kaolinite

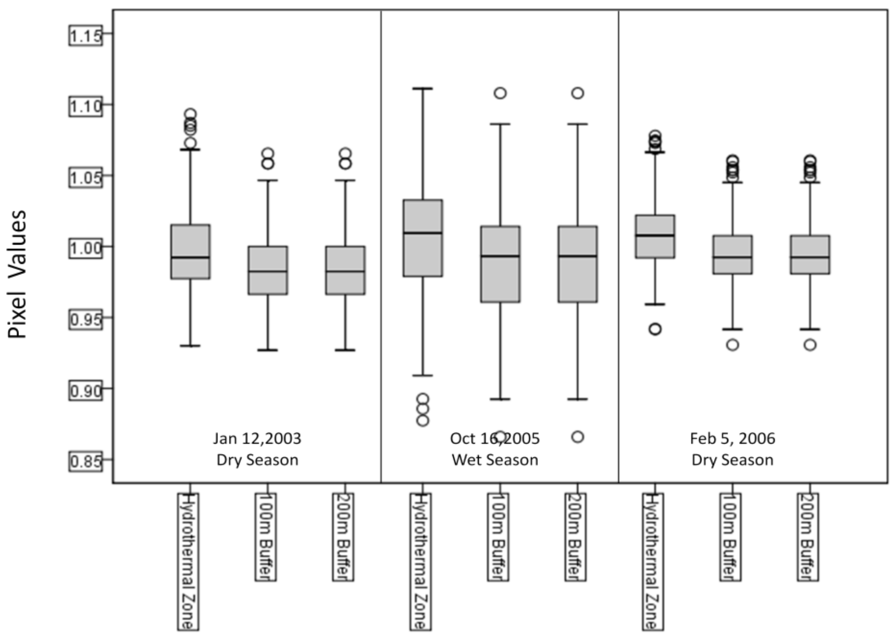

Tendaho- Kaolinite

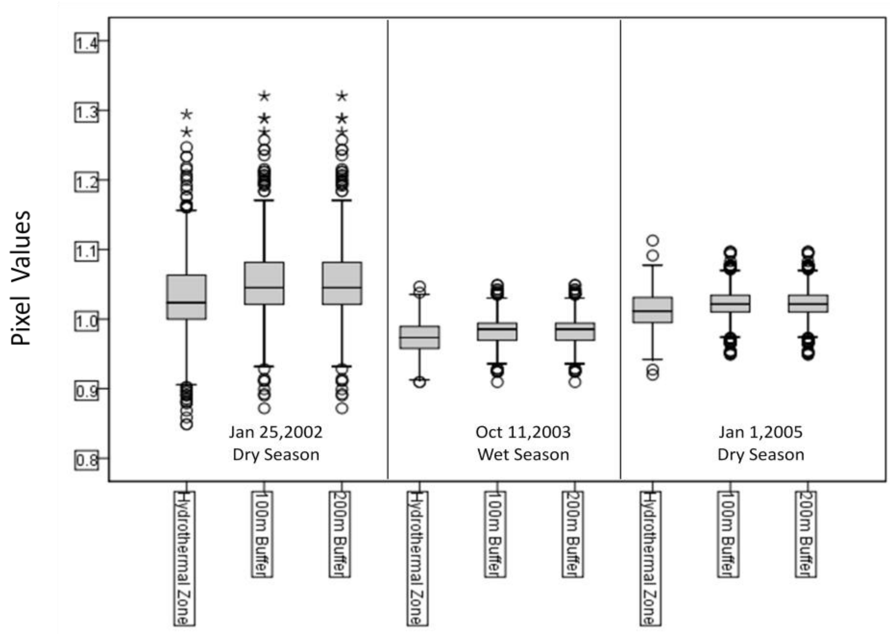

Berecha- Alteration

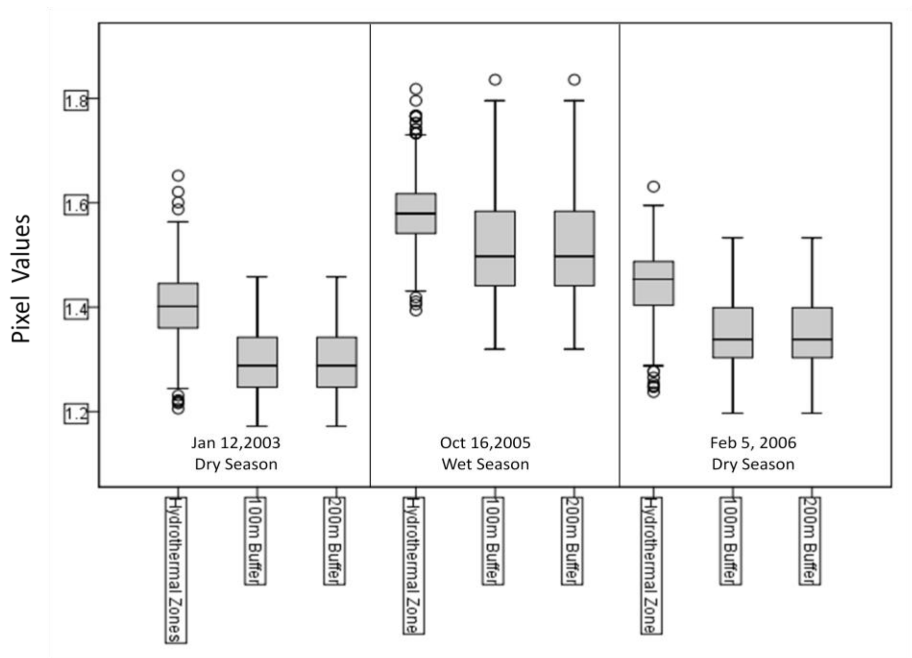

Tendaho- Alteration

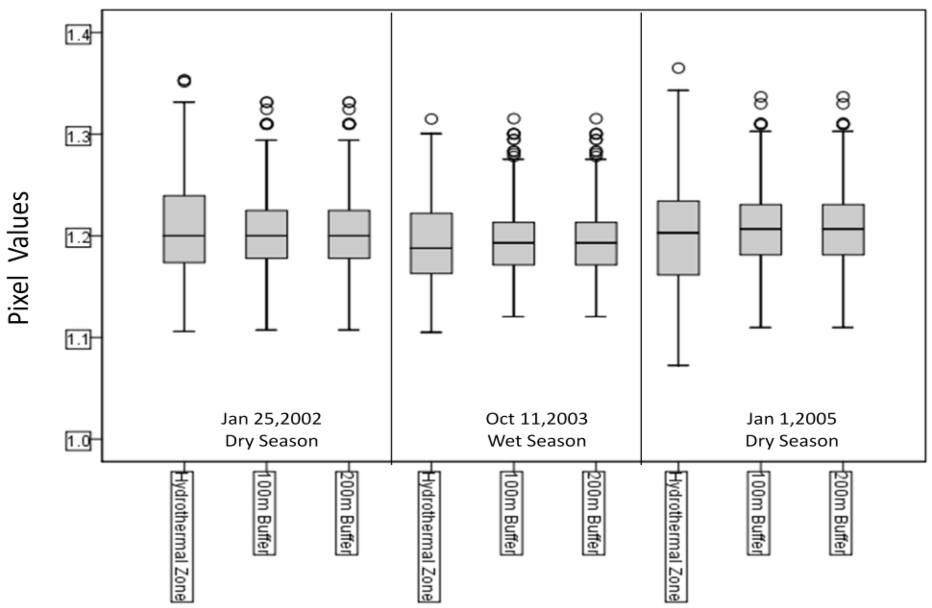

Silica 11/10

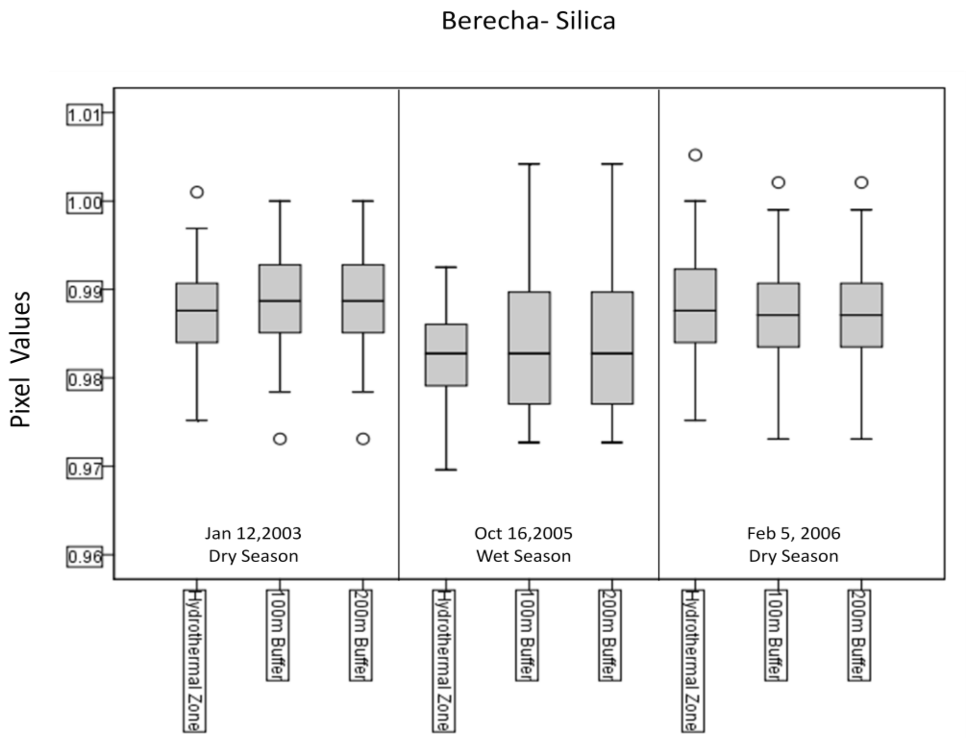
Berecha- Silica
Pixel Values
1.01
1.00
0.99
0.98
0.97
0.96
Jan 12,2003
Dry Season
Oct 16,2005
Wet Season
Feb 5, 2006
Dry Season
Hydrothermal Zone
100m Buffer
200m Buffer
Hydrothermal Zone
100m Buffer
200m Buffer
Hydrothermal Zone
100m Buffer
200m Buffer

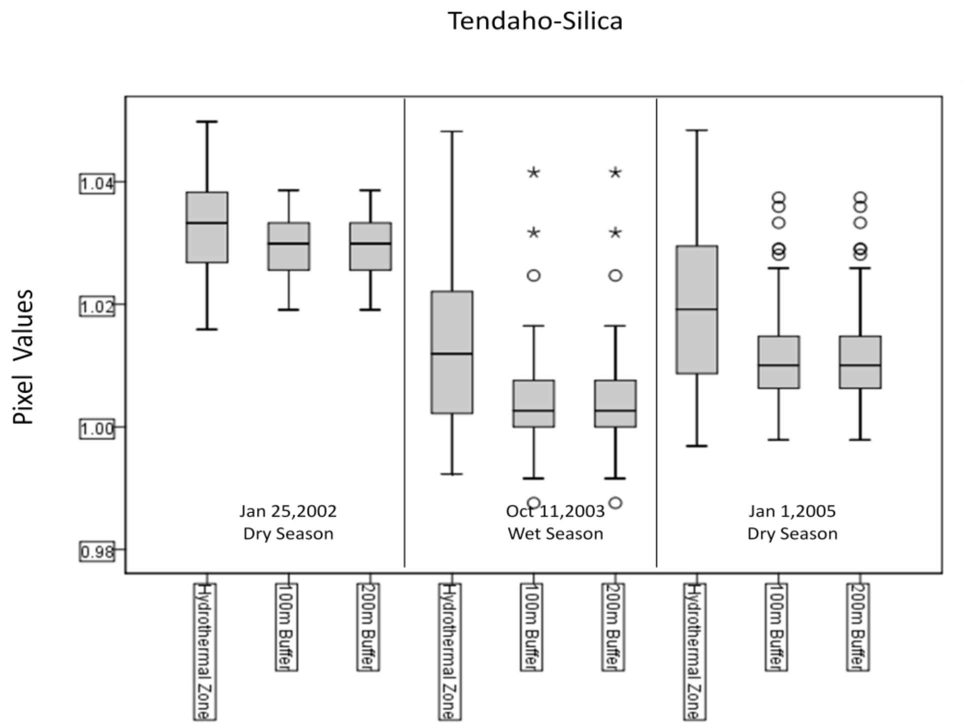
Tendaho-Silica
Pixel Values
1.04
1.02
1.00
0.98
Jan 25,2002
Dry Season
Oct 11,2003
Wet Season
Jan 1,2005
Dry Season
Hydrothermal Zone
100m Buffer
200m Buffer
Hydrothermal Zone
100m Buffer
200m Buffer
Hydrothermal Zone
100m Buffer
200m Buffer

Silica 11/12

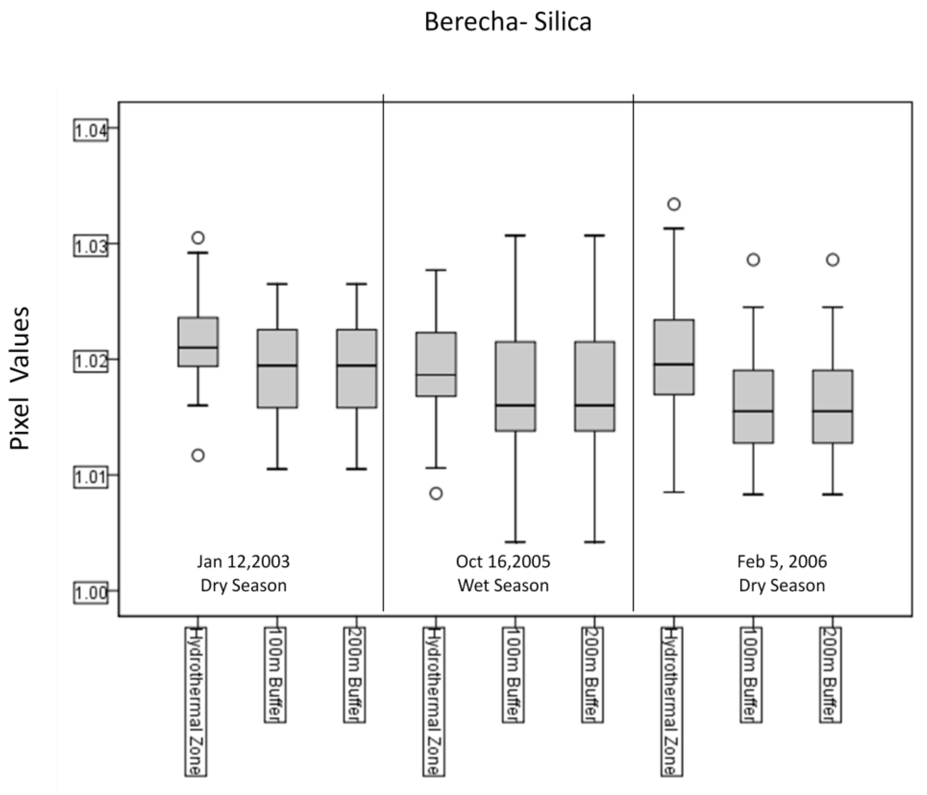
Berecha- Silica
Pixel Values
1.04
1.03
1.02
1.01
1.00
Jan 12,2003
Dry Season
Oct 16,2005
Wet Season
Feb 5, 2006
Dry Season
Hydrothermal Zone
100m Buffer
200m Buffer
Hydrothermal Zone
100m Buffer
200m Buffer
Hydrothermal Zone
100m Buffer
200m Buffer

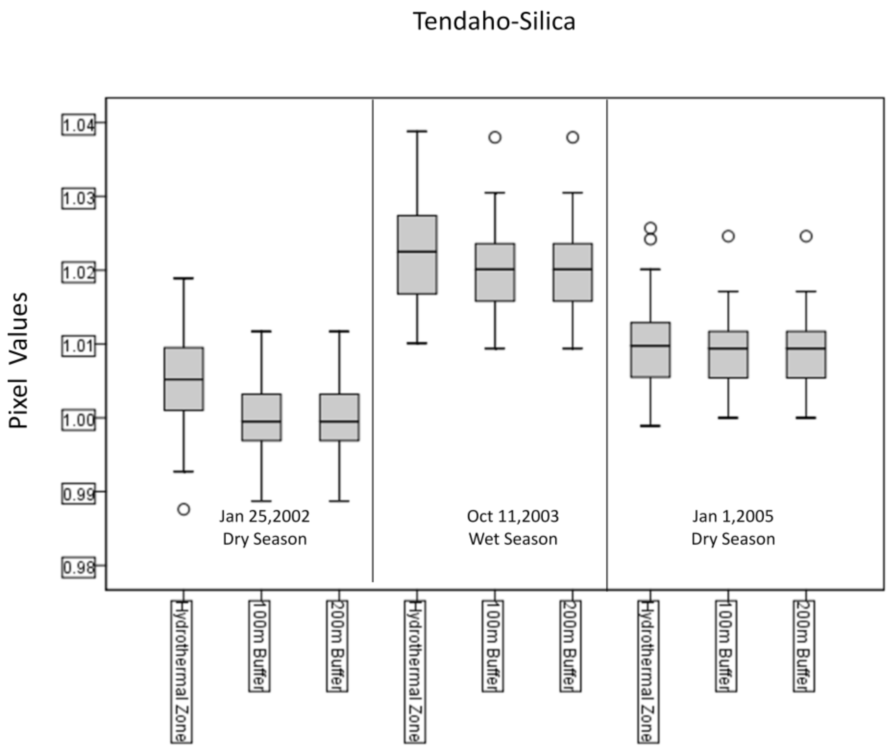
Tendaho-Silica
Pixel Values
1.04
1.03
1.02
1.01
1.00
0.99
0.98
Jan 25,2002
Dry Season
Oct 11,2003
Wet Season
Jan 1,2005
Dry Season
Hydrothermal Zone
100m Buffer
200m Buffer
Hydrothermal Zone
100m Buffer
200m Buffer
Hydrothermal Zone
100m Buffer
200m Buffer

Silica 13/10

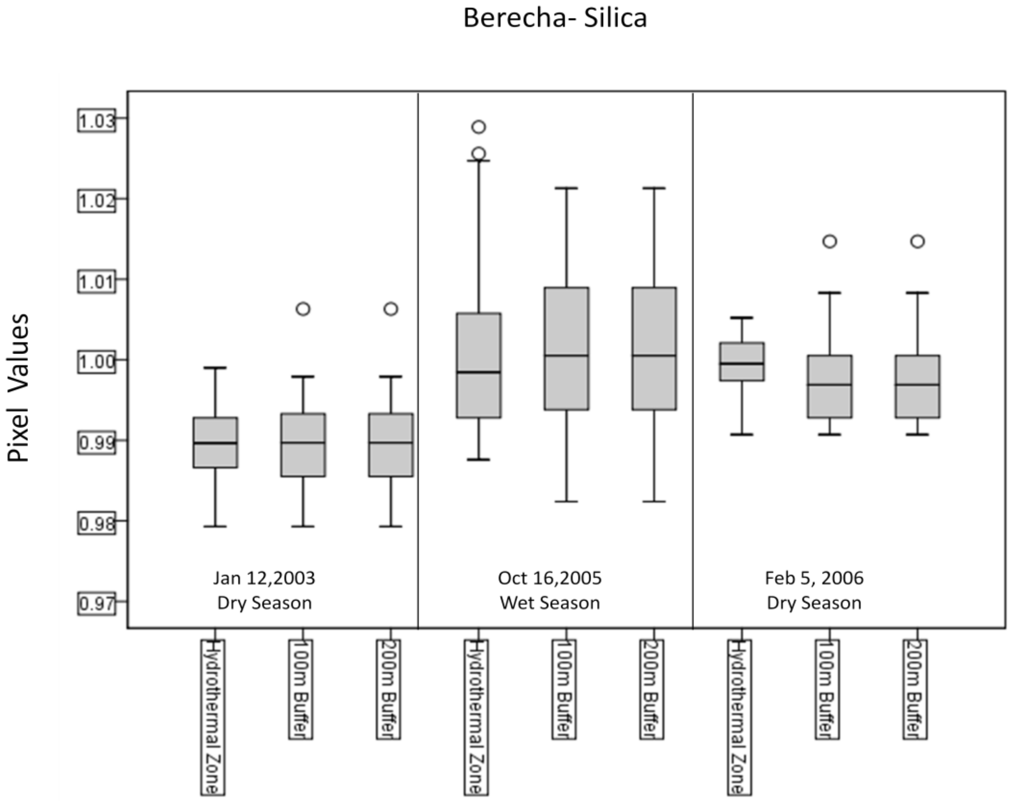
Berecha- Silica
Pixel Values
1.03
1.02
1.01
1.00
0.99
0.98
0.97
Jan 12,2003
Dry Season
Oct 16,2005
Wet Season
Feb 5, 2006
Dry Season
Hydrothermal Zone
100m Buffer
200m Buffer
Hydrothermal Zone
100m Buffer
200m Buffer
Hydrothermal Zone
100m Buffer
200m Buffer

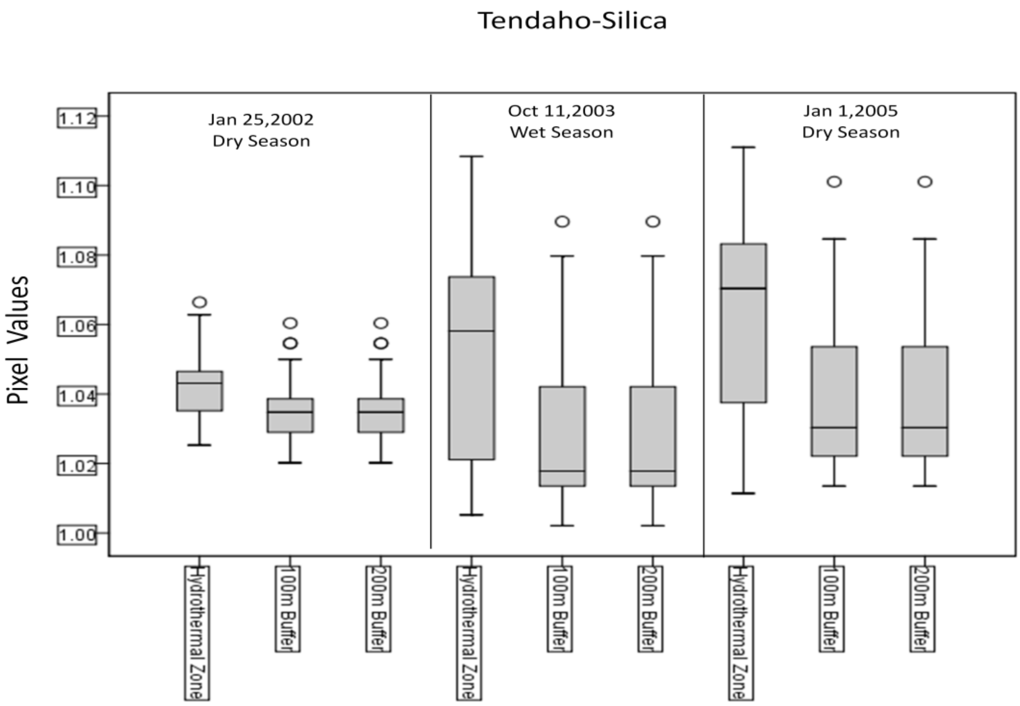
Tendaho-Silica
Pixel Values
1.12
1.10
1.08
1.06
1.04
1.02
1.00
Jan 25,2002
Dry Season
Oct 11,2003
Wet Season
Jan 1,2005
Dry Season
Hydrothermal Zone
100m Buffer
200m Buffer
Hydrothermal Zone
100m Buffer
200m Buffer
Hydrothermal Zone
100m Buffer
200m Buffer

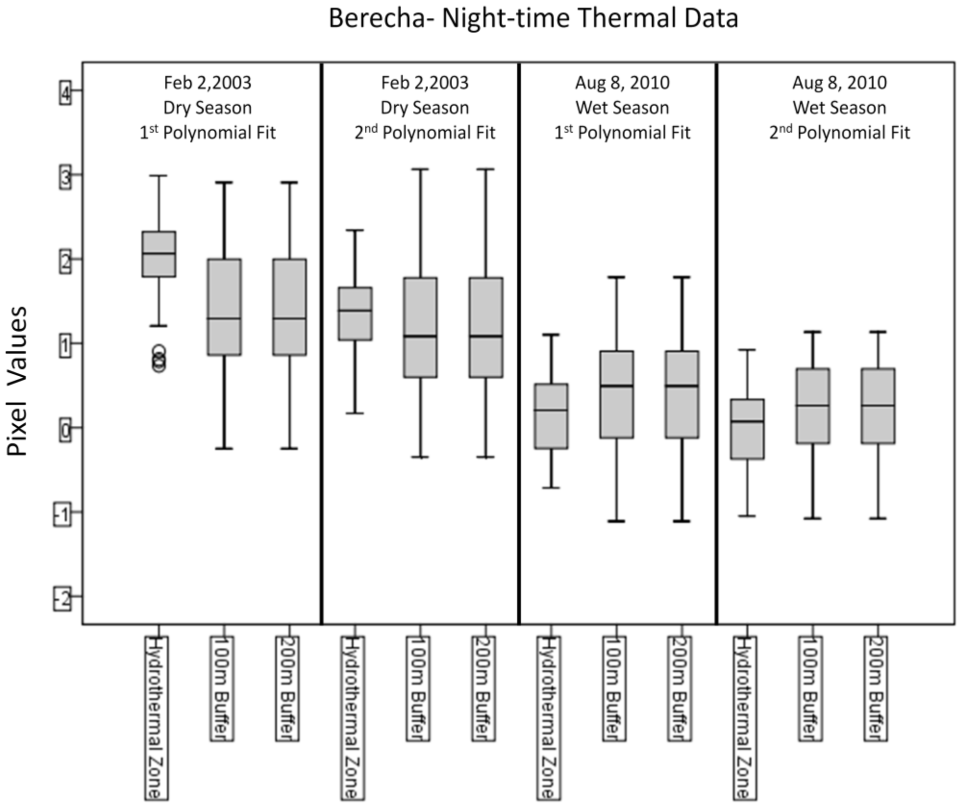
Berecha- Night-time Thermal Data
Pixel Values
4
3
2
1
0
-1
-2
Feb 2,2003
Dry Season
1st Polynomial Fit
Feb 2,2003
Dry Season
2nd Polynomial Fit
Aug 8, 2010
Wet Season
1st Polynomial Fit
Aug 8, 2010
Wet Season
2nd Polynomial Fit
Hydrothermal Zone
100m Buffer
200m Buffer
Hydrothermal Zone
100m Buffer
200m Buffer
Hydrothermal Zone
100m Buffer
200m Buffer
Hydrothermal Zone
100m Buffer
200m Buffer

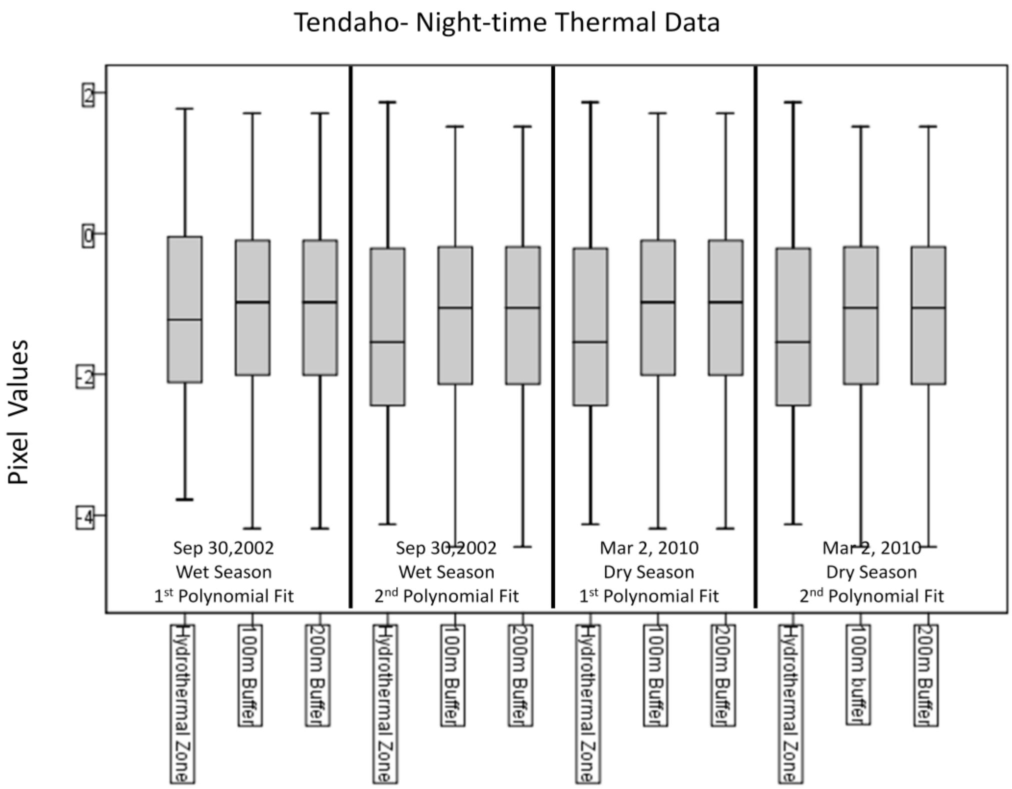
Tendaho- Night-time Thermal Data
Pixel Values
2
0
-2
-4
Sep 30,2002
Wet Season
1st Polynomial Fit
Sep 30,2002
Wet Season
2nd Polynomial Fit
Mar 2, 2010
Dry Season
1st Polynomial Fit
Mar 2, 2010
Dry Season
2nd Polynomial Fit
Hydrothermal Zone
100m Buffer
200m Buffer
Hydrothermal Zone
100m Buffer
200m Buffer
Hydrothermal Zone
100m Buffer
200m Buffer
Hydrothermal Zone
100m buffer
200m Buffer

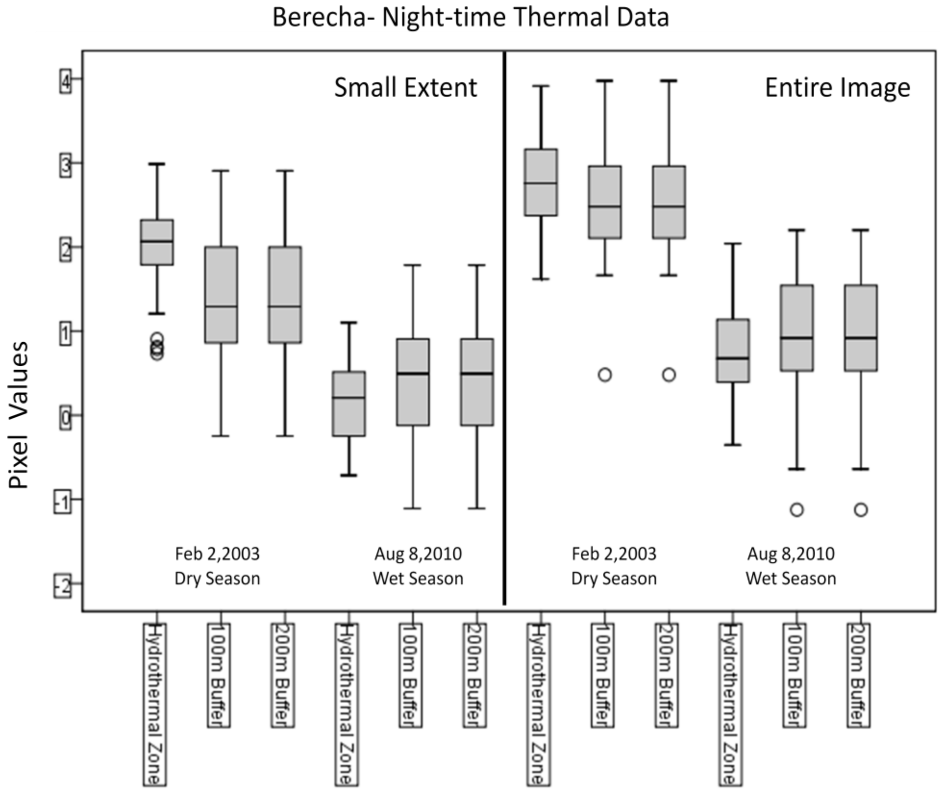
Berecha- Night-time Thermal Data
Small Extent
Entire Image
Pixel Values
4
3
2
1
0
-1
-2
Feb 2,2003
Dry Season
Aug 8,2010
Wet Season
Feb 2,2003
Dry Season
Aug 8,2010
Wet Season
Hydrothermal Zone
100m Buffer
200m Buffer
Hydrothermal Zone
100m Buffer
200m Buffer
Hydrothermal Zone
100m Buffer
200m Buffer
Hydrothermal Zone
100m Buffer
200m Buffer

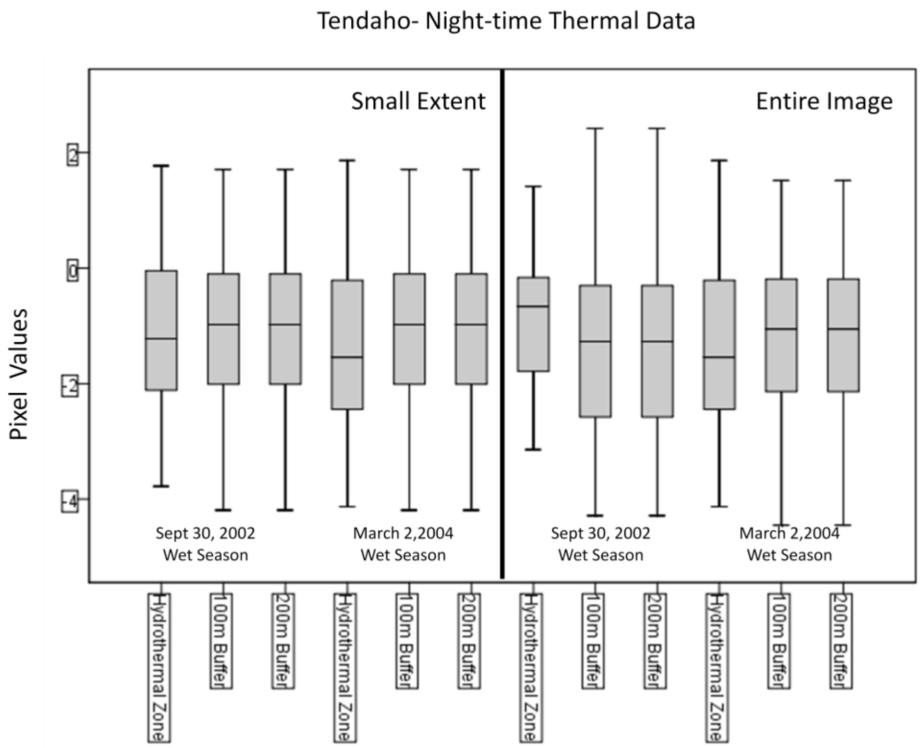
Tendaho- Night-time Thermal Data
Small Extent
Entire Image
Pixel Values
2
0
-2
-4
Sept 30, 2002
Wet Season
March 2,2004
Wet Season
Sept 30, 2002
Wet Season
March 2,2004
Wet Season
Hydrothermal Zone
100m Buffer
200m Buffer
Hydrothermal Zone
100m Buffer
200m Buffer
Hydrothermal Zone
100m Buffer
200m Buffer
Hydrothermal Zone
100m Buffer
200m Buffer

9. APPENDICES B

Berecha Carbonate

Carbonate (Jan 12, 2003)

Case Processing Summary

	HZ_Zones	Valid N	Valid Percent	Missing N	Missing Percent	Total N	Total Percent
Pixel_Values	Hydrothermal Zones ROI	808	100.0%	0	.0%	808	100.0%
	100m Buffer from Hydrothermal Zone ROI	413	100.0%	0	.0%	413	100.0%
	100m and 200m Buffer from Hydrothermal Zone ROI	903	100.0%	0	.0%	903	100.0%

ANOVA

Pixel_Values

	Sum of Squares	df	Mean Square	F	Sig.
Between Groups	.012	2	.006	2.643	.071
Within Groups	4.807	2121	.002		
Total	4.819	2123			

Multiple Comparisons

Dependent Variable:Pixel_Values

	(I) HZ_Zones	(J) HZ_Zones	Mean Difference (I-J)	Std. Error	Sig.	95% Confidence Interval Lower Bound	95% Confidence Interval Upper Bound
Tamhane	Hydrothermal Zones ROI	100m Buffer from Hydrothermal Zone ROI	.00128122	.00284026	.958	-.0055150	.0080774
		100m and 200m Buffer from Hydrothermal Zone ROI	-.00427957	.00229151	.175	-.0097565	.0011973
	100m Buffer from Hydrothermal Zone ROI	Hydrothermal Zones ROI	-.00128122	.00284026	.958	-.0080774	.0055150
		100m and 200m Buffer from Hydrothermal Zone ROI	-.00556080	.00287229	.151	-.0124330	.0013114
	100m and 200m Buffer from Hydrothermal Zone ROI	Hydrothermal Zones ROI	.00427957	.00229151	.175	-.0011973	.0097565
		100m Buffer from Hydrothermal Zone ROI	.00556080	.00287229	.151	-.0013114	.0124330
Dunnett T3	Hydrothermal Zones ROI	100m Buffer from Hydrothermal Zone ROI	.00128122	.00284026	.958	-.0055145	.0080769
		100m and 200m Buffer from Hydrothermal Zone ROI	-.00427957	.00229151	.175	-.0097563	.0011971
	100m Buffer from Hydrothermal Zone ROI	Hydrothermal Zones ROI	-.00128122	.00284026	.958	-.0080769	.0055145
		100m and 200m Buffer from Hydrothermal Zone ROI	-.00556080	.00287229	.151	-.0124325	.0013110
	100m and 200m Buffer from Hydrothermal Zone ROI	Hydrothermal Zones ROI	.00427957	.00229151	.175	-.0011971	.0097563
		100m Buffer from Hydrothermal Zone ROI	.00556080	.00287229	.151	-.0013110	.0124325

Carbonate (Oct 16, 2005)

Case Processing Summary

	HZ_Zones	Cases Valid N	Valid Percent	Missing N	Missing Percent	Total N	Total Percent
Pixel_Values	Hydrothermal Zones ROI	791	100.0%	0	.0%	791	100.0%
	100m Buffer from Hydrothermal Zone ROI	431	100.0%	0	.0%	431	100.0%
	100m and 200m Buffer from Hydrothermal Zone ROI	921	100.0%	0	.0%	921	100.0%

ANOVA

Pixel_Values

	Sum of Squares	df	Mean Square	F	Sig.
Between Groups	.114	2	.057	10.165	.000
Within Groups	11.967	2140	.006		
Total	12.081	2142			

Multiple Comparisons

Dependent Variable:Pixel_Values

	(I) HZ_Zones	(J) HZ_Zones	Mean Difference (I-J)	Std. Error	Sig.	95% Confidence Interval Lower Bound	95% Confidence Interval Upper Bound
Tamhane	Hydrothermal Zones ROI	100m Buffer from Hydrothermal Zone ROI	-.00480195	.00436499	.614	-.0152467	.0056428
		100m and 200m Buffer from Hydrothermal Zone ROI	-.01598429*	.00355447	.000	-.0244798	-.0074888
	100m Buffer from Hydrothermal Zone ROI	Hydrothermal Zones ROI	.00480195	.00436499	.614	-.0056428	.0152467
		100m and 200m Buffer from Hydrothermal Zone ROI	-.01118234*	.00453409	.041	-.0220291	-.0003356
	100m and 200m Buffer from Hydrothermal Zone ROI	Hydrothermal Zones ROI	.01598429*	.00355447	.000	.0074888	.0244798
		100m Buffer from Hydrothermal Zone ROI	.01118234*	.00453409	.041	.0003356	.0220291
Dunnett T3	Hydrothermal Zones ROI	100m Buffer from Hydrothermal Zone ROI	-.00480195	.00436499	.613	-.0152459	.0056420
		100m and 200m Buffer from Hydrothermal Zone ROI	-.01598429*	.00355447	.000	-.0244795	-.0074891
	100m Buffer from Hydrothermal Zone ROI	Hydrothermal Zones ROI	.00480195	.00436499	.613	-.0056420	.0152459
		100m and 200m Buffer from Hydrothermal Zone ROI	-.01118234*	.00453409	.041	-.0220284	-.0003363
	100m and 200m Buffer from Hydrothermal Zone ROI	Hydrothermal Zones ROI	.01598429*	.00355447	.000	.0074891	.0244795
		100m Buffer from Hydrothermal Zone ROI	.01118234*	.00453409	.041	.0003363	.0220284

*. The mean difference is significant at the 0.05 level.

Carbonate (Feb 5, 2006)

Case Processing Summary

	HZ_Zones	Cases Valid N	Valid Percent	Missing N	Missing Percent	Total N	Total Percent
Pixel_Values	Hydrothermal Zones ROI	813	100.0%	0	.0%	813	100.0%
	100m Buffer from Hydrothermal Zone ROI	411	100.0%	0	.0%	411	100.0%
	100m and 200m Buffer from Hydrothermal Zone ROI	895	100.0%	0	.0%	895	100.0%

ANOVA

Pixel_Values

	Sum of Squares	df	Mean Square	F	Sig.
Between Groups	.008	2	.004	1.849	.158
Within Groups	4.488	2116	.002		
Total	4.496	2118			

Multiple Comparisons

Dependent Variable:Pixel_Values

	(I) HZ_Zones	(J) HZ_Zones	Mean Difference (I-J)	Std. Error	Sig.	95% Confidence Interval Lower Bound	95% Confidence Interval Upper Bound
Tamhane	Hydrothermal Zones ROI	100m Buffer from Hydrothermal Zone ROI	-.00051406	.00282018	.997	-.0072633	.0062352
		100m and 200m Buffer from Hydrothermal Zone ROI	-.00404924	.00218840	.181	-.0092797	.0011812
	100m Buffer from Hydrothermal Zone ROI	Hydrothermal Zones ROI	.00051406	.00282018	.997	-.0062352	.0072633
		100m and 200m Buffer from Hydrothermal Zone ROI	-.00353518	.00288185	.526	-.0104310	.0033606
	100m and 200m Buffer from Hydrothermal Zone ROI	Hydrothermal Zones ROI	.00404924	.00218840	.181	-.0011812	.0092797
		100m Buffer from Hydrothermal Zone ROI	.00353518	.00288185	.526	-.0033606	.0104310
Dunnett T3	Hydrothermal Zones ROI	100m Buffer from Hydrothermal Zone ROI	-.00051406	.00282018	.997	-.0072628	.0062347
		100m and 200m Buffer from Hydrothermal Zone ROI	-.00404924	.00218840	.181	-.0092795	.0011810
	100m Buffer from Hydrothermal Zone ROI	Hydrothermal Zones ROI	.00051406	.00282018	.997	-.0062347	.0072628
		100m and 200m Buffer from Hydrothermal Zone ROI	-.00353518	.00288185	.526	-.0104305	.0033601
	100m and 200m Buffer from Hydrothermal Zone ROI	Hydrothermal Zones ROI	.00404924	.00218840	.181	-.0011810	.0092795
		100m Buffer from Hydrothermal Zone ROI	.00353518	.00288185	.526	-.0033601	.0104305

Tendaho Carbonate

Carbonate (Jan 25, 2002)

Case Processing Summary

		Cases					
		Valid		Missing		Total	
	HZ_Zones	N	Percent	N	Percent	N	Percent
Pixel_Values	Hydrothermal Zones ROI	743	100.0%	0	.0%	743	100.0%
	100m Buffer from Hydrothermal Zone ROI	608	100.0%	0	.0%	608	100.0%
	100m and 200m Buffer from Hydrothermal Zone ROI	1214	100.0%	0	.0%	1214	100.0%

ANOVA

Pixel_Values

	Sum of Squares	df	Mean Square	F	Sig.
Between Groups	.479	2	.239	37.274	.000
Within Groups	16.451	2562	.006		
Total	16.930	2564			

Multiple Comparisons

Dependent Variable:Pixel_Values

	(I) HZ_Zones	(J) HZ_Zones	Mean Difference (I-J)	Std. Error	Sig.	95% Confidence Interval Lower Bound	95% Confidence Interval Upper Bound
Tamhane	Hydrothermal Zones ROI	100m Buffer from Hydrothermal Zone ROI	-.03098480*	.00440467	.000	-.0415156	-.0204540
		100m and 200m Buffer from Hydrothermal Zone ROI	-.02964776*	.00374328	.000	-.0385954	-.0207001
	100m Buffer from Hydrothermal Zone ROI	Hydrothermal Zones ROI	.03098480*	.00440467	.000	.0204540	.0415156
		100m and 200m Buffer from Hydrothermal Zone ROI	.00133704	.00397897	.982	-.0081769	.0108510
	100m and 200m Buffer from Hydrothermal Zone ROI	Hydrothermal Zones ROI	.02964776*	.00374328	.000	.0207001	.0385954
		100m Buffer from Hydrothermal Zone ROI	-.00133704	.00397897	.982	-.0108510	.0081769
Dunnett T3	Hydrothermal Zones ROI	100m Buffer from Hydrothermal Zone ROI	-.03098480*	.00440467	.000	-.0415151	-.0204545
		100m and 200m Buffer from Hydrothermal Zone ROI	-.02964776*	.00374328	.000	-.0385951	-.0207005
	100m Buffer from Hydrothermal Zone ROI	Hydrothermal Zones ROI	.03098480*	.00440467	.000	.0204545	.0415151
		100m and 200m Buffer from Hydrothermal Zone ROI	.00133704	.00397897	.982	-.0081765	.0108506
	100m and 200m Buffer from Hydrothermal Zone ROI	Hydrothermal Zones ROI	.02964776*	.00374328	.000	.0207005	.0385951
		100m Buffer from Hydrothermal Zone ROI	-.00133704	.00397897	.982	-.0108506	.0081765

*. The mean difference is significant at the 0.05 level.

Carbonate (Oct 11, 2003)

Case Processing Summary

	HZ_Zones	Cases: Valid N	Valid Percent	Missing N	Missing Percent	Total N	Total Percent
Pixel_Values	Hydrothermal Zones ROI	742	100.0%	0	.0%	742	100.0%
	100m Buffer from Hydrothermal Zone ROI	606	100.0%	0	.0%	606	100.0%
	100m and 200m Buffer from Hydrothermal Zone ROI	1211	100.0%	0	.0%	1211	100.0%

ANOVA

Pixel_Values

	Sum of Squares	df	Mean Square	F	Sig.
Between Groups	.210	2	.105	39.037	.000
Within Groups	6.868	2556	.003		
Total	7.077	2558			

Multiple Comparisons

Dependent Variable:Pixel_Values

	(I) HZ_Zones	(J) HZ_Zones	Mean Difference (I-J)	Std. Error	Sig.	95% Confidence Interval Lower Bound	95% Confidence Interval Upper Bound
Tamhane	Hydrothermal Zones ROI	100m Buffer from Hydrothermal Zone ROI	-.01912980*	.00280561	.000	-.0258376	-.0124220
		100m and 200m Buffer from Hydrothermal Zone ROI	-.02032513*	.00240504	.000	-.0260737	-.0145765
	100m Buffer from Hydrothermal Zone ROI	Hydrothermal Zones ROI	.01912980*	.00280561	.000	.0124220	.0258376
		100m and 200m Buffer from Hydrothermal Zone ROI	-.00119533	.00257786	.954	-.0073589	.0049683
	100m and 200m Buffer from Hydrothermal Zone ROI	Hydrothermal Zones ROI	.02032513*	.00240504	.000	.0145765	.0260737
		100m Buffer from Hydrothermal Zone ROI	.00119533	.00257786	.954	-.0049683	.0073589
Dunnett T3	Hydrothermal Zones ROI	100m Buffer from Hydrothermal Zone ROI	-.01912980*	.00280561	.000	-.0258373	-.0124223
		100m and 200m Buffer from Hydrothermal Zone ROI	-.02032513*	.00240504	.000	-.0260735	-.0145767
	100m Buffer from Hydrothermal Zone ROI	Hydrothermal Zones ROI	.01912980*	.00280561	.000	.0124223	.0258373
		100m and 200m Buffer from Hydrothermal Zone ROI	-.00119533	.00257786	.954	-.0073587	.0049680
	100m and 200m Buffer from Hydrothermal Zone ROI	Hydrothermal Zones ROI	.02032513*	.00240504	.000	.0145767	.0260735
		100m Buffer from Hydrothermal Zone ROI	.00119533	.00257786	.954	-.0049680	.0073587

*. The mean difference is significant at the 0.05 level.

Carbonate (Jan 1, 2005)

Case Processing Summary

	HZ_Zones	Cases Valid N	Valid Percent	Missing N	Missing Percent	Total N	Total Percent
Pixel_Values	Hydrothermal Zones ROI	747	100.0%	0	.0%	747	100.0%
	100m Buffer from Hydrothermal Zone ROI	609	100.0%	0	.0%	609	100.0%
	100m and 200m Buffer from Hydrothermal Zone ROI	1207	100.0%	0	.0%	1207	100.0%

ANOVA

Pixel_Values

	Sum of Squares	df	Mean Square	F	Sig.
Between Groups	.181	2	.090	35.035	.000
Within Groups	6.604	2560	.003		
Total	6.784	2562			

Multiple Comparisons

Dependent Variable:Pixel_Values

	(I) HZ_Zones	(J) HZ_Zones	Mean Difference (I-J)	Std. Error	Sig.	95% Confidence Interval Lower Bound	95% Confidence Interval Upper Bound
Tamhane	Hydrothermal Zones ROI	100m Buffer from Hydrothermal Zone ROI	-.01675821*	.00276973	.000	-.0233799	-.0101365
		100m and 200m Buffer from Hydrothermal Zone ROI	-.01916701*	.00241496	.000	-.0249396	-.0133944
	100m Buffer from Hydrothermal Zone ROI	Hydrothermal Zones ROI	.01675821*	.00276973	.000	.0101365	.0233799
		100m and 200m Buffer from Hydrothermal Zone ROI	-.00240880	.00246022	.696	-.0082910	.0034734
	100m and 200m Buffer from Hydrothermal Zone ROI	Hydrothermal Zones ROI	.01916701*	.00241496	.000	.0133944	.0249396
		100m Buffer from Hydrothermal Zone ROI	.00240880	.00246022	.696	-.0034734	.0082910
Dunnett T3	Hydrothermal Zones ROI	100m Buffer from Hydrothermal Zone ROI	-.01675821*	.00276973	.000	-.0233797	-.0101368
		100m and 200m Buffer from Hydrothermal Zone ROI	-.01916701*	.00241496	.000	-.0249394	-.0133946
	100m Buffer from Hydrothermal Zone ROI	Hydrothermal Zones ROI	.01675821*	.00276973	.000	.0101368	.0233797
		100m and 200m Buffer from Hydrothermal Zone ROI	-.00240880	.00246022	.696	-.0082908	.0034732
	100m and 200m Buffer from Hydrothermal Zone ROI	Hydrothermal Zones ROI	.01916701*	.00241496	.000	.0133946	.0249394
		100m Buffer from Hydrothermal Zone ROI	.00240880	.00246022	.696	-.0034732	.0082908

*. The mean difference is significant at the 0.05 level.

Berecha Sericite/Muscovite/Illite/Smectite

Sericite/Muscovite/Illite/Smectite (Jan 12, 2003)

Case Processing Summary

	HZ_Zones	Cases Valid N	Valid Percent	Missing N	Missing Percent	Total N	Total Percent
Pixel_Values	Hydrothermal Zones ROI	808	100.0%	0	.0%	808	100.0%
	100m Buffer from Hydrothermal Zone ROI	413	100.0%	0	.0%	413	100.0%
	100m and 200m Buffer from Hydrothermal Zone ROI	903	100.0%	0	.0%	903	100.0%

ANOVA

Pixel_Values

	Sum of Squares	df	Mean Square	F	Sig.
Between Groups	.923	2	.461	248.687	.000
Within Groups	3.935	2121	.002		
Total	4.858	2123			

Multiple Comparisons

Dependent Variable:Pixel_Values

	(I) HZ_Zones	(J) HZ_Zones	Mean Difference (I-J)	Std. Error	Sig.	95% Confidence Interval Lower Bound	95% Confidence Interval Upper Bound
Tamhane	Hydrothermal Zones ROI	100m Buffer from Hydrothermal Zone ROI	.03646477*	.00255931	.000	.0303422	.0425873
		100m and 200m Buffer from Hydrothermal Zone ROI	.04516089*	.00211005	.000	.0401176	.0502042
	100m Buffer from Hydrothermal Zone ROI	Hydrothermal Zones ROI	-.03646477*	.00255931	.000	-.0425873	-.0303422
		100m and 200m Buffer from Hydrothermal Zone ROI	.00869613*	.00248127	.001	.0027595	.0146328
	100m and 200m Buffer from Hydrothermal Zone ROI	Hydrothermal Zones ROI	-.04516089*	.00211005	.000	-.0502042	-.0401176
		100m Buffer from Hydrothermal Zone ROI	-.00869613*	.00248127	.001	-.0146328	-.0027595
Dunnett T3	Hydrothermal Zones ROI	100m Buffer from Hydrothermal Zone ROI	.03646477*	.00255931	.000	.0303426	.0425869
		100m and 200m Buffer from Hydrothermal Zone ROI	.04516089*	.00211005	.000	.0401178	.0502040
	100m Buffer from Hydrothermal Zone ROI	Hydrothermal Zones ROI	-.03646477*	.00255931	.000	-.0425869	-.0303426
		100m and 200m Buffer from Hydrothermal Zone ROI	.00869613*	.00248127	.001	.0027599	.0146324
	100m and 200m Buffer from Hydrothermal Zone ROI	Hydrothermal Zones ROI	-.04516089*	.00211005	.000	-.0502040	-.0401178
		100m Buffer from Hydrothermal Zone ROI	-.00869613*	.00248127	.001	-.0146324	-.0027599

*. The mean difference is significant at the 0.05 level.

Sericite/Muscovite/Illite/Smectite (Oct 16, 2005)

Case Processing Summary

		Cases					
		Valid		Missing		Total	
	HZ_Zones	N	Percent	N	Percent	N	Percent
Pixel_Values	Hydrothermal Zones ROI	791	100.0%	0	.0%	791	100.0%
	100m Buffer from Hydrothermal Zone ROI	431	100.0%	0	.0%	431	100.0%
	100m and 200m Buffer from Hydrothermal Zone ROI	921	100.0%	0	.0%	921	100.0%

ANOVA

Pixel_Values

	Sum of Squares	df	Mean Square	F	Sig.
Between Groups	.971	2	.485	191.049	.000
Within Groups	5.436	2140	.003		
Total	6.406	2142			

Multiple Comparisons

Dependent Variable:Pixel_Values

	(I) HZ_Zones	(J) HZ_Zones	Mean Difference (I-J)	Std. Error	Sig.	95% Confidence Interval Lower Bound	95% Confidence Interval Upper Bound
Tamhane	Hydrothermal Zones ROI	100m Buffer from Hydrothermal Zone ROI	.03699351*	.00302436	.000	.0297581	.0442289
		100m and 200m Buffer from Hydrothermal Zone ROI	.04652904*	.00243186	.000	.0407166	.0523415
	100m Buffer from Hydrothermal Zone ROI	Hydrothermal Zones ROI	-.03699351*	.00302436	.000	-.0442289	-.0297581
		100m and 200m Buffer from Hydrothermal Zone ROI	.00953552*	.00297133	.004	.0024265	.0166445
	100m and 200m Buffer from Hydrothermal Zone ROI	Hydrothermal Zones ROI	-.04652904*	.00243186	.000	-.0523415	-.0407166
		100m Buffer from Hydrothermal Zone ROI	-.00953552*	.00297133	.004	-.0166445	-.0024265
Dunnett T3	Hydrothermal Zones ROI	100m Buffer from Hydrothermal Zone ROI	.03699351*	.00302436	.000	.0297586	.0442285
		100m and 200m Buffer from Hydrothermal Zone ROI	.04652904*	.00243186	.000	.0407168	.0523413
	100m Buffer from Hydrothermal Zone ROI	Hydrothermal Zones ROI	-.03699351*	.00302436	.000	-.0442285	-.0297586
		100m and 200m Buffer from Hydrothermal Zone ROI	.00953552*	.00297133	.004	.0024270	.0166440
	100m and 200m Buffer from Hydrothermal Zone ROI	Hydrothermal Zones ROI	-.04652904*	.00243186	.000	-.0523413	-.0407168
		100m Buffer from Hydrothermal Zone ROI	-.00953552*	.00297133	.004	-.0166440	-.0024270

*. The mean difference is significant at the 0.05 level.

Sericite/Muscovite/Illite/Smectite (Feb 5, 2005)

Case Processing Summary

	HZ_Zones	Cases					
		Valid		Missing		Total	
		N	Percent	N	Percent	N	Percent
Pixel_Values	Hydrothermal Zones ROI	813	100.0%	0	.0%	813	100.0%
	100m Buffer from Hydrothermal Zone ROI	411	100.0%	0	.0%	411	100.0%
	100m and 200m Buffer from Hydrothermal Zone ROI	895	100.0%	0	.0%	895	100.0%

ANOVA

Pixel_Values

	Sum of Squares	df	Mean Square	F	Sig.
Between Groups	.925	2	.462	247.826	.000
Within Groups	3.948	2116	.002		
Total	4.873	2118			

Multiple Comparisons

Dependent Variable:Pixel_Values

	(I) HZ_Zones	(J) HZ_Zones	Mean Difference (I-J)	Std. Error	Sig.	95% Confidence Interval	
						Lower Bound	Upper Bound
Tamhane	Hydrothermal Zones ROI	100m Buffer from Hydrothermal Zone ROI	.03711845*	.00266418	.000	.0307440	.0434929
		100m and 200m Buffer from Hydrothermal Zone ROI	.04504253*	.00208535	.000	.0400583	.0500268
	100m Buffer from Hydrothermal Zone ROI	Hydrothermal Zones ROI	-.03711845*	.00266418	.000	-.0434929	-.0307440
		100m and 200m Buffer from Hydrothermal Zone ROI	.00792408*	.00259441	.007	.0017157	.0141324
	100m and 200m Buffer from Hydrothermal Zone ROI	Hydrothermal Zones ROI	-.04504253*	.00208535	.000	-.0500268	-.0400583
		100m Buffer from Hydrothermal Zone ROI	-.00792408*	.00259441	.007	-.0141324	-.0017157
Dunnett T3	Hydrothermal Zones ROI	100m Buffer from Hydrothermal Zone ROI	.03711845*	.00266418	.000	.0307445	.0434925
		100m and 200m Buffer from Hydrothermal Zone ROI	.04504253*	.00208535	.000	.0400585	.0500266
	100m Buffer from Hydrothermal Zone ROI	Hydrothermal Zones ROI	-.03711845*	.00266418	.000	-.0434925	-.0307445
		100m and 200m Buffer from Hydrothermal Zone ROI	.00792408*	.00259441	.007	.0017162	.0141320
	100m and 200m Buffer from Hydrothermal Zone ROI	Hydrothermal Zones ROI	-.04504253*	.00208535	.000	-.0500266	-.0400585
		100m Buffer from Hydrothermal Zone ROI	-.00792408*	.00259441	.007	-.0141320	-.0017162

*. The mean difference is significant at the 0.05 level.

Tendaho Sericite/Muscovite/Illite/Smectite
Sericite/Muscovite/Illite/Smectite (Jan 25, 2002)

Case Processing Summary

		Cases					
		Valid		Missing		Total	
	HZ_Zones	N	Percent	N	Percent	N	Percent
Pixel_Values	Hydrothermal Zones ROI	747	100.0%	0	.0%	747	100.0%
	100m Buffer from Hydrothermal Zone ROI	609	100.0%	0	.0%	609	100.0%
	100m and 200m Buffer from Hydrothermal Zone ROI	1207	100.0%	0	.0%	1207	100.0%

ANOVA

Pixel_Values

	Sum of Squares	df	Mean Square	F	Sig.
Between Groups	.037	2	.019	11.198	.000
Within Groups	4.230	2560	.002		
Total	4.267	2562			

Multiple Comparisons

Dependent Variable:Pixel_Values

	(I) HZ_Zones	(J) HZ_Zones	Mean Difference (I-J)	Std. Error	Sig.	95% Confidence Interval Lower Bound	95% Confidence Interval Upper Bound
Tamhane	Hydrothermal Zones ROI	100m Buffer from Hydrothermal Zone ROI	.00602286*	.00224767	.022	.0006493	.0113964
		100m and 200m Buffer from Hydrothermal Zone ROI	.00894166*	.00196521	.000	.0042439	.0136395
	100m Buffer from Hydrothermal Zone ROI	Hydrothermal Zones ROI	-.00602286*	.00224767	.022	-.0113964	-.0006493
		100m and 200m Buffer from Hydrothermal Zone ROI	.00291880	.00194198	.348	-.0017244	.0075620
	100m and 200m Buffer from Hydrothermal Zone ROI	Hydrothermal Zones ROI	-.00894166*	.00196521	.000	-.0136395	-.0042439
		100m Buffer from Hydrothermal Zone ROI	-.00291880	.00194198	.348	-.0075620	.0017244
Dunnett T3	Hydrothermal Zones ROI	100m Buffer from Hydrothermal Zone ROI	.00602286*	.00224767	.022	.0006495	.0113962
		100m and 200m Buffer from Hydrothermal Zone ROI	.00894166*	.00196521	.000	.0042440	.0136393
	100m Buffer from Hydrothermal Zone ROI	Hydrothermal Zones ROI	-.00602286*	.00224767	.022	-.0113962	-.0006495
		100m and 200m Buffer from Hydrothermal Zone ROI	.00291880	.00194198	.348	-.0017242	.0075618
	100m and 200m Buffer from Hydrothermal Zone ROI	Hydrothermal Zones ROI	-.00894166*	.00196521	.000	-.0136393	-.0042440
		100m Buffer from Hydrothermal Zone ROI	-.00291880	.00194198	.348	-.0075618	.0017242

*. The mean difference is significant at the 0.05 level.

Sericite/Muscovite/Illite/Smectite (Oct 11, 2003)

Case Processing Summary

	HZ_Zones	Cases: Valid N	Valid Percent	Missing N	Missing Percent	Total N	Total Percent
Pixel_Values	Hydrothermal Zones ROI	742	100.0%	0	.0%	742	100.0%
	100m Buffer from Hydrothermal Zone ROI	606	100.0%	0	.0%	606	100.0%
	100m and 200m Buffer from Hydrothermal Zone ROI	1211	100.0%	0	.0%	1211	100.0%

ANOVA

Pixel_Values

	Sum of Squares	df	Mean Square	F	Sig.
Between Groups	.048	2	.024	15.644	.000
Within Groups	3.961	2556	.002		
Total	4.009	2558			

Multiple Comparisons

Dependent Variable:Pixel_Values

	(I) HZ_Zones	(J) HZ_Zones	Mean Difference (I-J)	Std. Error	Sig.	95% Confidence Interval Lower Bound	Upper Bound
Tamhane	Hydrothermal Zones ROI	100m Buffer from Hydrothermal Zone ROI	.00562647*	.00217794	.029	.0004195	.0108335
		100m and 200m Buffer from Hydrothermal Zone ROI	.01023960*	.00186224	.000	.0057881	.0146911
	100m Buffer from Hydrothermal Zone ROI	Hydrothermal Zones ROI	-.00562647*	.00217794	.029	-.0108335	-.0004195
		100m and 200m Buffer from Hydrothermal Zone ROI	.00461313	.00193645	.051	-.0000171	.0092433
	100m and 200m Buffer from Hydrothermal Zone ROI	Hydrothermal Zones ROI	-.01023960*	.00186224	.000	-.0146911	-.0057881
		100m Buffer from Hydrothermal Zone ROI	-.00461313	.00193645	.051	-.0092433	.0000171
Dunnett T3	Hydrothermal Zones ROI	100m Buffer from Hydrothermal Zone ROI	.00562647*	.00217794	.029	.0004197	.0108333
		100m and 200m Buffer from Hydrothermal Zone ROI	.01023960*	.00186224	.000	.0057883	.0146909
	100m Buffer from Hydrothermal Zone ROI	Hydrothermal Zones ROI	-.00562647*	.00217794	.029	-.0108333	-.0004197
		100m and 200m Buffer from Hydrothermal Zone ROI	.00461313	.00193645	.051	-.0000168	.0092431
	100m and 200m Buffer from Hydrothermal Zone ROI	Hydrothermal Zones ROI	-.01023960*	.00186224	.000	-.0146909	-.0057883
		100m Buffer from Hydrothermal Zone ROI	-.00461313	.00193645	.051	-.0092431	.0000168

*. The mean difference is significant at the 0.05 level.

Sericite/Muscovite/Illite/Smectite (Jan 1, 2003)

Case Processing Summary

	HZ_Zones	Cases					
		Valid		Missing		Total	
		N	Percent	N	Percent	N	Percent
Pixel_Values	Hydrothermal Zones ROI	747	100.0%	0	.0%	747	100.0%
	100m Buffer from Hydrothermal Zone ROI	609	100.0%	0	.0%	609	100.0%
	100m and 200m Buffer from Hydrothermal Zone ROI	1207	100.0%	0	.0%	1207	100.0%

ANOVA

Pixel_Values

	Sum of Squares	df	Mean Square	F	Sig.
Between Groups	.037	2	.019	11.198	.000
Within Groups	4.230	2560	.002		
Total	4.267	2562			

Multiple Comparisons

Dependent Variable:Pixel_Values

	(I) HZ_Zones	(J) HZ_Zones	Mean Difference (I-J)	Std. Error	Sig.	95% Confidence Interval Lower Bound	95% Confidence Interval Upper Bound
Tamhane	Hydrothermal Zones ROI	100m Buffer from Hydrothermal Zone ROI	.00602286*	.00224767	.022	.0006493	.0113964
		100m and 200m Buffer from Hydrothermal Zone ROI	.00894166*	.00196521	.000	.0042439	.0136395
	100m Buffer from Hydrothermal Zone ROI	Hydrothermal Zones ROI	-.00602286*	.00224767	.022	-.0113964	-.0006493
		100m and 200m Buffer from Hydrothermal Zone ROI	.00291880	.00194198	.348	-.0017244	.0075620
	100m and 200m Buffer from Hydrothermal Zone ROI	Hydrothermal Zones ROI	-.00894166*	.00196521	.000	-.0136395	-.0042439
		100m Buffer from Hydrothermal Zone ROI	-.00291880	.00194198	.348	-.0075620	.0017244
Dunnett T3	Hydrothermal Zones ROI	100m Buffer from Hydrothermal Zone ROI	.00602286*	.00224767	.022	.0006495	.0113962
		100m and 200m Buffer from Hydrothermal Zone ROI	.00894166*	.00196521	.000	.0042440	.0136393
	100m Buffer from Hydrothermal Zone ROI	Hydrothermal Zones ROI	-.00602286*	.00224767	.022	-.0113962	-.0006495
		100m and 200m Buffer from Hydrothermal Zone ROI	.00291880	.00194198	.348	-.0017242	.0075618
	100m and 200m Buffer from Hydrothermal Zone ROI	Hydrothermal Zones ROI	-.00894166*	.00196521	.000	-.0136393	-.0042440
		100m Buffer from Hydrothermal Zone ROI	-.00291880	.00194198	.348	-.0075618	.0017242

*. The mean difference is significant at the 0.05 level.

Berecha Alunite/ Kaolinite/ Pyrophyllite

Alunite/ Kaolinite/ Pyrophyllite (Jan 12, 2003)

Case Processing Summary

		Cases					
		Valid		Missing		Total	
	HZ_Zones	N	Percent	N	Percent	N	Percent
Pixel_Values	Hydrothermal Zones ROI	808	100.0%	0	.0%	808	100.0%
	100m Buffer from Hydrothermal Zone ROI	413	100.0%	0	.0%	413	100.0%
	100m and 200m Buffer from Hydrothermal Zone ROI	903	100.0%	0	.0%	903	100.0%

ANOVA

Pixel_Values

	Sum of Squares	df	Mean Square	F	Sig.
Between Groups	5.466	2	2.733	463.337	.000
Within Groups	12.510	2121	.006		
Total	17.975	2123			

Multiple Comparisons

Dependent Variable:Pixel_Values

	(I) HZ_Zones	(J) HZ_Zones	Mean Difference (I-J)	Std. Error	Sig.	95% Confidence Interval Lower Bound	95% Confidence Interval Upper Bound
Tamhane	Hydrothermal Zones ROI	100m Buffer from Hydrothermal Zone ROI	.09662683*	.00467467	.000	.0854453	.1078084
		100m and 200m Buffer from Hydrothermal Zone ROI	.10760429*	.00380435	.000	.0985108	.1166978
	100m Buffer from Hydrothermal Zone ROI	Hydrothermal Zones ROI	-.09662683*	.00467467	.000	-.1078084	-.0854453
		100m and 200m Buffer from Hydrothermal Zone ROI	.01097746*	.00427827	.031	.0007399	.0212150
	100m and 200m Buffer from Hydrothermal Zone ROI	Hydrothermal Zones ROI	-.10760429*	.00380435	.000	-.1166978	-.0985108
		100m Buffer from Hydrothermal Zone ROI	-.01097746*	.00427827	.031	-.0212150	-.0007399
Dunnett T3	Hydrothermal Zones ROI	100m Buffer from Hydrothermal Zone ROI	.09662683*	.00467467	.000	.0854460	.1078077
		100m and 200m Buffer from Hydrothermal Zone ROI	.10760429*	.00380435	.000	.0985111	.1166975
	100m Buffer from Hydrothermal Zone ROI	Hydrothermal Zones ROI	-.09662683*	.00467467	.000	-.1078077	-.0854460
		100m and 200m Buffer from Hydrothermal Zone ROI	.01097746*	.00427827	.031	.0007406	.0212143
	100m and 200m Buffer from Hydrothermal Zone ROI	Hydrothermal Zones ROI	-.10760429*	.00380435	.000	-.1166975	-.0985111
		100m Buffer from Hydrothermal Zone ROI	-.01097746*	.00427827	.031	-.0212143	-.0007406

*. The mean difference is significant at the 0.05 level.

Alunite/ Kaolinite/ Pyrophyllite (Oct 16, 2005)

Case Processing Summary

	HZ_Zones	Cases					
		Valid		Missing		Total	
		N	Percent	N	Percent	N	Percent
Pixel_Values	Hydrothermal Zones ROI	791	100.0%	0	.0%	791	100.0%
	100m Buffer from Hydrothermal Zone ROI	431	100.0%	0	.0%	431	100.0%
	100m and 200m Buffer from Hydrothermal Zone ROI	921	100.0%	0	.0%	921	100.0%

ANOVA

Pixel_Values

	Sum of Squares	df	Mean Square	F	Sig.
Between Groups	1.671	2	.836	75.035	.000
Within Groups	23.831	2140	.011		
Total	25.502	2142			

Multiple Comparisons

Dependent Variable:Pixel_Values

	(I) HZ_Zones	(J) HZ_Zones	Mean Difference (I-J)	Std. Error	Sig.	95% Confidence Interval	
						Lower Bound	Upper Bound
Tamhane	Hydrothermal Zones ROI	100m Buffer from Hydrothermal Zone ROI	.05475465*	.00619122	.000	.0399340	.0695753
		100m and 200m Buffer from Hydrothermal Zone ROI	.05917970*	.00485343	.000	.0475789	.0707805
	100m Buffer from Hydrothermal Zone ROI	Hydrothermal Zones ROI	-.05475465*	.00619122	.000	-.0695753	-.0399340
		100m and 200m Buffer from Hydrothermal Zone ROI	.00442504	.00678471	.886	-.0118061	.0206562
	100m and 200m Buffer from Hydrothermal Zone ROI	Hydrothermal Zones ROI	-.05917970*	.00485343	.000	-.0707805	-.0475789
		100m Buffer from Hydrothermal Zone ROI	-.00442504	.00678471	.886	-.0206562	.0118061
Dunnett T3	Hydrothermal Zones ROI	100m Buffer from Hydrothermal Zone ROI	.05475465*	.00619122	.000	.0399353	.0695740
		100m and 200m Buffer from Hydrothermal Zone ROI	.05917970*	.00485343	.000	.0475793	.0707801
	100m Buffer from Hydrothermal Zone ROI	Hydrothermal Zones ROI	-.05475465*	.00619122	.000	-.0695740	-.0399353
		100m and 200m Buffer from Hydrothermal Zone ROI	.00442504	.00678471	.885	-.0118050	.0206551
	100m and 200m Buffer from Hydrothermal Zone ROI	Hydrothermal Zones ROI	-.05917970*	.00485343	.000	-.0707801	-.0475793
		100m Buffer from Hydrothermal Zone ROI	-.00442504	.00678471	.885	-.0206551	.0118050

*. The mean difference is significant at the 0.05 level.

Alunite/ Kaolinite/ Pyrophyllite (Feb 5, 2006)

Case Processing Summary

		Cases					
		Valid		Missing		Total	
	HZ_Zones	N	Percent	N	Percent	N	Percent
Pixel_Values	Hydrothermal Zones ROI	813	100.0%	0	.0%	813	100.0%
	100m Buffer from Hydrothermal Zone ROI	411	100.0%	0	.0%	411	100.0%
	100m and 200m Buffer from Hydrothermal Zone ROI	895	100.0%	0	.0%	895	100.0%

ANOVA

Pixel_Values

	Sum of Squares	df	Mean Square	F	Sig.
Between Groups	3.600	2	1.800	281.193	.000
Within Groups	13.545	2116	.006		
Total	17.145	2118			

Multiple Comparisons

Dependent Variable:Pixel_Values

	(I) HZ_Zones	(J) HZ_Zones	Mean Difference (I-J)	Std. Error	Sig.	95% Confidence Interval Lower Bound	95% Confidence Interval Upper Bound
Tamhane	Hydrothermal Zones ROI	100m Buffer from Hydrothermal Zone ROI	.08009132*	.00491777	.000	.0683240	.0918587
		100m and 200m Buffer from Hydrothermal Zone ROI	.08669644*	.00384234	.000	.0775129	.0958800
	100m Buffer from Hydrothermal Zone ROI	Hydrothermal Zones ROI	-.08009132*	.00491777	.000	-.0918587	-.0683240
		100m and 200m Buffer from Hydrothermal Zone ROI	.00660513	.00487438	.440	-.0050588	.0182691
	100m and 200m Buffer from Hydrothermal Zone ROI	Hydrothermal Zones ROI	-.08669644*	.00384234	.000	-.0958800	-.0775129
		100m Buffer from Hydrothermal Zone ROI	-.00660513	.00487438	.440	-.0182691	.0050588
Dunnett T3	Hydrothermal Zones ROI	100m Buffer from Hydrothermal Zone ROI	.08009132*	.00491777	.000	.0683248	.0918578
		100m and 200m Buffer from Hydrothermal Zone ROI	.08669644*	.00384234	.000	.0775132	.0958797
	100m Buffer from Hydrothermal Zone ROI	Hydrothermal Zones ROI	-.08009132*	.00491777	.000	-.0918578	-.0683248
		100m and 200m Buffer from Hydrothermal Zone ROI	.00660513	.00487438	.440	-.0050580	.0182682
	100m and 200m Buffer from Hydrothermal Zone ROI	Hydrothermal Zones ROI	-.08669644*	.00384234	.000	-.0958797	-.0775132
		100m Buffer from Hydrothermal Zone ROI	-.00660513	.00487438	.440	-.0182682	.0050580

*. The mean difference is significant at the 0.05 level.

Tendaho Alunite/ Kaolinite/ Pyrophyllite

Alunite/ Kaolinite/ Pyrophyllite (Jan 25, 2002)

Case Processing Summary

		Cases					
		Valid		Missing		Total	
	HZ_Zones	N	Percent	N	Percent	N	Percent
Pixel_Values	Hydrothermal Zones ROI	743	100.0%	0	.0%	743	100.0%
	100m Buffer from Hydrothermal Zone ROI	608	100.0%	0	.0%	608	100.0%
	100m and 200m Buffer from Hydrothermal Zone ROI	1214	100.0%	0	.0%	1214	100.0%

ANOVA

Pixel_Values

	Sum of Squares	df	Mean Square	F	Sig.
Between Groups	.133	2	.067	26.127	.000
Within Groups	6.543	2562	.003		
Total	6.677	2564			

Multiple Comparisons

Dependent Variable:Pixel_Values

						95% Confidence Interval	
	(I) HZ_Zones	(J) HZ_Zones	Mean Difference (I-J)	Std. Error	Sig.	Lower Bound	Upper Bound
Tamhane	Hydrothermal Zones ROI	100m Buffer from Hydrothermal Zone ROI	-.01394389*	.00276572	.000	-.0205560	-.0073318
		100m and 200m Buffer from Hydrothermal Zone ROI	-.01662108*	.00244405	.000	-.0224635	-.0107787
	100m Buffer from Hydrothermal Zone ROI	Hydrothermal Zones ROI	.01394389*	.00276572	.000	.0073318	.0205560
		100m and 200m Buffer from Hydrothermal Zone ROI	-.00267719	.00239890	.602	-.0084127	.0030584
	100m and 200m Buffer from Hydrothermal Zone ROI	Hydrothermal Zones ROI	.01662108*	.00244405	.000	.0107787	.0224635
		100m Buffer from Hydrothermal Zone ROI	.00267719	.00239890	.602	-.0030584	.0084127
Dunnett T3	Hydrothermal Zones ROI	100m Buffer from Hydrothermal Zone ROI	-.01394389*	.00276572	.000	-.0205557	-.0073321
		100m and 200m Buffer from Hydrothermal Zone ROI	-.01662108*	.00244405	.000	-.0224633	-.0107789
	100m Buffer from Hydrothermal Zone ROI	Hydrothermal Zones ROI	.01394389*	.00276572	.000	.0073321	.0205557
		100m and 200m Buffer from Hydrothermal Zone ROI	-.00267719	.00239890	.602	-.0084125	.0030581
	100m and 200m Buffer from Hydrothermal Zone ROI	Hydrothermal Zones ROI	.01662108*	.00244405	.000	.0107789	.0224633
		100m Buffer from Hydrothermal Zone ROI	.00267719	.00239890	.602	-.0030581	.0084125

*. The mean difference is significant at the 0.05 level.

Alunite/ Kaolinite/ Pyrophyllite (Oct 11, 2003)

Case Processing Summary

	HZ_Zones	Cases					
		Valid		Missing		Total	
		N	Percent	N	Percent	N	Percent
Pixel_Values	Hydrothermal Zones ROI	742	100.0%	0	.0%	742	100.0%
	100m Buffer from Hydrothermal Zone ROI	606	100.0%	0	.0%	606	100.0%
	100m and 200m Buffer from Hydrothermal Zone ROI	1211	100.0%	0	.0%	1211	100.0%

ANOVA

Pixel_Values

	Sum of Squares	df	Mean Square	F	Sig.
Between Groups	.108	2	.054	26.154	.000
Within Groups	5.300	2556	.002		
Total	5.409	2558			

Multiple Comparisons

Dependent Variable:Pixel_Values

	(I) HZ_Zones	(J) HZ_Zones	Mean Difference (I-J)	Std. Error	Sig.	95% Confidence Interval Lower Bound	95% Confidence Interval Upper Bound
Tamhane	Hydrothermal Zones ROI	100m Buffer from Hydrothermal Zone ROI	-.00990007*	.00250336	.000	-.0158850	-.0039151
		100m and 200m Buffer from Hydrothermal Zone ROI	-.01534957*	.00216007	.000	-.0205130	-.0101862
	100m Buffer from Hydrothermal Zone ROI	Hydrothermal Zones ROI	.00990007*	.00250336	.000	.0039151	.0158850
		100m and 200m Buffer from Hydrothermal Zone ROI	-.00544951*	.00222520	.043	-.0107700	-.0001290
	100m and 200m Buffer from Hydrothermal Zone ROI	Hydrothermal Zones ROI	.01534957*	.00216007	.000	.0101862	.0205130
		100m Buffer from Hydrothermal Zone ROI	.00544951*	.00222520	.043	.0001290	.0107700
Dunnett T3	Hydrothermal Zones ROI	100m Buffer from Hydrothermal Zone ROI	-.00990007*	.00250336	.000	-.0158848	-.0039153
		100m and 200m Buffer from Hydrothermal Zone ROI	-.01534957*	.00216007	.000	-.0205128	-.0101864
	100m Buffer from Hydrothermal Zone ROI	Hydrothermal Zones ROI	.00990007*	.00250336	.000	.0039153	.0158848
		100m and 200m Buffer from Hydrothermal Zone ROI	-.00544951*	.00222520	.043	-.0107697	-.0001293
	100m and 200m Buffer from Hydrothermal Zone ROI	Hydrothermal Zones ROI	.01534957*	.00216007	.000	.0101864	.0205128
		100m Buffer from Hydrothermal Zone ROI	.00544951*	.00222520	.043	.0001293	.0107697

*. The mean difference is significant at the 0.05 level.

Alunite/ Kaolinite/ Pyrophyllite (Jan 1, 2003)

Case Processing Summary

		Cases					
		Valid		Missing		Total	
	HZ_Zones	N	Percent	N	Percent	N	Percent
Pixel_Values	Hydrothermal Zones ROI	747	100.0%	0	.0%	747	100.0%
	100m Buffer from Hydrothermal Zone ROI	609	100.0%	0	.0%	609	100.0%
	100m and 200m Buffer from Hydrothermal Zone ROI	1207	100.0%	0	.0%	1207	100.0%

ANOVA

Pixel_Values

	Sum of Squares	df	Mean Square	F	Sig.
Between Groups	.190	2	.095	34.537	.000
Within Groups	7.026	2560	.003		
Total	7.216	2562			

Multiple Comparisons

Dependent Variable:Pixel_Values

	(I) HZ_Zones	(J) HZ_Zones	Mean Difference (I-J)	Std. Error	Sig.	95% Confidence Interval Lower Bound	95% Confidence Interval Upper Bound
Tamhane	Hydrothermal Zones ROI	100m Buffer from Hydrothermal Zone ROI	-.01656163*	.00290548	.000	-.0235079	-.0096154
		100m and 200m Buffer from Hydrothermal Zone ROI	-.01979853*	.00251175	.000	-.0258028	-.0137943
	100m Buffer from Hydrothermal Zone ROI	Hydrothermal Zones ROI	.01656163*	.00290548	.000	.0096154	.0235079
		100m and 200m Buffer from Hydrothermal Zone ROI	-.00323691	.00253422	.491	-.0092963	.0028225
	100m and 200m Buffer from Hydrothermal Zone ROI	Hydrothermal Zones ROI	.01979853*	.00251175	.000	.0137943	.0258028
		100m Buffer from Hydrothermal Zone ROI	.00323691	.00253422	.491	-.0028225	.0092963
Dunnett T3	Hydrothermal Zones ROI	100m Buffer from Hydrothermal Zone ROI	-.01656163*	.00290548	.000	-.0235076	-.0096157
		100m and 200m Buffer from Hydrothermal Zone ROI	-.01979853*	.00251175	.000	-.0258025	-.0137945
	100m Buffer from Hydrothermal Zone ROI	Hydrothermal Zones ROI	.01656163*	.00290548	.000	.0096157	.0235076
		100m and 200m Buffer from Hydrothermal Zone ROI	-.00323691	.00253422	.491	-.0092960	.0028222
	100m and 200m Buffer from Hydrothermal Zone ROI	Hydrothermal Zones ROI	.01979853*	.00251175	.000	.0137945	.0258025
		100m Buffer from Hydrothermal Zone ROI	.00323691	.00253422	.491	-.0028222	.0092960

*. The mean difference is significant at the 0.05 level.

Berecha Kaolinite

Kaolinite (Jan 12, 2003)

Case Processing Summary

		Cases					
		Valid		Missing		Total	
	HZ_Zones	N	Percent	N	Percent	N	Percent
Pixel_Values	Hydrothermal Zones ROI	808	100.0%	0	.0%	808	100.0%
	100m Buffer from Hydrothermal Zone ROI	413	100.0%	0	.0%	413	100.0%
	100m and 200m Buffer from Hydrothermal Zone ROI	903	100.0%	0	.0%	903	100.0%

ANOVA

Pixel_Values

	Sum of Squares	df	Mean Square	F	Sig.
Between Groups	.295	2	.148	214.815	.000
Within Groups	1.458	2121	.001		
Total	1.754	2123			

Multiple Comparisons

Dependent Variable:Pixel_Values

	(I) HZ_Zones	(J) HZ_Zones	Mean Difference (I-J)	Std. Error	Sig.	95% Confidence Interval Lower Bound	95% Confidence Interval Upper Bound
Tamhane	Hydrothermal Zones ROI	100m Buffer from Hydrothermal Zone ROI	.02359251*	.00155826	.000	.0198658	.0273192
		100m and 200m Buffer from Hydrothermal Zone ROI	.02459549*	.00132293	.000	.0214332	.0277578
	100m Buffer from Hydrothermal Zone ROI	Hydrothermal Zones ROI	-.02359251*	.00155826	.000	-.0273192	-.0198658
		100m and 200m Buffer from Hydrothermal Zone ROI	.00100298	.00137558	.848	-.0022884	.0042943
	100m and 200m Buffer from Hydrothermal Zone ROI	Hydrothermal Zones ROI	-.02459549*	.00132293	.000	-.0277578	-.0214332
		100m Buffer from Hydrothermal Zone ROI	-.00100298	.00137558	.848	-.0042943	.0022884
Dunnett T3	Hydrothermal Zones ROI	100m Buffer from Hydrothermal Zone ROI	.02359251*	.00155826	.000	.0198660	.0273190
		100m and 200m Buffer from Hydrothermal Zone ROI	.02459549*	.00132293	.000	.0214333	.0277577
	100m Buffer from Hydrothermal Zone ROI	Hydrothermal Zones ROI	-.02359251*	.00155826	.000	-.0273190	-.0198660
		100m and 200m Buffer from Hydrothermal Zone ROI	.00100298	.00137558	.848	-.0022881	.0042941
	100m and 200m Buffer from Hydrothermal Zone ROI	Hydrothermal Zones ROI	-.02459549*	.00132293	.000	-.0277577	-.0214333
		100m Buffer from Hydrothermal Zone ROI	-.00100298	.00137558	.848	-.0042941	.0022881

*. The mean difference is significant at the 0.05 level.

Kaolinite (Oct 16, 2005)

Case Processing Summary

		Cases					
		Valid		Missing		Total	
	HZ_Zones	N	Percent	N	Percent	N	Percent
Pixel_Values	Hydrothermal Zones ROI	791	100.0%	0	.0%	791	100.0%
	100m Buffer from Hydrothermal Zone ROI	431	100.0%	0	.0%	431	100.0%
	100m and 200m Buffer from Hydrothermal Zone ROI	921	100.0%	0	.0%	921	100.0%

ANOVA

Pixel_Values

	Sum of Squares	df	Mean Square	F	Sig.
Between Groups	.452	2	.226	136.182	.000
Within Groups	3.550	2140	.002		
Total	4.002	2142			

Multiple Comparisons

Dependent Variable:Pixel_Values

	(I) HZ_Zones	(J) HZ_Zones	Mean Difference (I-J)	Std. Error	Sig.	95% Confidence Interval Lower Bound	95% Confidence Interval Upper Bound
Tamhane	Hydrothermal Zones ROI	100m Buffer from Hydrothermal Zone ROI	.02452007*	.00246071	.000	.0186346	.0304055
		100m and 200m Buffer from Hydrothermal Zone ROI	.03190524*	.00202327	.000	.0270690	.0367415
	100m Buffer from Hydrothermal Zone ROI	Hydrothermal Zones ROI	-.02452007*	.00246071	.000	-.0304055	-.0186346
		100m and 200m Buffer from Hydrothermal Zone ROI	.00738517*	.00224567	.003	.0020121	.0127583
	100m and 200m Buffer from Hydrothermal Zone ROI	Hydrothermal Zones ROI	-.03190524*	.00202327	.000	-.0367415	-.0270690
		100m Buffer from Hydrothermal Zone ROI	-.00738517*	.00224567	.003	-.0127583	-.0020121
Dunnett T3	Hydrothermal Zones ROI	100m Buffer from Hydrothermal Zone ROI	.02452007*	.00246071	.000	.0186350	.0304052
		100m and 200m Buffer from Hydrothermal Zone ROI	.03190524*	.00202327	.000	.0270691	.0367413
	100m Buffer from Hydrothermal Zone ROI	Hydrothermal Zones ROI	-.02452007*	.00246071	.000	-.0304052	-.0186350
		100m and 200m Buffer from Hydrothermal Zone ROI	.00738517*	.00224567	.003	.0020125	.0127579
	100m and 200m Buffer from Hydrothermal Zone ROI	Hydrothermal Zones ROI	-.03190524*	.00202327	.000	-.0367413	-.0270691
		100m Buffer from Hydrothermal Zone ROI	-.00738517*	.00224567	.003	-.0127579	-.0020125

*. The mean difference is significant at the 0.05 level.

Kaolinite (Feb 5, 2006)

Case Processing Summary

	HZ_Zones	Cases					
		Valid		Missing		Total	
		N	Percent	N	Percent	N	Percent
Pixel_Values	Hydrothermal Zones ROI	813	100.0%	0	.0%	813	100.0%
	100m Buffer from Hydrothermal Zone ROI	411	100.0%	0	.0%	411	100.0%
	100m and 200m Buffer from Hydrothermal Zone ROI	895	100.0%	0	.0%	895	100.0%

Pixel_Values

	Sum of Squares	df	Mean Square	F	Sig.
Between Groups	.333	2	.166	275.139	.000
Within Groups	1.279	2116	.001		
Total	1.612	2118			

Multiple Comparisons

Dependent Variable:Pixel_Values

	(I) HZ_Zones	(J) HZ_Zones	Mean Difference (I-J)	Std. Error	Sig.	95% Confidence Interval Lower Bound	95% Confidence Interval Upper Bound
Tamhane	Hydrothermal Zones ROI	100m Buffer from Hydrothermal Zone ROI	.02563128*	.00147013	.000	.0221150	.0291475
		100m and 200m Buffer from Hydrothermal Zone ROI	.02582667*	.00122778	.000	.0228919	.0287614
	100m Buffer from Hydrothermal Zone ROI	Hydrothermal Zones ROI	-.02563128*	.00147013	.000	-.0291475	-.0221150
		100m and 200m Buffer from Hydrothermal Zone ROI	.00019540	.00133442	.998	-.0029975	.0033883
	100m and 200m Buffer from Hydrothermal Zone ROI	Hydrothermal Zones ROI	-.02582667*	.00122778	.000	-.0287614	-.0228919
		100m Buffer from Hydrothermal Zone ROI	-.00019540	.00133442	.998	-.0033883	.0029975
Dunnett T3	Hydrothermal Zones ROI	100m Buffer from Hydrothermal Zone ROI	.02563128*	.00147013	.000	.0221152	.0291473
		100m and 200m Buffer from Hydrothermal Zone ROI	.02582667*	.00122778	.000	.0228920	.0287613
	100m Buffer from Hydrothermal Zone ROI	Hydrothermal Zones ROI	-.02563128*	.00147013	.000	-.0291473	-.0221152
		100m and 200m Buffer from Hydrothermal Zone ROI	.00019540	.00133442	.998	-.0029973	.0033881
	100m and 200m Buffer from Hydrothermal Zone ROI	Hydrothermal Zones ROI	-.02582667*	.00122778	.000	-.0287613	-.0228920
		100m Buffer from Hydrothermal Zone ROI	-.00019540	.00133442	.998	-.0033881	.0029973

*. The mean difference is significant at the 0.05 level.

Tendaho Kaolinite

Kaolinite (Jan 25, 2002)

Case Processing Summary

		Cases					
		Valid		Missing		Total	
	HZ_Zones	N	Percent	N	Percent	N	Percent
Pixel_Values	Hydrothermal Zones ROI	743	100.0%	0	.0%	743	100.0%
	100m Buffer from Hydrothermal Zone ROI	608	100.0%	0	.0%	608	100.0%
	100m and 200m Buffer from Hydrothermal Zone ROI	1214	100.0%	0	.0%	1214	100.0%

ANOVA

Pixel_Values

	Sum of Squares	df	Mean Square	F	Sig.
Between Groups	.163	2	.081	24.005	.000
Within Groups	8.678	2562	.003		
Total	8.841	2564			

Multiple Comparisons

Dependent Variable:Pixel_Values

	(I) HZ_Zones	(J) HZ_Zones	Mean Difference (I-J)	Std. Error	Sig.	95% Confidence Interval Lower Bound	95% Confidence Interval Upper Bound
Tamhane	Hydrothermal Zones ROI	100m Buffer from Hydrothermal Zone ROI	-.01988683*	.00322559	.000	-.0275987	-.0121750
		100m and 200m Buffer from Hydrothermal Zone ROI	-.01584308*	.00271787	.000	-.0223397	-.0093464
	100m Buffer from Hydrothermal Zone ROI	Hydrothermal Zones ROI	.01988683*	.00322559	.000	.0121750	.0275987
		100m and 200m Buffer from Hydrothermal Zone ROI	.00404375	.00290353	.416	-.0028989	.0109864
	100m and 200m Buffer from Hydrothermal Zone ROI	Hydrothermal Zones ROI	.01584308*	.00271787	.000	.0093464	.0223397
		100m Buffer from Hydrothermal Zone ROI	-.00404375	.00290353	.416	-.0109864	.0028989
Dunnett T3	Hydrothermal Zones ROI	100m Buffer from Hydrothermal Zone ROI	-.01988683*	.00322559	.000	-.0275983	-.0121753
		100m and 200m Buffer from Hydrothermal Zone ROI	-.01584308*	.00271787	.000	-.0223395	-.0093467
	100m Buffer from Hydrothermal Zone ROI	Hydrothermal Zones ROI	.01988683*	.00322559	.000	.0121753	.0275983
		100m and 200m Buffer from Hydrothermal Zone ROI	.00404375	.00290353	.415	-.0028986	.0109861
	100m and 200m Buffer from Hydrothermal Zone ROI	Hydrothermal Zones ROI	.01584308*	.00271787	.000	.0093467	.0223395
		100m Buffer from Hydrothermal Zone ROI	-.00404375	.00290353	.415	-.0109861	.0028986

*. The mean difference is significant at the 0.05 level.

Kaolinite (Oct 11, 2003)

Case Processing Summary

		Cases					
		Valid		Missing		Total	
	HZ_Zones	N	Percent	N	Percent	N	Percent
Pixel_Values	Hydrothermal Zones ROI	742	100.0%	0	.0%	742	100.0%
	100m Buffer from Hydrothermal Zone ROI	606	100.0%	0	.0%	606	100.0%
	100m and 200m Buffer from Hydrothermal Zone ROI	1211	100.0%	0	.0%	1211	100.0%

ANOVA

Pixel_Values

	Sum of Squares	df	Mean Square	F	Sig.
Between Groups	.025	2	.012	25.423	.000
Within Groups	1.238	2556	.000		
Total	1.262	2558			

Multiple Comparisons

Dependent Variable:Pixel_Values

	(I) HZ_Zones	(J) HZ_Zones	Mean Difference (I-J)	Std. Error	Sig.	95% Confidence Interval Lower Bound	95% Confidence Interval Upper Bound
Tamhane	Hydrothermal Zones ROI	100m Buffer from Hydrothermal Zone ROI	-.00612723*	.00122706	.000	-.0090609	-.0031935
		100m and 200m Buffer from Hydrothermal Zone ROI	-.00710987*	.00103251	.000	-.0095780	-.0046418
	100m Buffer from Hydrothermal Zone ROI	Hydrothermal Zones ROI	.00612723*	.00122706	.000	.0031935	.0090609
		100m and 200m Buffer from Hydrothermal Zone ROI	-.00098264	.00109762	.751	-.0036072	.0016419
	100m and 200m Buffer from Hydrothermal Zone ROI	Hydrothermal Zones ROI	.00710987*	.00103251	.000	.0046418	.0095780
		100m Buffer from Hydrothermal Zone ROI	.00098264	.00109762	.751	-.0016419	.0036072
Dunnett T3	Hydrothermal Zones ROI	100m Buffer from Hydrothermal Zone ROI	-.00612723*	.00122706	.000	-.0090608	-.0031937
		100m and 200m Buffer from Hydrothermal Zone ROI	-.00710987*	.00103251	.000	-.0095779	-.0046419
	100m Buffer from Hydrothermal Zone ROI	Hydrothermal Zones ROI	.00612723*	.00122706	.000	.0031937	.0090608
		100m and 200m Buffer from Hydrothermal Zone ROI	-.00098264	.00109762	.751	-.0036071	.0016418
	100m and 200m Buffer from Hydrothermal Zone ROI	Hydrothermal Zones ROI	.00710987*	.00103251	.000	.0046419	.0095779
		100m Buffer from Hydrothermal Zone ROI	.00098264	.00109762	.751	-.0016418	.0036071

*. The mean difference is significant at the 0.05 level.

Kaolinite (Jan 1, 2005)

Case Processing Summary

	HZ_Zones	Cases					
		Valid		Missing		Total	
		N	Percent	N	Percent	N	Percent
Pixel_Values	Hydrothermal Zones ROI	747	100.0%	0	.0%	747	100.0%
	100m Buffer from Hydrothermal Zone ROI	609	100.0%	0	.0%	609	100.0%
	100m and 200m Buffer from Hydrothermal Zone ROI	1207	100.0%	0	.0%	1207	100.0%

ANOVA

Pixel_Values

	Sum of Squares	df	Mean Square	F	Sig.
Between Groups	.045	2	.022	31.595	.000
Within Groups	1.803	2560	.001		
Total	1.848	2562			

Multiple Comparisons

Dependent Variable:Pixel_Values

	(I) HZ_Zones	(J) HZ_Zones	Mean Difference (I-J)	Std. Error	Sig.	95% Confidence Interval	
						Lower Bound	Upper Bound
Tamhane	Hydrothermal Zones ROI	100m Buffer from Hydrothermal Zone ROI	-.00827320*	.00145940	.000	-.0117623	-.0047841
		100m and 200m Buffer from Hydrothermal Zone ROI	-.00952467*	.00124751	.000	-.0125066	-.0065427
	100m Buffer from Hydrothermal Zone ROI	Hydrothermal Zones ROI	.00827320*	.00145940	.000	.0047841	.0117623
		100m and 200m Buffer from Hydrothermal Zone ROI	-.00125147	.00130936	.712	-.0043822	.0018793
	100m and 200m Buffer from Hydrothermal Zone ROI	Hydrothermal Zones ROI	.00952467*	.00124751	.000	.0065427	.0125066
		100m Buffer from Hydrothermal Zone ROI	.00125147	.00130936	.712	-.0018793	.0043822
Dunnett T3	Hydrothermal Zones ROI	100m Buffer from Hydrothermal Zone ROI	-.00827320*	.00145940	.000	-.0117622	-.0047842
		100m and 200m Buffer from Hydrothermal Zone ROI	-.00952467*	.00124751	.000	-.0125065	-.0065428
	100m Buffer from Hydrothermal Zone ROI	Hydrothermal Zones ROI	.00827320*	.00145940	.000	.0047842	.0117622
		100m and 200m Buffer from Hydrothermal Zone ROI	-.00125147	.00130936	.711	-.0043821	.0018791
	100m and 200m Buffer from Hydrothermal Zone ROI	Hydrothermal Zones ROI	.00952467*	.00124751	.000	.0065428	.0125065
		100m Buffer from Hydrothermal Zone ROI	.00125147	.00130936	.711	-.0018791	.0043821

*. The mean difference is significant at the 0.05 level.

Berecha Alteration

Alteration (Jan 12, 2003)

Case Processing Summary

	HZ_Zones	Cases					
		Valid		Missing		Total	
		N	Percent	N	Percent	N	Percent
Pixel_Values	Hydrothermal Zones ROI	808	100.0%	0	.0%	808	100.0%
	100m Buffer from Hydrothermal Zone ROI	413	100.0%	0	.0%	413	100.0%
	100m and 200m Buffer from Hydrothermal Zone ROI	903	100.0%	0	.0%	903	100.0%

ANOVA

Pixel_Values

	Sum of Squares	df	Mean Square	F	Sig.
Between Groups	6.467	2	3.234	702.026	.000
Within Groups	9.769	2121	.005		
Total	16.236	2123			

Multiple Comparisons

Dependent Variable:Pixel_Values

	(I) HZ_Zones	(J) HZ_Zones	Mean Difference (I-J)	Std. Error	Sig.	95% Confidence Interval	
						Lower Bound	Upper Bound
Tamhane	Hydrothermal Zones ROI	100m Buffer from Hydrothermal Zone ROI	.10289139*	.00415644	.000	.0929510	.1128318
		100m and 200m Buffer from Hydrothermal Zone ROI	.11777533*	.00341905	.000	.1096020	.1259487
	100m Buffer from Hydrothermal Zone ROI	Hydrothermal Zones ROI	-.10289139*	.00415644	.000	-.1128318	-.0929510
		100m and 200m Buffer from Hydrothermal Zone ROI	.01488394*	.00357491	.000	.0063288	.0234391
	100m and 200m Buffer from Hydrothermal Zone ROI	Hydrothermal Zones ROI	-.11777533*	.00341905	.000	-.1259487	-.1096020
		100m Buffer from Hydrothermal Zone ROI	-.01488394*	.00357491	.000	-.0234391	-.0063288
Dunnett T3	Hydrothermal Zones ROI	100m Buffer from Hydrothermal Zone ROI	.10289139*	.00415644	.000	.0929515	.1128313
		100m and 200m Buffer from Hydrothermal Zone ROI	.11777533*	.00341905	.000	.1096023	.1259484
	100m Buffer from Hydrothermal Zone ROI	Hydrothermal Zones ROI	-.10289139*	.00415644	.000	-.1128313	-.0929515
		100m and 200m Buffer from Hydrothermal Zone ROI	.01488394*	.00357491	.000	.0063294	.0234385
	100m and 200m Buffer from Hydrothermal Zone ROI	Hydrothermal Zones ROI	-.11777533*	.00341905	.000	-.1259484	-.1096023
		100m Buffer from Hydrothermal Zone ROI	-.01488394*	.00357491	.000	-.0234385	-.0063294

*. The mean difference is significant at the 0.05 level.

Alteration (Oct 16, 2005)

Case Processing Summary

	HZ_Zones	Cases					
		Valid		Missing		Total	
		N	Percent	N	Percent	N	Percent
Pixel_Values	Hydrothermal Zones ROI	791	100.0%	0	.0%	791	100.0%
	100m Buffer from Hydrothermal Zone ROI	431	100.0%	0	.0%	431	100.0%
	100m and 200m Buffer from Hydrothermal Zone ROI	921	100.0%	0	.0%	921	100.0%

ANOVA

Pixel_Values

	Sum of Squares	df	Mean Square	F	Sig.
Between Groups	2.148	2	1.074	113.077	.000
Within Groups	20.327	2140	.009		
Total	22.475	2142			

Multiple Comparisons

Dependent Variable:Pixel_Values

	(I) HZ_Zones	(J) HZ_Zones	Mean Difference (I-J)	Std. Error	Sig.	95% Confidence Interval Lower Bound	95% Confidence Interval Upper Bound
Tamhane	Hydrothermal Zones ROI	100m Buffer from Hydrothermal Zone ROI	.06158695*	.00575059	.000	.0478204	.0753535
		100m and 200m Buffer from Hydrothermal Zone ROI	.06727776*	.00446091	.000	.0566151	.0779404
	100m Buffer from Hydrothermal Zone ROI	Hydrothermal Zones ROI	-.06158695*	.00575059	.000	-.0753535	-.0478204
		100m and 200m Buffer from Hydrothermal Zone ROI	.00569081	.00631707	.747	-.0094218	.0208034
	100m and 200m Buffer from Hydrothermal Zone ROI	Hydrothermal Zones ROI	-.06727776*	.00446091	.000	-.0779404	-.0566151
		100m Buffer from Hydrothermal Zone ROI	-.00569081	.00631707	.747	-.0208034	.0094218
Dunnett T3	Hydrothermal Zones ROI	100m Buffer from Hydrothermal Zone ROI	.06158695*	.00575059	.000	.0478216	.0753523
		100m and 200m Buffer from Hydrothermal Zone ROI	.06727776*	.00446091	.000	.0566155	.0779401
	100m Buffer from Hydrothermal Zone ROI	Hydrothermal Zones ROI	-.06158695*	.00575059	.000	-.0753523	-.0478216
		100m and 200m Buffer from Hydrothermal Zone ROI	.00569081	.00631707	.747	-.0094208	.0208025
	100m and 200m Buffer from Hydrothermal Zone ROI	Hydrothermal Zones ROI	-.06727776*	.00446091	.000	-.0779401	-.0566155
		100m Buffer from Hydrothermal Zone ROI	-.00569081	.00631707	.747	-.0208025	.0094208

*. The mean difference is significant at the 0.05 level.

Alteration (Feb 5, 2006)

Case Processing Summary

	HZ_Zones	Cases					
		Valid		Missing		Total	
		N	Percent	N	Percent	N	Percent
Pixel_Values	Hydrothermal Zones ROI	813	100.0%	0	.0%	813	100.0%
	100m Buffer from Hydrothermal Zone ROI	411	100.0%	0	.0%	411	100.0%
	100m and 200m Buffer from Hydrothermal Zone ROI	895	100.0%	0	.0%	895	100.0%

ANOVA

Pixel_Values

	Sum of Squares	df	Mean Square	F	Sig.
Between Groups	4.377	2	2.188	439.798	.000
Within Groups	10.528	2116	.005		
Total	14.905	2118			

Multiple Comparisons

Dependent Variable:Pixel_Values

	(I) HZ_Zones	(J) HZ_Zones	Mean Difference (I-J)	Std. Error	Sig.	95% Confidence Interval	
						Lower Bound	Upper Bound
Tamhane	Hydrothermal Zones ROI	100m Buffer from Hydrothermal Zone ROI	.08594496*	.00433968	.000	.0755632	.0963267
		100m and 200m Buffer from Hydrothermal Zone ROI	.09642459*	.00344656	.000	.0881866	.1046625
	100m Buffer from Hydrothermal Zone ROI	Hydrothermal Zones ROI	-.08594496*	.00433968	.000	-.0963267	-.0755632
		100m and 200m Buffer from Hydrothermal Zone ROI	.01047964*	.00409571	.032	.0006786	.0202807
	100m and 200m Buffer from Hydrothermal Zone ROI	Hydrothermal Zones ROI	-.09642459*	.00344656	.000	-.1046625	-.0881866
		100m Buffer from Hydrothermal Zone ROI	-.01047964*	.00409571	.032	-.0202807	-.0006786
Dunnett T3	Hydrothermal Zones ROI	100m Buffer from Hydrothermal Zone ROI	.08594496*	.00433968	.000	.0755638	.0963261
		100m and 200m Buffer from Hydrothermal Zone ROI	.09642459*	.00344656	.000	.0881869	.1046622
	100m Buffer from Hydrothermal Zone ROI	Hydrothermal Zones ROI	-.08594496*	.00433968	.000	-.0963261	-.0755638
		100m and 200m Buffer from Hydrothermal Zone ROI	.01047964*	.00409571	.032	.0006793	.0202800
	100m and 200m Buffer from Hydrothermal Zone ROI	Hydrothermal Zones ROI	-.09642459*	.00344656	.000	-.1046622	-.0881869
		100m Buffer from Hydrothermal Zone ROI	-.01047964*	.00409571	.032	-.0202800	-.0006793

*. The mean difference is significant at the 0.05 level.

Tendaho Alteration

Alteration (Jan 25, 2002)

Case Processing Summary

		Cases					
		Valid		Missing		Total	
	HZ_Zones	N	Percent	N	Percent	N	Percent
Pixel_Values	Hydrothermal Zones ROI	743	100.0%	0	.0%	743	100.0%
	100m Buffer from Hydrothermal Zone ROI	608	100.0%	0	.0%	608	100.0%
	100m and 200m Buffer from Hydrothermal Zone ROI	1214	100.0%	0	.0%	1214	100.0%

ANOVA

Pixel_Values

	Sum of Squares	df	Mean Square	F	Sig.
Between Groups	.030	2	.015	9.869	.000
Within Groups	3.910	2562	.002		
Total	3.940	2564			

Multiple Comparisons

Dependent Variable:Pixel_Values

	(I) HZ_Zones	(J) HZ_Zones	Mean Difference (I-J)	Std. Error	Sig.	95% Confidence Interval Lower Bound	95% Confidence Interval Upper Bound
Tamhane	Hydrothermal Zones ROI	100m Buffer from Hydrothermal Zone ROI	-.00601864*	.00223288	.021	-.0113569	-.0006804
		100m and 200m Buffer from Hydrothermal Zone ROI	-.00801613*	.00199550	.000	-.0127872	-.0032451
	100m Buffer from Hydrothermal Zone ROI	Hydrothermal Zones ROI	.00601864*	.00223288	.021	.0006804	.0113569
		100m and 200m Buffer from Hydrothermal Zone ROI	-.00199749	.00175714	.588	-.0061988	.0022038
	100m and 200m Buffer from Hydrothermal Zone ROI	Hydrothermal Zones ROI	.00801613*	.00199550	.000	.0032451	.0127872
		100m Buffer from Hydrothermal Zone ROI	.00199749	.00175714	.588	-.0022038	.0061988
Dunnett T3	Hydrothermal Zones ROI	100m Buffer from Hydrothermal Zone ROI	-.00601864*	.00223288	.021	-.0113566	-.0006807
		100m and 200m Buffer from Hydrothermal Zone ROI	-.00801613*	.00199550	.000	-.0127870	-.0032453
	100m Buffer from Hydrothermal Zone ROI	Hydrothermal Zones ROI	.00601864*	.00223288	.021	.0006807	.0113566
		100m and 200m Buffer from Hydrothermal Zone ROI	-.00199749	.00175714	.588	-.0061986	.0022037
	100m and 200m Buffer from Hydrothermal Zone ROI	Hydrothermal Zones ROI	.00801613*	.00199550	.000	.0032453	.0127870
		100m Buffer from Hydrothermal Zone ROI	.00199749	.00175714	.588	-.0022037	.0061986

*. The mean difference is significant at the 0.05 level.

Alteration (Oct 11, 2003)

Case Processing Summary

		Cases					
		Valid		Missing		Total	
	HZ_Zones	N	Percent	N	Percent	N	Percent
Pixel_Values	Hydrothermal Zones ROI	742	100.0%	0	.0%	742	100.0%
	100m Buffer from Hydrothermal Zone ROI	606	100.0%	0	.0%	606	100.0%
	100m and 200m Buffer from Hydrothermal Zone ROI	1211	100.0%	0	.0%	1211	100.0%

ANOVA

Pixel_Values

	Sum of Squares	df	Mean Square	F	Sig.
Between Groups	.020	2	.010	8.439	.000
Within Groups	3.069	2556	.001		
Total	3.090	2558			

Multiple Comparisons

Dependent Variable:Pixel_Values

	(I) HZ_Zones	(J) HZ_Zones	Mean Difference (I-J)	Std. Error	Sig.	95% Confidence Interval Lower Bound	95% Confidence Interval Upper Bound
Tamhane	Hydrothermal Zones ROI	100m Buffer from Hydrothermal Zone ROI	-.00401206	.00197188	.121	-.0087263	.0007021
		100m and 200m Buffer from Hydrothermal Zone ROI	-.00663643*	.00173675	.000	-.0107886	-.0024842
	100m Buffer from Hydrothermal Zone ROI	Hydrothermal Zones ROI	.00401206	.00197188	.121	-.0007021	.0087263
		100m and 200m Buffer from Hydrothermal Zone ROI	-.00262437	.00160441	.276	-.0064606	.0012119
	100m and 200m Buffer from Hydrothermal Zone ROI	Hydrothermal Zones ROI	.00663643*	.00173675	.000	.0024842	.0107886
		100m Buffer from Hydrothermal Zone ROI	.00262437	.00160441	.276	-.0012119	.0064606
Dunnett T3	Hydrothermal Zones ROI	100m Buffer from Hydrothermal Zone ROI	-.00401206	.00197188	.121	-.0087261	.0007019
		100m and 200m Buffer from Hydrothermal Zone ROI	-.00663643*	.00173675	.000	-.0107884	-.0024844
	100m Buffer from Hydrothermal Zone ROI	Hydrothermal Zones ROI	.00401206	.00197188	.121	-.0007019	.0087261
		100m and 200m Buffer from Hydrothermal Zone ROI	-.00262437	.00160441	.276	-.0064604	.0012117
	100m and 200m Buffer from Hydrothermal Zone ROI	Hydrothermal Zones ROI	.00663643*	.00173675	.000	.0024844	.0107884
		100m Buffer from Hydrothermal Zone ROI	.00262437	.00160441	.276	-.0012117	.0064604

*. The mean difference is significant at the 0.05 level.

Alteration (Jan 1, 2005)

Case Processing Summary

	HZ_Zones	Cases					
		Valid		Missing		Total	
		N	Percent	N	Percent	N	Percent
Pixel_Values	Hydrothermal Zones ROI	747	100.0%	0	.0%	747	100.0%
	100m Buffer from Hydrothermal Zone ROI	609	100.0%	0	.0%	609	100.0%
	100m and 200m Buffer from Hydrothermal Zone ROI	1207	100.0%	0	.0%	1207	100.0%

ANOVA

Pixel_Values

	Sum of Squares	df	Mean Square	F	Sig.
Between Groups	.056	2	.028	17.463	.000
Within Groups	4.136	2560	.002		
Total	4.193	2562			

Multiple Comparisons

Dependent Variable:Pixel_Values

	(I) HZ_Zones	(J) HZ_Zones	Mean Difference (I-J)	Std. Error	Sig.	95% Confidence Interval	
						Lower Bound	Upper Bound
Tamhane	Hydrothermal Zones ROI	100m Buffer from Hydrothermal Zone ROI	-.00953089*	.00231717	.000	-.0150705	-.0039912
		100m and 200m Buffer from Hydrothermal Zone ROI	-.01065603*	.00202489	.000	-.0154973	-.0058148
	100m Buffer from Hydrothermal Zone ROI	Hydrothermal Zones ROI	.00953089*	.00231717	.000	.0039912	.0150705
		100m and 200m Buffer from Hydrothermal Zone ROI	-.00112514	.00185666	.906	-.0055647	.0033144
	100m and 200m Buffer from Hydrothermal Zone ROI	Hydrothermal Zones ROI	.01065603*	.00202489	.000	.0058148	.0154973
		100m Buffer from Hydrothermal Zone ROI	.00112514	.00185666	.906	-.0033144	.0055647
Dunnett T3	Hydrothermal Zones ROI	100m Buffer from Hydrothermal Zone ROI	-.00953089*	.00231717	.000	-.0150703	-.0039915
		100m and 200m Buffer from Hydrothermal Zone ROI	-.01065603*	.00202489	.000	-.0154971	-.0058150
	100m Buffer from Hydrothermal Zone ROI	Hydrothermal Zones ROI	.00953089*	.00231717	.000	.0039915	.0150703
		100m and 200m Buffer from Hydrothermal Zone ROI	-.00112514	.00185666	.905	-.0055645	.0033142
	100m and 200m Buffer from Hydrothermal Zone ROI	Hydrothermal Zones ROI	.01065603*	.00202489	.000	.0058150	.0154971
		100m Buffer from Hydrothermal Zone ROI	.00112514	.00185666	.905	-.0033142	.0055645

*. The mean difference is significant at the 0.05 level.

Berecha Silica

Silica (11/10) (Jan 12, 2003)

Case Processing Summary

		Cases					
		Valid		Missing		Total	
	HZ_Zones	N	Percent	N	Percent	N	Percent
Pixel_Values	Hydrothermal Zones ROI	96	100.0%	0	.0%	96	100.0%
	100m Buffer from Hydrothermal Zone ROI	46	100.0%	0	.0%	46	100.0%
	100m and 200m Buffer from Hydrothermal Zone ROI	100	100.0%	0	.0%	100	100.0%

ANOVA

Pixel_Values

	Sum of Squares	df	Mean Square	F	Sig.
Between Groups	.000	2	.000	6.821	.001
Within Groups	.005	239	.000		
Total	.005	241			

Multiple Comparisons

Dependent Variable:Pixel_Values

	(I) HZ_Zones	(J) HZ_Zones	Mean Difference (I-J)	Std. Error	Sig.	95% Confidence Interval Lower Bound	95% Confidence Interval Upper Bound
Tamhane	Hydrothermal Zones ROI	100m Buffer from Hydrothermal Zone ROI	.00140788	.00075260	.182	-.0004234	.0032392
		100m and 200m Buffer from Hydrothermal Zone ROI	.00236975*	.00065134	.001	.0008008	.0039387
	100m Buffer from Hydrothermal Zone ROI	Hydrothermal Zones ROI	-.00140788	.00075260	.182	-.0032392	.0004234
		100m and 200m Buffer from Hydrothermal Zone ROI	.00096187	.00078757	.534	-.0009503	.0028740
	100m and 200m Buffer from Hydrothermal Zone ROI	Hydrothermal Zones ROI	-.00236975*	.00065134	.001	-.0039387	-.0008008
		100m Buffer from Hydrothermal Zone ROI	-.00096187	.00078757	.534	-.0028740	.0009503
Dunnett T3	Hydrothermal Zones ROI	100m Buffer from Hydrothermal Zone ROI	.00140788	.00075260	.181	-.0004222	.0032379
		100m and 200m Buffer from Hydrothermal Zone ROI	.00236975*	.00065134	.001	.0008013	.0039382
	100m Buffer from Hydrothermal Zone ROI	Hydrothermal Zones ROI	-.00140788	.00075260	.181	-.0032379	.0004222
		100m and 200m Buffer from Hydrothermal Zone ROI	.00096187	.00078757	.532	-.0009492	.0028729
	100m and 200m Buffer from Hydrothermal Zone ROI	Hydrothermal Zones ROI	-.00236975*	.00065134	.001	-.0039382	-.0008013
		100m Buffer from Hydrothermal Zone ROI	-.00096187	.00078757	.532	-.0028729	.0009492

*. The mean difference is significant at the 0.05 level.

Silica (11/10) (Oct 16, 2005)

Case Processing Summary

	HZ_Zones	Cases					
		Valid		Missing		Total	
		N	Percent	N	Percent	N	Percent
Pixel_Values	Hydrothermal Zones ROI	95	100.0%	0	.0%	95	100.0%
	100m Buffer from Hydrothermal Zone ROI	44	100.0%	0	.0%	44	100.0%
	100m and 200m Buffer from Hydrothermal Zone ROI	100	100.0%	0	.0%	100	100.0%

ANOVA

Pixel_Values

	Sum of Squares	df	Mean Square	F	Sig.
Between Groups	.000	2	.000	7.401	.001
Within Groups	.008	236	.000		
Total	.008	238			

Multiple Comparisons

Dependent Variable:Pixel_Values

	(I) HZ_Zones	(J) HZ_Zones	Mean Difference (I-J)	Std. Error	Sig.	95% Confidence Interval	
						Lower Bound	Upper Bound
Tamhane	Hydrothermal Zones ROI	100m Buffer from Hydrothermal Zone ROI	.00271031*	.00105673	.036	.0001302	.0052905
		100m and 200m Buffer from Hydrothermal Zone ROI	.00298995*	.00080929	.001	.0010406	.0049393
	100m Buffer from Hydrothermal Zone ROI	Hydrothermal Zones ROI	-.00271031*	.00105673	.036	-.0052905	-.0001302
		100m and 200m Buffer from Hydrothermal Zone ROI	.00027964	.00108187	.992	-.0023576	.0029169
	100m and 200m Buffer from Hydrothermal Zone ROI	Hydrothermal Zones ROI	-.00298995*	.00080929	.001	-.0049393	-.0010406
		100m Buffer from Hydrothermal Zone ROI	-.00027964	.00108187	.992	-.0029169	.0023576
Dunnett T3	Hydrothermal Zones ROI	100m Buffer from Hydrothermal Zone ROI	.00271031*	.00105673	.036	.0001323	.0052883
		100m and 200m Buffer from Hydrothermal Zone ROI	.00298995*	.00080929	.001	.0010412	.0049387
	100m Buffer from Hydrothermal Zone ROI	Hydrothermal Zones ROI	-.00271031*	.00105673	.036	-.0052883	-.0001323
		100m and 200m Buffer from Hydrothermal Zone ROI	.00027964	.00108187	.991	-.0023556	.0029149
	100m and 200m Buffer from Hydrothermal Zone ROI	Hydrothermal Zones ROI	-.00298995*	.00080929	.001	-.0049387	-.0010412
		100m Buffer from Hydrothermal Zone ROI	-.00027964	.00108187	.991	-.0029149	.0023556

*. The mean difference is significant at the 0.05 level.

Silica (11/10) (Feb 5, 2006)

Case Processing Summary

		Cases					
		Valid		Missing		Total	
	HZ_Zones	N	Percent	N	Percent	N	Percent
Pixel_Values	Hydrothermal Zones ROI	93	100.0%	0	.0%	93	100.0%
	100m Buffer from Hydrothermal Zone ROI	49	100.0%	0	.0%	49	100.0%
	100m and 200m Buffer from Hydrothermal Zone ROI	98	100.0%	0	.0%	98	100.0%

ANOVA

Pixel_Values

	Sum of Squares	df	Mean Square	F	Sig.
Between Groups	.000	2	.000	1.503	.225
Within Groups	.008	237	.000		
Total	.008	239			

Multiple Comparisons

Dependent Variable:Pixel_Values

	(I) HZ_Zones	(J) HZ_Zones	Mean Difference (I-J)	Std. Error	Sig.	95% Confidence Interval Lower Bound	95% Confidence Interval Upper Bound
Tamhane	Hydrothermal Zones ROI	100m Buffer from Hydrothermal Zone ROI	-.00018508	.00104694	.997	-.0027353	.0023651
		100m and 200m Buffer from Hydrothermal Zone ROI	-.00137896	.00082085	.258	-.0033566	.0005987
	100m Buffer from Hydrothermal Zone ROI	Hydrothermal Zones ROI	.00018508	.00104694	.997	-.0023651	.0027353
		100m and 200m Buffer from Hydrothermal Zone ROI	-.00119388	.00108138	.615	-.0038230	.0014353
	100m and 200m Buffer from Hydrothermal Zone ROI	Hydrothermal Zones ROI	.00137896	.00082085	.258	-.0005987	.0033566
		100m Buffer from Hydrothermal Zone ROI	.00119388	.00108138	.615	-.0014353	.0038230
Dunnett T3	Hydrothermal Zones ROI	100m Buffer from Hydrothermal Zone ROI	-.00018508	.00104694	.997	-.0027334	.0023632
		100m and 200m Buffer from Hydrothermal Zone ROI	-.00137896	.00082085	.257	-.0033560	.0005980
	100m Buffer from Hydrothermal Zone ROI	Hydrothermal Zones ROI	.00018508	.00104694	.997	-.0023632	.0027334
		100m and 200m Buffer from Hydrothermal Zone ROI	-.00119388	.00108138	.612	-.0038213	.0014335
	100m and 200m Buffer from Hydrothermal Zone ROI	Hydrothermal Zones ROI	.00137896	.00082085	.257	-.0005980	.0033560
		100m Buffer from Hydrothermal Zone ROI	.00119388	.00108138	.612	-.0014335	.0038213

Tendaho Silica

Silica (11/10) (Jan 25, 2002)

Case Processing Summary

	HZ_Zones	Cases					
		Valid		Missing		Total	
		N	Percent	N	Percent	N	Percent
Pixel_Values	Hydrothermal Zones ROI	91	100.0%	0	.0%	91	100.0%
	100m Buffer from Hydrothermal Zone ROI	62	100.0%	0	.0%	62	100.0%
	100m and 200m Buffer from Hydrothermal Zone ROI	130	100.0%	0	.0%	130	100.0%

ANOVA

Pixel_Values

	Sum of Squares	df	Mean Square	F	Sig.
Between Groups	.000	2	.000	6.499	.002
Within Groups	.010	280	.000		
Total	.010	282			

Multiple Comparisons

Dependent Variable:Pixel_Values

	(I) HZ_Zones	(J) HZ_Zones	Mean Difference (I-J)	Std. Error	Sig.	95% Confidence Interval Lower Bound	Upper Bound
Tamhane	Hydrothermal Zones ROI	100m Buffer from Hydrothermal Zone ROI	.00266111*	.00097102	.021	.0003163	.0050059
		100m and 200m Buffer from Hydrothermal Zone ROI	.00274791*	.00086743	.005	.0006559	.0048399
	100m Buffer from Hydrothermal Zone ROI	Hydrothermal Zones ROI	-.00266111*	.00097102	.021	-.0050059	-.0003163
		100m and 200m Buffer from Hydrothermal Zone ROI	.00008680	.00081840	.999	-.0018930	.0020666
	100m and 200m Buffer from Hydrothermal Zone ROI	Hydrothermal Zones ROI	-.00274791*	.00086743	.005	-.0048399	-.0006559
		100m Buffer from Hydrothermal Zone ROI	-.00008680	.00081840	.999	-.0020666	.0018930
Dunnett T3	Hydrothermal Zones ROI	100m Buffer from Hydrothermal Zone ROI	.00266111*	.00097102	.020	.0003172	.0050050
		100m and 200m Buffer from Hydrothermal Zone ROI	.00274791*	.00086743	.005	.0006566	.0048392
	100m Buffer from Hydrothermal Zone ROI	Hydrothermal Zones ROI	-.00266111*	.00097102	.020	-.0050050	-.0003172
		100m and 200m Buffer from Hydrothermal Zone ROI	.00008680	.00081840	.999	-.0018921	.0020657
	100m and 200m Buffer from Hydrothermal Zone ROI	Hydrothermal Zones ROI	-.00274791*	.00086743	.005	-.0048392	-.0006566
		100m Buffer from Hydrothermal Zone ROI	-.00008680	.00081840	.999	-.0020657	.0018921

*. The mean difference is significant at the 0.05 level.

Silica (11/10) (Oct 11, 2003)

Case Processing Summary

	HZ_Zones	Cases					
		Valid		Missing		Total	
		N	Percent	N	Percent	N	Percent
Pixel_Values	Hydrothermal Zones ROI	88	100.0%	0	.0%	88	100.0%
	100m Buffer from Hydrothermal Zone ROI	63	100.0%	0	.0%	63	100.0%
	100m and 200m Buffer from Hydrothermal Zone ROI	133	100.0%	0	.0%	133	100.0%

ANOVA

Pixel_Values

	Sum of Squares	df	Mean Square	F	Sig.
Between Groups	.004	2	.002	23.454	.000
Within Groups	.024	281	.000		
Total	.028	283			

Multiple Comparisons

Dependent Variable:Pixel_Values

	(I) HZ_Zones	(J) HZ_Zones	Mean Difference (I-J)	Std. Error	Sig.	95% Confidence Interval Lower Bound	95% Confidence Interval Upper Bound
Tamhane	Hydrothermal Zones ROI	100m Buffer from Hydrothermal Zone ROI	.00674738*	.00164210	.000	.0027814	.0107133
		100m and 200m Buffer from Hydrothermal Zone ROI	.00851689*	.00137323	.000	.0051985	.0118353
	100m Buffer from Hydrothermal Zone ROI	Hydrothermal Zones ROI	-.00674738*	.00164210	.000	-.0107133	-.0027814
		100m and 200m Buffer from Hydrothermal Zone ROI	.00176951	.00130620	.445	-.0013987	.0049377
	100m and 200m Buffer from Hydrothermal Zone ROI	Hydrothermal Zones ROI	-.00851689*	.00137323	.000	-.0118353	-.0051985
		100m Buffer from Hydrothermal Zone ROI	-.00176951	.00130620	.445	-.0049377	.0013987
Dunnett T3	Hydrothermal Zones ROI	100m Buffer from Hydrothermal Zone ROI	.00674738*	.00164210	.000	.0027830	.0107117
		100m and 200m Buffer from Hydrothermal Zone ROI	.00851689*	.00137323	.000	.0051999	.0118339
	100m Buffer from Hydrothermal Zone ROI	Hydrothermal Zones ROI	-.00674738*	.00164210	.000	-.0107117	-.0027830
		100m and 200m Buffer from Hydrothermal Zone ROI	.00176951	.00130620	.443	-.0013969	.0049359
	100m and 200m Buffer from Hydrothermal Zone ROI	Hydrothermal Zones ROI	-.00851689*	.00137323	.000	-.0118339	-.0051999
		100m Buffer from Hydrothermal Zone ROI	-.00176951	.00130620	.443	-.0049359	.0013969

*. The mean difference is significant at the 0.05 level.

Silica (11/10) (Jan 1, 2005)

Case Processing Summary

		Cases					
		Valid		Missing		Total	
	HZ_Zones	N	Percent	N	Percent	N	Percent
Pixel_Values	Hydrothermal Zones ROI	92	100.0%	0	.0%	92	100.0%
	100m Buffer from Hydrothermal Zone ROI	62	100.0%	0	.0%	62	100.0%
	100m and 200m Buffer from Hydrothermal Zone ROI	127	100.0%	0	.0%	127	100.0%

ANOVA

Pixel_Values

	Sum of Squares	df	Mean Square	F	Sig.
Between Groups	.003	2	.002	18.519	.000
Within Groups	.026	278	.000		
Total	.029	280			

Multiple Comparisons

Dependent Variable:Pixel_Values

	(I) HZ_Zones	(J) HZ_Zones	Mean Difference (I-J)	Std. Error	Sig.	95% Confidence Interval Lower Bound	95% Confidence Interval Upper Bound
Tamhane	Hydrothermal Zones ROI	100m Buffer from Hydrothermal Zone ROI	.00579516*	.00171055	.003	.0016647	.0099256
		100m and 200m Buffer from Hydrothermal Zone ROI	.00791969*	.00142917	.000	.0044666	.0113728
	100m Buffer from Hydrothermal Zone ROI	Hydrothermal Zones ROI	-.00579516*	.00171055	.003	-.0099256	-.0016647
		100m and 200m Buffer from Hydrothermal Zone ROI	.00212452	.00133964	.309	-.0011266	.0053757
	100m and 200m Buffer from Hydrothermal Zone ROI	Hydrothermal Zones ROI	-.00791969*	.00142917	.000	-.0113728	-.0044666
		100m Buffer from Hydrothermal Zone ROI	-.00212452	.00133964	.309	-.0053757	.0011266
Dunnett T3	Hydrothermal Zones ROI	100m Buffer from Hydrothermal Zone ROI	.00579516*	.00171055	.003	.0016663	.0099240
		100m and 200m Buffer from Hydrothermal Zone ROI	.00791969*	.00142917	.000	.0044680	.0113714
	100m Buffer from Hydrothermal Zone ROI	Hydrothermal Zones ROI	-.00579516*	.00171055	.003	-.0099240	-.0016663
		100m and 200m Buffer from Hydrothermal Zone ROI	.00212452	.00133964	.307	-.0011247	.0053738
	100m and 200m Buffer from Hydrothermal Zone ROI	Hydrothermal Zones ROI	-.00791969*	.00142917	.000	-.0113714	-.0044680
		100m Buffer from Hydrothermal Zone ROI	-.00212452	.00133964	.307	-.0053738	.0011247

*. The mean difference is significant at the 0.05 level.

Berecha (Silica (11/12))

(Silica (11/12)) (Jan 12, 2003)

Case Processing Summary

	HZ_Zones	Cases					
		Valid		Missing		Total	
		N	Percent	N	Percent	N	Percent
Pixel_Values	Hydrothermal Zones ROI	92	100.0%	0	.0%	92	100.0%
	100m Buffer from Hydrothermal Zone ROI	62	100.0%	0	.0%	62	100.0%
	100m and 200m Buffer from Hydrothermal Zone ROI	127	100.0%	0	.0%	127	100.0%

ANOVA

Pixel_Values

	Sum of Squares	df	Mean Square	F	Sig.
Between Groups	.000	2	.000	1.122	.327
Within Groups	.007	278	.000		
Total	.007	280			

Multiple Comparisons

Dependent Variable:Pixel_Values

	(I) HZ_Zones	(J) HZ_Zones	Mean Difference (I-J)	Std. Error	Sig.	95% Confidence Interval	
						Lower Bound	Upper Bound
Tamhane	Hydrothermal Zones ROI	100m Buffer from Hydrothermal Zone ROI	-.00097447	.00083853	.574	-.0030032	.0010542
		100m and 200m Buffer from Hydrothermal Zone ROI	-.00091231	.00066791	.436	-.0025214	.0006968
	100m Buffer from Hydrothermal Zone ROI	Hydrothermal Zones ROI	.00097447	.00083853	.574	-.0010542	.0030032
		100m and 200m Buffer from Hydrothermal Zone ROI	.00006217	.00077736	1.000	-.0018223	.0019466
	100m and 200m Buffer from Hydrothermal Zone ROI	Hydrothermal Zones ROI	.00091231	.00066791	.436	-.0006968	.0025214
		100m Buffer from Hydrothermal Zone ROI	-.00006217	.00077736	1.000	-.0019466	.0018223
Dunnett T3	Hydrothermal Zones ROI	100m Buffer from Hydrothermal Zone ROI	-.00097447	.00083853	.572	-.0030022	.0010533
		100m and 200m Buffer from Hydrothermal Zone ROI	-.00091231	.00066791	.434	-.0025209	.0006963
	100m Buffer from Hydrothermal Zone ROI	Hydrothermal Zones ROI	.00097447	.00083853	.572	-.0010533	.0030022
		100m and 200m Buffer from Hydrothermal Zone ROI	.00006217	.00077736	1.000	-.0018213	.0019456
	100m and 200m Buffer from Hydrothermal Zone ROI	Hydrothermal Zones ROI	.00091231	.00066791	.434	-.0006963	.0025209
		100m Buffer from Hydrothermal Zone ROI	-.00006217	.00077736	1.000	-.0019456	.0018213

(Silica (11/12)) (Oct 16, 2005)

Case Processing Summary

		Cases					
		Valid		Missing		Total	
	HZ_Zones	N	Percent	N	Percent	N	Percent
Pixel_Values	Hydrothermal Zones ROI	95	100.0%	0	.0%	95	100.0%
	100m Buffer from Hydrothermal Zone ROI	44	100.0%	0	.0%	44	100.0%
	100m and 200m Buffer from Hydrothermal Zone ROI	100	100.0%	0	.0%	100	100.0%

ANOVA

Pixel_Values

	Sum of Squares	df	Mean Square	F	Sig.
Between Groups	.000	2	.000	2.456	.088
Within Groups	.011	236	.000		
Total	.011	238			

Multiple Comparisons

Dependent Variable:Pixel_Values

	(I) HZ_Zones	(J) HZ_Zones	Mean Difference (I-J)	Std. Error	Sig.	95% Confidence Interval	
						Lower Bound	Upper Bound
Tamhane	Hydrothermal Zones ROI	100m Buffer from Hydrothermal Zone ROI	-.00215964	.00128338	.264	-.0053031	.0009838
		100m and 200m Buffer from Hydrothermal Zone ROI	-.00192537	.00094890	.126	-.0042118	.0003611
	100m Buffer from Hydrothermal Zone ROI	Hydrothermal Zones ROI	.00215964	.00128338	.264	-.0009838	.0053031
		100m and 200m Buffer from Hydrothermal Zone ROI	.00023427	.00136405	.997	-.0030913	.0035598
	100m and 200m Buffer from Hydrothermal Zone ROI	Hydrothermal Zones ROI	.00192537	.00094890	.126	-.0003611	.0042118
		100m Buffer from Hydrothermal Zone ROI	-.00023427	.00136405	.997	-.0035598	.0030913
Dunnett T3	Hydrothermal Zones ROI	100m Buffer from Hydrothermal Zone ROI	-.00215964	.00128338	.262	-.0053001	.0009808
		100m and 200m Buffer from Hydrothermal Zone ROI	-.00192537	.00094890	.126	-.0042111	.0003603
	100m Buffer from Hydrothermal Zone ROI	Hydrothermal Zones ROI	.00215964	.00128338	.262	-.0009808	.0053001
		100m and 200m Buffer from Hydrothermal Zone ROI	.00023427	.00136405	.997	-.0030888	.0035573
	100m and 200m Buffer from Hydrothermal Zone ROI	Hydrothermal Zones ROI	.00192537	.00094890	.126	-.0003603	.0042111
		100m Buffer from Hydrothermal Zone ROI	-.00023427	.00136405	.997	-.0035573	.0030888

(Silica (11/12)) (Feb 5, 2006)

Case Processing Summary

	HZ_Zones	Cases					
		Valid		Missing		Total	
		N	Percent	N	Percent	N	Percent
Pixel_Values	Hydrothermal Zones ROI	93	100.0%	0	.0%	93	100.0%
	100m Buffer from Hydrothermal Zone ROI	49	100.0%	0	.0%	49	100.0%
	100m and 200m Buffer from Hydrothermal Zone ROI	98	100.0%	0	.0%	98	100.0%

ANOVA

Pixel_Values

	Sum of Squares	df	Mean Square	F	Sig.
Between Groups	.000	2	.000	7.287	.001
Within Groups	.005	237	.000		
Total	.006	239			

Multiple Comparisons

Dependent Variable:Pixel_Values

	(I) HZ_Zones	(J) HZ_Zones	Mean Difference (I-J)	Std. Error	Sig.	95% Confidence Interval	
						Lower Bound	Upper Bound
Tamhane	Hydrothermal Zones ROI	100m Buffer from Hydrothermal Zone ROI	.00248710*	.00080395	.007	.0005387	.0044355
		100m and 200m Buffer from Hydrothermal Zone ROI	.00230546*	.00069531	.003	.0006300	.0039809
	100m Buffer from Hydrothermal Zone ROI	Hydrothermal Zones ROI	-.00248710*	.00080395	.007	-.0044355	-.0005387
		100m and 200m Buffer from Hydrothermal Zone ROI	-.00018163	.00075962	.993	-.0020260	.0016627
	100m and 200m Buffer from Hydrothermal Zone ROI	Hydrothermal Zones ROI	-.00230546*	.00069531	.003	-.0039809	-.0006300
		100m Buffer from Hydrothermal Zone ROI	.00018163	.00075962	.993	-.0016627	.0020260
Dunnett T3	Hydrothermal Zones ROI	100m Buffer from Hydrothermal Zone ROI	.00248710*	.00080395	.007	.0005398	.0044344
		100m and 200m Buffer from Hydrothermal Zone ROI	.00230546*	.00069531	.003	.0006305	.0039804
	100m Buffer from Hydrothermal Zone ROI	Hydrothermal Zones ROI	-.00248710*	.00080395	.007	-.0044344	-.0005398
		100m and 200m Buffer from Hydrothermal Zone ROI	-.00018163	.00075962	.993	-.0020248	.0016616
	100m and 200m Buffer from Hydrothermal Zone ROI	Hydrothermal Zones ROI	-.00230546*	.00069531	.003	-.0039804	-.0006305
		100m Buffer from Hydrothermal Zone ROI	.00018163	.00075962	.993	-.0016616	.0020248

*. The mean difference is significant at the 0.05 level.

Tendaho (Silica (11/12))

(Silica (11/12)) (Jan 25, 2002)

Case Processing Summary

	HZ_Zones	Cases					
		Valid		Missing		Total	
		N	Percent	N	Percent	N	Percent
Pixel_Values	Hydrothermal Zones ROI	91	100.0%	0	.0%	91	100.0%
	100m Buffer from Hydrothermal Zone ROI	62	100.0%	0	.0%	62	100.0%
	100m and 200m Buffer from Hydrothermal Zone ROI	130	100.0%	0	.0%	130	100.0%

ANOVA

Pixel_Values

	Sum of Squares	df	Mean Square	F	Sig.
Between Groups	.000	2	.000	6.499	.002
Within Groups	.010	280	.000		
Total	.010	282			

Multiple Comparisons

Dependent Variable:Pixel_Values

	(I) HZ_Zones	(J) HZ_Zones	Mean Difference (I-J)	Std. Error	Sig.	95% Confidence Interval Lower Bound	95% Confidence Interval Upper Bound
Tamhane	Hydrothermal Zones ROI	100m Buffer from Hydrothermal Zone ROI	.00266111*	.00097102	.021	.0003163	.0050059
		100m and 200m Buffer from Hydrothermal Zone ROI	.00274791*	.00086743	.005	.0006559	.0048399
	100m Buffer from Hydrothermal Zone ROI	Hydrothermal Zones ROI	-.00266111*	.00097102	.021	-.0050059	-.0003163
		100m and 200m Buffer from Hydrothermal Zone ROI	.00008680	.00081840	.999	-.0018930	.0020666
	100m and 200m Buffer from Hydrothermal Zone ROI	Hydrothermal Zones ROI	-.00274791*	.00086743	.005	-.0048399	-.0006559
		100m Buffer from Hydrothermal Zone ROI	-.00008680	.00081840	.999	-.0020666	.0018930
Dunnett T3	Hydrothermal Zones ROI	100m Buffer from Hydrothermal Zone ROI	.00266111*	.00097102	.020	.0003172	.0050050
		100m and 200m Buffer from Hydrothermal Zone ROI	.00274791*	.00086743	.005	.0006566	.0048392
	100m Buffer from Hydrothermal Zone ROI	Hydrothermal Zones ROI	-.00266111*	.00097102	.020	-.0050050	-.0003172
		100m and 200m Buffer from Hydrothermal Zone ROI	.00008680	.00081840	.999	-.0018921	.0020657
	100m and 200m Buffer from Hydrothermal Zone ROI	Hydrothermal Zones ROI	-.00274791*	.00086743	.005	-.0048392	-.0006566
		100m Buffer from Hydrothermal Zone ROI	-.00008680	.00081840	.999	-.0020657	.0018921

*. The mean difference is significant at the 0.05 level.

(Silica (11/12)) (Oct 11, 2003)

Case Processing Summary

		Cases					
		Valid		Missing		Total	
	HZ_Zones	N	Percent	N	Percent	N	Percent
Pixel_Values	Hydrothermal Zones ROI	88	100.0%	0	.0%	88	100.0%
	100m Buffer from Hydrothermal Zone ROI	63	100.0%	0	.0%	63	100.0%
	100m and 200m Buffer from Hydrothermal Zone ROI	133	100.0%	0	.0%	133	100.0%

ANOVA

Pixel_Values

	Sum of Squares	df	Mean Square	F	Sig.
Between Groups	.004	2	.002	23.454	.000
Within Groups	.024	281	.000		
Total	.028	283			

Multiple Comparisons

Dependent Variable:Pixel_Values

	(I) HZ_Zones	(J) HZ_Zones	Mean Difference (I-J)	Std. Error	Sig.	95% Confidence Interval Lower Bound	95% Confidence Interval Upper Bound
Tamhane	Hydrothermal Zones ROI	100m Buffer from Hydrothermal Zone ROI	.00674738*	.00164210	.000	.0027814	.0107133
		100m and 200m Buffer from Hydrothermal Zone ROI	.00851689*	.00137323	.000	.0051985	.0118353
	100m Buffer from Hydrothermal Zone ROI	Hydrothermal Zones ROI	-.00674738*	.00164210	.000	-.0107133	-.0027814
		100m and 200m Buffer from Hydrothermal Zone ROI	.00176951	.00130620	.445	-.0013987	.0049377
	100m and 200m Buffer from Hydrothermal Zone ROI	Hydrothermal Zones ROI	-.00851689*	.00137323	.000	-.0118353	-.0051985
		100m Buffer from Hydrothermal Zone ROI	-.00176951	.00130620	.445	-.0049377	.0013987
Dunnett T3	Hydrothermal Zones ROI	100m Buffer from Hydrothermal Zone ROI	.00674738*	.00164210	.000	.0027830	.0107117
		100m and 200m Buffer from Hydrothermal Zone ROI	.00851689*	.00137323	.000	.0051999	.0118339
	100m Buffer from Hydrothermal Zone ROI	Hydrothermal Zones ROI	-.00674738*	.00164210	.000	-.0107117	-.0027830
		100m and 200m Buffer from Hydrothermal Zone ROI	.00176951	.00130620	.443	-.0013969	.0049359
	100m and 200m Buffer from Hydrothermal Zone ROI	Hydrothermal Zones ROI	-.00851689*	.00137323	.000	-.0118339	-.0051999
		100m Buffer from Hydrothermal Zone ROI	-.00176951	.00130620	.443	-.0049359	.0013969

*. The mean difference is significant at the 0.05 level.

(Silica (11/12)) (Jan 1, 2005)

Case Processing Summary

	HZ_Zones	Cases					
		Valid		Missing		Total	
		N	Percent	N	Percent	N	Percent
Pixel_Values	Hydrothermal Zones ROI	92	100.0%	0	.0%	92	100.0%
	100m Buffer from Hydrothermal Zone ROI	62	100.0%	0	.0%	62	100.0%
	100m and 200m Buffer from Hydrothermal Zone ROI	127	100.0%	0	.0%	127	100.0%

ANOVA

Pixel_Values

	Sum of Squares	df	Mean Square	F	Sig.
Between Groups	.003	2	.002	18.519	.000
Within Groups	.026	278	.000		
Total	.029	280			

Multiple Comparisons

Dependent Variable:Pixel_Values

	(I) HZ_Zones	(J) HZ_Zones	Mean Difference (I-J)	Std. Error	Sig.	95% Confidence Interval Lower Bound	95% Confidence Interval Upper Bound
Tamhane	Hydrothermal Zones ROI	100m Buffer from Hydrothermal Zone ROI	.00579516*	.00171055	.003	.0016647	.0099256
		100m and 200m Buffer from Hydrothermal Zone ROI	.00791969*	.00142917	.000	.0044666	.0113728
	100m Buffer from Hydrothermal Zone ROI	Hydrothermal Zones ROI	-.00579516*	.00171055	.003	-.0099256	-.0016647
		100m and 200m Buffer from Hydrothermal Zone ROI	.00212452	.00133964	.309	-.0011266	.0053757
	100m and 200m Buffer from Hydrothermal Zone ROI	Hydrothermal Zones ROI	-.00791969*	.00142917	.000	-.0113728	-.0044666
		100m Buffer from Hydrothermal Zone ROI	-.00212452	.00133964	.309	-.0053757	.0011266
Dunnett T3	Hydrothermal Zones ROI	100m Buffer from Hydrothermal Zone ROI	.00579516*	.00171055	.003	.0016663	.0099240
		100m and 200m Buffer from Hydrothermal Zone ROI	.00791969*	.00142917	.000	.0044680	.0113714
	100m Buffer from Hydrothermal Zone ROI	Hydrothermal Zones ROI	-.00579516*	.00171055	.003	-.0099240	-.0016663
		100m and 200m Buffer from Hydrothermal Zone ROI	.00212452	.00133964	.307	-.0011247	.0053738
	100m and 200m Buffer from Hydrothermal Zone ROI	Hydrothermal Zones ROI	-.00791969*	.00142917	.000	-.0113714	-.0044680
		100m Buffer from Hydrothermal Zone ROI	-.00212452	.00133964	.307	-.0053738	.0011247

*. The mean difference is significant at the 0.05 level.

Berecha (Silica (13/10))

(Silica (13/10)) (Jan 12, 2003)

Case Processing Summary

	HZ_Zones	Cases Valid N	Valid Percent	Missing N	Missing Percent	Total N	Total Percent
Pixel_Values	Hydrothermal Zones ROI	96	100.0%	0	.0%	96	100.0%
	100m Buffer from Hydrothermal Zone ROI	46	100.0%	0	.0%	46	100.0%
	100m and 200m Buffer from Hydrothermal Zone ROI	100	100.0%	0	.0%	100	100.0%

ANOVA

Pixel_Values

	Sum of Squares	df	Mean Square	F	Sig.
Between Groups	.001	2	.000	9.373	.000
Within Groups	.009	239	.000		
Total	.010	241			

Multiple Comparisons

Dependent Variable:Pixel_Values

	(I) HZ_Zones	(J) HZ_Zones	Mean Difference (I-J)	Std. Error	Sig.	95% Confidence Interval Lower Bound	95% Confidence Interval Upper Bound
Tamhane	Hydrothermal Zones ROI	100m Buffer from Hydrothermal Zone ROI	.00290784*	.00110610	.029	.0002261	.0055896
		100m and 200m Buffer from Hydrothermal Zone ROI	.00371079*	.00090320	.000	.0015334	.0058882
	100m Buffer from Hydrothermal Zone ROI	Hydrothermal Zones ROI	-.00290784*	.00110610	.029	-.0055896	-.0002261
		100m and 200m Buffer from Hydrothermal Zone ROI	.00080296	.00098597	.803	-.0015997	.0032056
	100m and 200m Buffer from Hydrothermal Zone ROI	Hydrothermal Zones ROI	-.00371079*	.00090320	.000	-.0058882	-.0015334
		100m Buffer from Hydrothermal Zone ROI	-.00080296	.00098597	.803	-.0032056	.0015997
Dunnett T3	Hydrothermal Zones ROI	100m Buffer from Hydrothermal Zone ROI	.00290784*	.00110610	.029	.0002275	.0055881
		100m and 200m Buffer from Hydrothermal Zone ROI	.00371079*	.00090320	.000	.0015341	.0058875
	100m Buffer from Hydrothermal Zone ROI	Hydrothermal Zones ROI	-.00290784*	.00110610	.029	-.0055881	-.0002275
		100m and 200m Buffer from Hydrothermal Zone ROI	.00080296	.00098597	.800	-.0015979	.0032038
	100m and 200m Buffer from Hydrothermal Zone ROI	Hydrothermal Zones ROI	-.00371079*	.00090320	.000	-.0058875	-.0015341
		100m Buffer from Hydrothermal Zone ROI	-.00080296	.00098597	.800	-.0032038	.0015979

*. The mean difference is significant at the 0.05 level.

(Silica (13/10)) (Oct 16, 2005)

Case Processing Summary

		Cases					
		Valid		Missing		Total	
	HZ_Zones	N	Percent	N	Percent	N	Percent
Pixel_Values	Hydrothermal Zones ROI	95	100.0%	0	.0%	95	100.0%
	100m Buffer from Hydrothermal Zone ROI	44	100.0%	0	.0%	44	100.0%
	100m and 200m Buffer from Hydrothermal Zone ROI	100	100.0%	0	.0%	100	100.0%

ANOVA

Pixel_Values

	Sum of Squares	df	Mean Square	F	Sig.
Between Groups	.000	2	.000	1.847	.160
Within Groups	.023	236	.000		
Total	.024	238			

Multiple Comparisons

Dependent Variable:Pixel_Values

	(I) HZ_Zones	(J) HZ_Zones	Mean Difference (I-J)	Std. Error	Sig.	95% Confidence Interval Lower Bound	95% Confidence Interval Upper Bound
Tamhane	Hydrothermal Zones ROI	100m Buffer from Hydrothermal Zone ROI	-.00041206	.00183179	.994	-.0048691	.0040450
		100m and 200m Buffer from Hydrothermal Zone ROI	.00235858	.00143351	.275	-.0010951	.0058122
	100m Buffer from Hydrothermal Zone ROI	Hydrothermal Zones ROI	.00041206	.00183179	.994	-.0040450	.0048691
		100m and 200m Buffer from Hydrothermal Zone ROI	.00277064	.00175184	.313	-.0015026	.0070438
	100m and 200m Buffer from Hydrothermal Zone ROI	Hydrothermal Zones ROI	-.00235858	.00143351	.275	-.0058122	.0010951
		100m Buffer from Hydrothermal Zone ROI	-.00277064	.00175184	.313	-.0070438	.0015026
Dunnett T3	Hydrothermal Zones ROI	100m Buffer from Hydrothermal Zone ROI	-.00041206	.00183179	.994	-.0048660	.0040419
		100m and 200m Buffer from Hydrothermal Zone ROI	.00235858	.00143351	.274	-.0010940	.0058111
	100m Buffer from Hydrothermal Zone ROI	Hydrothermal Zones ROI	.00041206	.00183179	.994	-.0040419	.0048660
		100m and 200m Buffer from Hydrothermal Zone ROI	.00277064	.00175184	.311	-.0014992	.0070405
	100m and 200m Buffer from Hydrothermal Zone ROI	Hydrothermal Zones ROI	-.00235858	.00143351	.274	-.0058111	.0010940
		100m Buffer from Hydrothermal Zone ROI	-.00277064	.00175184	.311	-.0070405	.0014992

(Silica (13/10)) (Feb 5, 2006)

Case Processing Summary

	HZ_Zones	Cases					
		Valid		Missing		Total	
		N	Percent	N	Percent	N	Percent
Pixel_Values	Hydrothermal Zones ROI	93	100.0%	0	.0%	93	100.0%
	100m Buffer from Hydrothermal Zone ROI	49	100.0%	0	.0%	49	100.0%
	100m and 200m Buffer from Hydrothermal Zone ROI	98	100.0%	0	.0%	98	100.0%

ANOVA

Pixel_Values

	Sum of Squares	df	Mean Square	F	Sig.
Between Groups	.001	2	.000	12.953	.000
Within Groups	.005	237	.000		
Total	.006	239			

Multiple Comparisons

Dependent Variable:Pixel_Values

	(I) HZ_Zones	(J) HZ_Zones	Mean Difference (I-J)	Std. Error	Sig.	95% Confidence Interval	
						Lower Bound	Upper Bound
Tamhane	Hydrothermal Zones ROI	100m Buffer from Hydrothermal Zone ROI	.00274648*	.00082126	.004	.0007465	.0047464
		100m and 200m Buffer from Hydrothermal Zone ROI	.00341689*	.00068691	.000	.0017616	.0050722
	100m Buffer from Hydrothermal Zone ROI	Hydrothermal Zones ROI	-.00274648*	.00082126	.004	-.0047464	-.0007465
		100m and 200m Buffer from Hydrothermal Zone ROI	.00067041	.00087683	.830	-.0014578	.0027986
	100m and 200m Buffer from Hydrothermal Zone ROI	Hydrothermal Zones ROI	-.00341689*	.00068691	.000	-.0050722	-.0017616
		100m Buffer from Hydrothermal Zone ROI	-.00067041	.00087683	.830	-.0027986	.0014578
Dunnett T3	Hydrothermal Zones ROI	100m Buffer from Hydrothermal Zone ROI	.00274648*	.00082126	.004	.0007480	.0047450
		100m and 200m Buffer from Hydrothermal Zone ROI	.00341689*	.00068691	.000	.0017621	.0050716
	100m Buffer from Hydrothermal Zone ROI	Hydrothermal Zones ROI	-.00274648*	.00082126	.004	-.0047450	-.0007480
		100m and 200m Buffer from Hydrothermal Zone ROI	.00067041	.00087683	.829	-.0014566	.0027974
	100m and 200m Buffer from Hydrothermal Zone ROI	Hydrothermal Zones ROI	-.00341689*	.00068691	.000	-.0050716	-.0017621
		100m Buffer from Hydrothermal Zone ROI	-.00067041	.00087683	.829	-.0027974	.0014566

*. The mean difference is significant at the 0.05 level.

Tendaho (Silica (13/10))

(Silica (13/10)) (Jan 25, 2002)

Case Processing Summary

		Cases					
		Valid		Missing		Total	
	HZ_Zones	N	Percent	N	Percent	N	Percent
Pixel_Values	Hydrothermal Zones ROI	91	100.0%	0	.0%	91	100.0%
	100m Buffer from Hydrothermal Zone ROI	62	100.0%	0	.0%	62	100.0%
	100m and 200m Buffer from Hydrothermal Zone ROI	130	100.0%	0	.0%	130	100.0%

ANOVA

Pixel_Values

	Sum of Squares	df	Mean Square	F	Sig.
Between Groups	.003	2	.002	22.788	.000
Within Groups	.019	280	.000		
Total	.022	282			

Multiple Comparisons

Dependent Variable:Pixel_Values

	(I) HZ_Zones	(J) HZ_Zones	Mean Difference (I-J)	Std. Error	Sig.	95% Confidence Interval Lower Bound	95% Confidence Interval Upper Bound
Tamhane	Hydrothermal Zones ROI	100m Buffer from Hydrothermal Zone ROI	.00481611*	.00137087	.002	.0015024	.0081298
		100m and 200m Buffer from Hydrothermal Zone ROI	.00760495*	.00114975	.000	.0048344	.0103755
	100m Buffer from Hydrothermal Zone ROI	Hydrothermal Zones ROI	-.00481611*	.00137087	.002	-.0081298	-.0015024
		100m and 200m Buffer from Hydrothermal Zone ROI	.00278883	.00124398	.078	-.0002237	.0058014
	100m and 200m Buffer from Hydrothermal Zone ROI	Hydrothermal Zones ROI	-.00760495*	.00114975	.000	-.0103755	-.0048344
		100m Buffer from Hydrothermal Zone ROI	-.00278883	.00124398	.078	-.0058014	.0002237
Dunnett T3	Hydrothermal Zones ROI	100m Buffer from Hydrothermal Zone ROI	.00481611*	.00137087	.002	.0015038	.0081284
		100m and 200m Buffer from Hydrothermal Zone ROI	.00760495*	.00114975	.000	.0048353	.0103746
	100m Buffer from Hydrothermal Zone ROI	Hydrothermal Zones ROI	-.00481611*	.00137087	.002	-.0081284	-.0015038
		100m and 200m Buffer from Hydrothermal Zone ROI	.00278883	.00124398	.078	-.0002222	.0057998
	100m and 200m Buffer from Hydrothermal Zone ROI	Hydrothermal Zones ROI	-.00760495*	.00114975	.000	-.0103746	-.0048353
		100m Buffer from Hydrothermal Zone ROI	-.00278883	.00124398	.078	-.0057998	.0002222

*. The mean difference is significant at the 0.05 level.

(Silica (13/10)) (Oct 11, 2003)

Case Processing Summary

	HZ_Zones	Cases					
		Valid		Missing		Total	
		N	Percent	N	Percent	N	Percent
Pixel_Values	Hydrothermal Zones ROI	88	100.0%	0	.0%	88	100.0%
	100m Buffer from Hydrothermal Zone ROI	63	100.0%	0	.0%	63	100.0%
	100m and 200m Buffer from Hydrothermal Zone ROI	133	100.0%	0	.0%	133	100.0%

ANOVA

Pixel_Values

	Sum of Squares	df	Mean Square	F	Sig.
Between Groups	.046	2	.023	50.027	.000
Within Groups	.130	281	.000		
Total	.176	283			

Multiple Comparisons

Dependent Variable:Pixel_Values

	(I) HZ_Zones	(J) HZ_Zones	Mean Difference (I-J)	Std. Error	Sig.	95% Confidence Interval	
						Lower Bound	Upper Bound
Tamhane	Hydrothermal Zones ROI	100m Buffer from Hydrothermal Zone ROI	.02268220*	.00381670	.000	.0134631	.0319013
		100m and 200m Buffer from Hydrothermal Zone ROI	.02915413*	.00316598	.000	.0215069	.0368013
	100m Buffer from Hydrothermal Zone ROI	Hydrothermal Zones ROI	-.02268220*	.00381670	.000	-.0319013	-.0134631
		100m and 200m Buffer from Hydrothermal Zone ROI	.00647193	.00311381	.115	-.0010797	.0140236
	100m and 200m Buffer from Hydrothermal Zone ROI	Hydrothermal Zones ROI	-.02915413*	.00316598	.000	-.0368013	-.0215069
		100m Buffer from Hydrothermal Zone ROI	-.00647193	.00311381	.115	-.0140236	.0010797
Dunnett T3	Hydrothermal Zones ROI	100m Buffer from Hydrothermal Zone ROI	.02268220*	.00381670	.000	.0134668	.0318976
		100m and 200m Buffer from Hydrothermal Zone ROI	.02915413*	.00316598	.000	.0215100	.0367982
	100m Buffer from Hydrothermal Zone ROI	Hydrothermal Zones ROI	-.02268220*	.00381670	.000	-.0318976	-.0134668
		100m and 200m Buffer from Hydrothermal Zone ROI	.00647193	.00311381	.115	-.0010755	.0140194
	100m and 200m Buffer from Hydrothermal Zone ROI	Hydrothermal Zones ROI	-.02915413*	.00316598	.000	-.0367982	-.0215100
		100m Buffer from Hydrothermal Zone ROI	-.00647193	.00311381	.115	-.0140194	.0010755

*. The mean difference is significant at the 0.05 level.

(Silica (13/10)) (Jan 1, 2005)

Case Processing Summary

		Cases					
		Valid		Missing		Total	
	HZ_Zones	N	Percent	N	Percent	N	Percent
Pixel_Values	Hydrothermal Zones ROI	92	100.0%	0	.0%	92	100.0%
	100m Buffer from Hydrothermal Zone ROI	62	100.0%	0	.0%	62	100.0%
	100m and 200m Buffer from Hydrothermal Zone ROI	127	100.0%	0	.0%	127	100.0%

ANOVA

Pixel_Values

	Sum of Squares	df	Mean Square	F	Sig.
Between Groups	.028	2	.014	28.251	.000
Within Groups	.139	278	.000		
Total	.167	280			

Multiple Comparisons

Dependent Variable:Pixel_Values

	(I) HZ_Zones	(J) HZ_Zones	Mean Difference (I-J)	Std. Error	Sig.	95% Confidence Interval Lower Bound	95% Confidence Interval Upper Bound
Tamhane	Hydrothermal Zones ROI	100m Buffer from Hydrothermal Zone ROI	.01670687*	.00398660	.000	.0070754	.0263383
		100m and 200m Buffer from Hydrothermal Zone ROI	.02275409*	.00321565	.000	.0149916	.0305166
	100m Buffer from Hydrothermal Zone ROI	Hydrothermal Zones ROI	-.01670687*	.00398660	.000	-.0263383	-.0070754
		100m and 200m Buffer from Hydrothermal Zone ROI	.00604722	.00332165	.200	-.0020156	.0141101
	100m and 200m Buffer from Hydrothermal Zone ROI	Hydrothermal Zones ROI	-.02275409*	.00321565	.000	-.0305166	-.0149916
		100m Buffer from Hydrothermal Zone ROI	-.00604722	.00332165	.200	-.0141101	.0020156
Dunnett T3	Hydrothermal Zones ROI	100m Buffer from Hydrothermal Zone ROI	.01670687*	.00398660	.000	.0070794	.0263343
		100m and 200m Buffer from Hydrothermal Zone ROI	.02275409*	.00321565	.000	.0149945	.0305136
	100m Buffer from Hydrothermal Zone ROI	Hydrothermal Zones ROI	-.01670687*	.00398660	.000	-.0263343	-.0070794
		100m and 200m Buffer from Hydrothermal Zone ROI	.00604722	.00332165	.199	-.0020108	.0141053
	100m and 200m Buffer from Hydrothermal Zone ROI	Hydrothermal Zones ROI	-.02275409*	.00321565	.000	-.0305136	-.0149945
		100m Buffer from Hydrothermal Zone ROI	-.00604722	.00332165	.199	-.0141053	.0020108

*. The mean difference is significant at the 0.05 level.

Berecha (Thermal) Feb 2

(Feb 2, 2003) 1st polynomial

Case Processing Summary

	HZ_Zones	Cases					
		Valid		Missing		Total	
		N	Percent	N	Percent	N	Percent
Pixel_Values	Hydrothermal Zones ROI	95	100.0%	0	.0%	95	100.0%
	100m Buffer from Hydrothermal Zone ROI	41	100.0%	0	.0%	41	100.0%
	100m and 200m Buffer from Hydrothermal Zone ROI	98	100.0%	0	.0%	98	100.0%

ANOVA

Pixel_Values

	Sum of Squares	df	Mean Square	F	Sig.
Between Groups	15.881	2	7.940	17.186	.000
Within Groups	106.730	231	.462		
Total	122.611	233			

Multiple Comparisons

Dependent Variable:Pixel_Values

	(I) HZ_Zones	(J) HZ_Zones	Mean Difference (I-J)	Std. Error	Sig.	95% Confidence Interval Lower Bound	95% Confidence Interval Upper Bound
Tamhane	Hydrothermal Zones ROI	100m Buffer from Hydrothermal Zone ROI	.46120064*	.13403702	.003	.1310599	.7913414
		100m and 200m Buffer from Hydrothermal Zone ROI	.55360639*	.09358618	.000	.3279019	.7793109
	100m Buffer from Hydrothermal Zone ROI	Hydrothermal Zones ROI	-.46120064*	.13403702	.003	-.7913414	-.1310599
		100m and 200m Buffer from Hydrothermal Zone ROI	.09240575	.14600368	.895	-.2643598	.4491713
	100m and 200m Buffer from Hydrothermal Zone ROI	Hydrothermal Zones ROI	-.55360639*	.09358618	.000	-.7793109	-.3279019
		100m Buffer from Hydrothermal Zone ROI	-.09240575	.14600368	.895	-.4491713	.2643598
Dunnett T3	Hydrothermal Zones ROI	100m Buffer from Hydrothermal Zone ROI	.46120064*	.13403702	.003	.1314517	.7909495
		100m and 200m Buffer from Hydrothermal Zone ROI	.55360639*	.09358618	.000	.3279808	.7792320
	100m Buffer from Hydrothermal Zone ROI	Hydrothermal Zones ROI	-.46120064*	.13403702	.003	-.7909495	-.1314517
		100m and 200m Buffer from Hydrothermal Zone ROI	.09240575	.14600368	.894	-.2640549	.4488664
	100m and 200m Buffer from Hydrothermal Zone ROI	Hydrothermal Zones ROI	-.55360639*	.09358618	.000	-.7792320	-.3279808
		100m Buffer from Hydrothermal Zone ROI	-.09240575	.14600368	.894	-.4488664	.2640549

*. The mean difference is significant at the 0.05 level.

(Feb 2, 2003) 2nd polynomial

Case Processing Summary

	HZ_Zones	Cases: Valid N	Valid Percent	Missing N	Missing Percent	Total N	Total Percent
Pixel_Values	Hydrothermal Zones ROI	95	100.0%	0	.0%	95	100.0%
	100m Buffer from Hydrothermal Zone ROI	41	100.0%	0	.0%	41	100.0%
	100m and 200m Buffer from Hydrothermal Zone ROI	98	100.0%	0	.0%	98	100.0%

ANOVA

Pixel_Values

	Sum of Squares	df	Mean Square	F	Sig.
Between Groups	7.740	2	3.870	6.500	.002
Within Groups	137.538	231	.595		
Total	145.278	233			

Multiple Comparisons

Dependent Variable:Pixel_Values

	(I) HZ_Zones	(J) HZ_Zones	Mean Difference (I-J)	Std. Error	Sig.	95% Confidence Interval Lower Bound	Upper Bound
Tamhane	Hydrothermal Zones ROI	100m Buffer from Hydrothermal Zone ROI	.26979422	.14885869	.209	-.0962784	.6358668
		100m and 200m Buffer from Hydrothermal Zone ROI	.39643840*	.10745021	.001	.1373780	.6554988
	100m Buffer from Hydrothermal Zone ROI	Hydrothermal Zones ROI	-.26979422	.14885869	.209	-.6358668	.0962784
		100m and 200m Buffer from Hydrothermal Zone ROI	.12664418	.16119567	.819	-.2670102	.5202986
	100m and 200m Buffer from Hydrothermal Zone ROI	Hydrothermal Zones ROI	-.39643840*	.10745021	.001	-.6554988	-.1373780
		100m Buffer from Hydrothermal Zone ROI	-.12664418	.16119567	.819	-.5202986	.2670102
Dunnett T3	Hydrothermal Zones ROI	100m Buffer from Hydrothermal Zone ROI	.26979422	.14885869	.207	-.0958685	.6354569
		100m and 200m Buffer from Hydrothermal Zone ROI	.39643840*	.10745021	.001	.1374656	.6554112
	100m Buffer from Hydrothermal Zone ROI	Hydrothermal Zones ROI	-.26979422	.14885869	.207	-.6354569	.0958685
		100m and 200m Buffer from Hydrothermal Zone ROI	.12664418	.16119567	.817	-.2666833	.5199716
	100m and 200m Buffer from Hydrothermal Zone ROI	Hydrothermal Zones ROI	-.39643840*	.10745021	.001	-.6554112	-.1374656
		100m Buffer from Hydrothermal Zone ROI	-.12664418	.16119567	.817	-.5199716	.2666833

*. The mean difference is significant at the 0.05 level.

Berecha (Thermal) Aug 8

(Aug 8, 2010) 1st polynomial

Case Processing Summary

		Cases					
		Valid		Missing		Total	
	HZ_Zones	N	Percent	N	Percent	N	Percent
Pixel_Values	Hydrothermal Zones ROI	95	100.0%	0	.0%	95	100.0%
	100m Buffer from Hydrothermal Zone ROI	41	100.0%	0	.0%	41	100.0%
	100m and 200m Buffer from Hydrothermal Zone ROI	98	100.0%	0	.0%	98	100.0%

ANOVA

Pixel_Values

	Sum of Squares	df	Mean Square	F	Sig.
Between Groups	2.676	2	1.338	3.079	.048
Within Groups	100.381	231	.435		
Total	103.057	233			

Multiple Comparisons

Dependent Variable:Pixel_Values

						95% Confidence Interval	
	(I) HZ_Zones	(J) HZ_Zones	Mean Difference (I-J)	Std. Error	Sig.	Lower Bound	Upper Bound
Tamhane	Hydrothermal Zones ROI	100m Buffer from Hydrothermal Zone ROI	.28505651	.11996435	.057	-.0065533	.5766663
		100m and 200m Buffer from Hydrothermal Zone ROI	.16414466	.09714602	.253	-.0699983	.3982876
	100m Buffer from Hydrothermal Zone ROI	Hydrothermal Zones ROI	-.28505651	.11996435	.057	-.5766663	.0065533
		100m and 200m Buffer from Hydrothermal Zone ROI	-.12091185	.11025834	.621	-.3901664	.1483427
	100m and 200m Buffer from Hydrothermal Zone ROI	Hydrothermal Zones ROI	-.16414466	.09714602	.253	-.3982876	.0699983
		100m Buffer from Hydrothermal Zone ROI	.12091185	.11025834	.621	-.1483427	.3901664
Dunnett T3	Hydrothermal Zones ROI	100m Buffer from Hydrothermal Zone ROI	.28505651	.11996435	.057	-.0063647	.5764777
		100m and 200m Buffer from Hydrothermal Zone ROI	.16414466	.09714602	.253	-.0699217	.3982111
	100m Buffer from Hydrothermal Zone ROI	Hydrothermal Zones ROI	-.28505651	.11996435	.057	-.5764777	.0063647
		100m and 200m Buffer from Hydrothermal Zone ROI	-.12091185	.11025834	.618	-.3899430	.1481193
	100m and 200m Buffer from Hydrothermal Zone ROI	Hydrothermal Zones ROI	-.16414466	.09714602	.253	-.3982111	.0699217
		100m Buffer from Hydrothermal Zone ROI	.12091185	.11025834	.618	-.1481193	.3899430

(Aug 8, 2010) 2nd polynomial

Case Processing Summary

	HZ_Zones	Cases					
		Valid		Missing		Total	
		N	Percent	N	Percent	N	Percent
Pixel_Values	Hydrothermal Zones ROI	95	100.0%	0	.0%	95	100.0%
	100m Buffer from Hydrothermal Zone ROI	41	100.0%	0	.0%	41	100.0%
	100m and 200m Buffer from Hydrothermal Zone ROI	98	100.0%	0	.0%	98	100.0%

ANOVA

Pixel_Values

	Sum of Squares	df	Mean Square	F	Sig.
Between Groups	3.325	2	1.663	3.861	.022
Within Groups	99.465	231	.431		
Total	102.790	233			

Multiple Comparisons

Dependent Variable:Pixel_Values

	(I) HZ_Zones	(J) HZ_Zones	Mean Difference (I-J)	Std. Error	Sig.	95% Confidence Interval	
						Lower Bound	Upper Bound
Tamhane	Hydrothermal Zones ROI	100m Buffer from Hydrothermal Zone ROI	.32221340*	.11740516	.021	.0372660	.6071608
		100m and 200m Buffer from Hydrothermal Zone ROI	.17570887	.09766705	.205	-.0597745	.4111922
	100m Buffer from Hydrothermal Zone ROI	Hydrothermal Zones ROI	-.32221340*	.11740516	.021	-.6071608	-.0372660
		100m and 200m Buffer from Hydrothermal Zone ROI	-.14650453	.10417355	.415	-.4007976	.1077885
	100m and 200m Buffer from Hydrothermal Zone ROI	Hydrothermal Zones ROI	-.17570887	.09766705	.205	-.4111922	.0597745
		100m Buffer from Hydrothermal Zone ROI	.14650453	.10417355	.415	-.1077885	.4007976
Dunnett T3	Hydrothermal Zones ROI	100m Buffer from Hydrothermal Zone ROI	.32221340*	.11740516	.021	.0374332	.6069936
		100m and 200m Buffer from Hydrothermal Zone ROI	.17570887	.09766705	.205	-.0596945	.4111122
	100m Buffer from Hydrothermal Zone ROI	Hydrothermal Zones ROI	-.32221340*	.11740516	.021	-.6069936	-.0374332
		100m and 200m Buffer from Hydrothermal Zone ROI	-.14650453	.10417355	.412	-.4005907	.1075817
	100m and 200m Buffer from Hydrothermal Zone ROI	Hydrothermal Zones ROI	-.17570887	.09766705	.205	-.4111122	.0596945
		100m Buffer from Hydrothermal Zone ROI	.14650453	.10417355	.412	-.1075817	.4005907

*. The mean difference is significant at the 0.05 level.

Tendaho (Thermal) Sept 30, 2002

(Sept 30, 2002) 1nd polynomial

Case Processing Summary

		Cases					
		Valid		Missing		Total	
	HZ_Zones	N	Percent	N	Percent	N	Percent
Pixel_Values	Hydrothermal Zones ROI	90	100.0%	0	.0%	90	100.0%
	100m Buffer from Hydrothermal Zone ROI	66	100.0%	0	.0%	66	100.0%
	100m and 200m Buffer from Hydrothermal Zone ROI	128	100.0%	0	.0%	128	100.0%

ANOVA

Pixel_Values

	Sum of Squares	df	Mean Square	F	Sig.
Between Groups	4.427	2	2.214	1.125	.326
Within Groups	553.090	281	1.968		
Total	557.517	283			

Multiple Comparisons

Dependent Variable:Pixel_Values

	(I) HZ_Zones	(J) HZ_Zones	Mean Difference (I-J)	Std. Error	Sig.	95% Confidence Interval Lower Bound	95% Confidence Interval Upper Bound
Tamhane	Hydrothermal Zones ROI	100m Buffer from Hydrothermal Zone ROI	.33046697	.21791368	.345	-.1961316	.8570655
		100m and 200m Buffer from Hydrothermal Zone ROI	.20164370	.19245030	.651	-.2617290	.6650164
	100m Buffer from Hydrothermal Zone ROI	Hydrothermal Zones ROI	-.33046697	.21791368	.345	-.8570655	.1961316
		100m and 200m Buffer from Hydrothermal Zone ROI	-.12882327	.21025538	.903	-.6368352	.3791887
	100m and 200m Buffer from Hydrothermal Zone ROI	Hydrothermal Zones ROI	-.20164370	.19245030	.651	-.6650164	.2617290
		100m Buffer from Hydrothermal Zone ROI	.12882327	.21025538	.903	-.3791887	.6368352
Dunnett T3	Hydrothermal Zones ROI	100m Buffer from Hydrothermal Zone ROI	.33046697	.21791368	.344	-.1959088	.8568427
		100m and 200m Buffer from Hydrothermal Zone ROI	.20164370	.19245030	.650	-.2615947	.6648821
	100m Buffer from Hydrothermal Zone ROI	Hydrothermal Zones ROI	-.33046697	.21791368	.344	-.8568427	.1959088
		100m and 200m Buffer from Hydrothermal Zone ROI	-.12882327	.21025538	.903	-.6366233	.3789767
	100m and 200m Buffer from Hydrothermal Zone ROI	Hydrothermal Zones ROI	-.20164370	.19245030	.650	-.6648821	.2615947
		100m Buffer from Hydrothermal Zone ROI	.12882327	.21025538	.903	-.3789767	.6366233

(Sept 30, 2002) 2nd polynomial

Case Processing Summary

	HZ_Zones	Cases					
		Valid		Missing		Total	
		N	Percent	N	Percent	N	Percent
Pixel_Values	Hydrothermal Zones ROI	90	100.0%	0	.0%	90	100.0%
	100m Buffer from Hydrothermal Zone ROI	66	100.0%	0	.0%	66	100.0%
	100m and 200m Buffer from Hydrothermal Zone ROI	128	100.0%	0	.0%	128	100.0%

ANOVA

Pixel_Values

	Sum of Squares	df	Mean Square	F	Sig.
Between Groups	2.131	2	1.066	.502	.606
Within Groups	596.598	281	2.123		
Total	598.730	283			

Multiple Comparisons

Dependent Variable:Pixel_Values

	(I) HZ_Zones	(J) HZ_Zones	Mean Difference (I-J)	Std. Error	Sig.	95% Confidence Interval	
						Lower Bound	Upper Bound
Tamhane	Hydrothermal Zones ROI	100m Buffer from Hydrothermal Zone ROI	.23650980	.22758987	.658	-.3132837	.7863033
		100m and 200m Buffer from Hydrothermal Zone ROI	.09534936	.20265796	.953	-.3927163	.5834150
	100m Buffer from Hydrothermal Zone ROI	Hydrothermal Zones ROI	-.23650980	.22758987	.658	-.7863033	.3132837
		100m and 200m Buffer from Hydrothermal Zone ROI	-.14116044	.21466767	.884	-.6598128	.3774919
	100m and 200m Buffer from Hydrothermal Zone ROI	Hydrothermal Zones ROI	-.09534936	.20265796	.953	-.5834150	.3927163
		100m Buffer from Hydrothermal Zone ROI	.14116044	.21466767	.884	-.3774919	.6598128
Dunnett T3	Hydrothermal Zones ROI	100m Buffer from Hydrothermal Zone ROI	.23650980	.22758987	.656	-.3130581	.7860777
		100m and 200m Buffer from Hydrothermal Zone ROI	.09534936	.20265796	.952	-.3925707	.5832694
	100m Buffer from Hydrothermal Zone ROI	Hydrothermal Zones ROI	-.23650980	.22758987	.656	-.7860777	.3130581
		100m and 200m Buffer from Hydrothermal Zone ROI	-.14116044	.21466767	.883	-.6595971	.3772762
	100m and 200m Buffer from Hydrothermal Zone ROI	Hydrothermal Zones ROI	-.09534936	.20265796	.952	-.5832694	.3925707
		100m Buffer from Hydrothermal Zone ROI	.14116044	.21466767	.883	-.3772762	.6595971

Tendaho (Thermal) March 2, 2010

(March 2, 2010) 1nd polynomial

Case Processing Summary

		Cases					
		Valid		Missing		Total	
	HZ_Zones	N	Percent	N	Percent	N	Percent
Pixel_Values	Hydrothermal Zones ROI	90	100.0%	0	.0%	90	100.0%
	100m Buffer from Hydrothermal Zone ROI	66	100.0%	0	.0%	66	100.0%
	100m and 200m Buffer from Hydrothermal Zone ROI	128	100.0%	0	.0%	128	100.0%

ANOVA

Pixel_Values

	Sum of Squares	df	Mean Square	F	Sig.
Between Groups	2.131	2	1.066	.502	.606
Within Groups	596.598	281	2.123		
Total	598.730	283			

Multiple Comparisons

Dependent Variable:Pixel_Values

	(I) HZ_Zones	(J) HZ_Zones	Mean Difference (I-J)	Std. Error	Sig.	95% Confidence Interval Lower Bound	95% Confidence Interval Upper Bound
Tamhane	Hydrothermal Zones ROI	100m Buffer from Hydrothermal Zone ROI	.23650980	.22758987	.658	-.3132837	.7863033
		100m and 200m Buffer from Hydrothermal Zone ROI	.09534936	.20265796	.953	-.3927163	.5834150
	100m Buffer from Hydrothermal Zone ROI	Hydrothermal Zones ROI	-.23650980	.22758987	.658	-.7863033	.3132837
		100m and 200m Buffer from Hydrothermal Zone ROI	-.14116044	.21466767	.884	-.6598128	.3774919
	100m and 200m Buffer from Hydrothermal Zone ROI	Hydrothermal Zones ROI	-.09534936	.20265796	.953	-.5834150	.3927163
		100m Buffer from Hydrothermal Zone ROI	.14116044	.21466767	.884	-.3774919	.6598128
Dunnett T3	Hydrothermal Zones ROI	100m Buffer from Hydrothermal Zone ROI	.23650980	.22758987	.656	-.3130581	.7860777
		100m and 200m Buffer from Hydrothermal Zone ROI	.09534936	.20265796	.952	-.3925707	.5832694
	100m Buffer from Hydrothermal Zone ROI	Hydrothermal Zones ROI	-.23650980	.22758987	.656	-.7860777	.3130581
		100m and 200m Buffer from Hydrothermal Zone ROI	-.14116044	.21466767	.883	-.6595971	.3772762
	100m and 200m Buffer from Hydrothermal Zone ROI	Hydrothermal Zones ROI	-.09534936	.20265796	.952	-.5832694	.3925707
		100m Buffer from Hydrothermal Zone ROI	.14116044	.21466767	.883	-.3772762	.6595971

(March 2, 2010) 2nd polynomial

Case Processing Summary

		Cases					
		Valid		Missing		Total	
	HZ_Zones	N	Percent	N	Percent	N	Percent
Pixel_Values	Hydrothermal Zones ROI	90	100.0%	0	.0%	90	100.0%
	100m Buffer from Hydrothermal Zone ROI	66	100.0%	0	.0%	66	100.0%
	100m and 200m Buffer from Hydrothermal Zone ROI	128	100.0%	0	.0%	128	100.0%

ANOVA

Pixel_Values

	Sum of Squares	df	Mean Square	F	Sig.
Between Groups	2.042	2	1.021	.479	.620
Within Groups	598.574	281	2.130		
Total	600.615	283			

Multiple Comparisons

Dependent Variable:Pixel_Values

						95% Confidence Interval	
	(I) HZ_Zones	(J) HZ_Zones	Mean Difference (I-J)	Std. Error	Sig.	Lower Bound	Upper Bound
Tamhane	Hydrothermal Zones ROI	100m Buffer from Hydrothermal Zone ROI	.23127970	.22816640	.675	-.3199012	.7824606
		100m and 200m Buffer from Hydrothermal Zone ROI	.08952510	.20309671	.961	-.3996047	.5786549
	100m Buffer from Hydrothermal Zone ROI	Hydrothermal Zones ROI	-.23127970	.22816640	.675	-.7824606	.3199012
		100m and 200m Buffer from Hydrothermal Zone ROI	-.14175459	.21493402	.883	-.6610576	.3775484
	100m and 200m Buffer from Hydrothermal Zone ROI	Hydrothermal Zones ROI	-.08952510	.20309671	.961	-.5786549	.3996047
		100m Buffer from Hydrothermal Zone ROI	.14175459	.21493402	.883	-.3775484	.6610576
Dunnett T3	Hydrothermal Zones ROI	100m Buffer from Hydrothermal Zone ROI	.23127970	.22816640	.673	-.3196752	.7822346
		100m and 200m Buffer from Hydrothermal Zone ROI	.08952510	.20309671	.960	-.3994585	.5785087
	100m Buffer from Hydrothermal Zone ROI	Hydrothermal Zones ROI	-.23127970	.22816640	.673	-.7822346	.3196752
		100m and 200m Buffer from Hydrothermal Zone ROI	-.14175459	.21493402	.882	-.6608414	.3773322
	100m and 200m Buffer from Hydrothermal Zone ROI	Hydrothermal Zones ROI	-.08952510	.20309671	.960	-.5785087	.3994585
		100m Buffer from Hydrothermal Zone ROI	.14175459	.21493402	.882	-.3773322	.6608414